

**Repair of Partially Penetrated Weld Joints in Copper-Nickel  
Seawater Piping on Naval Ships**

by

Alan A. Rechel

B.S., Aeronautical Engineering  
Embry-Riddle Aeronautical University (1989)

Submitted to the Department of Ocean Engineering and the  
Department of Materials Science and Engineering  
in Partial Fulfillment of the Requirements for the Degrees of  
Master of Science in Naval Architecture and Marine Engineering  
and  
Master of Science in Materials Science and Engineering

at the

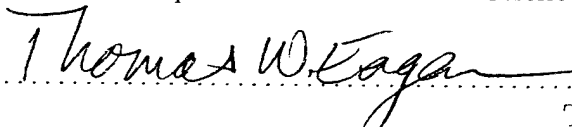
Massachusetts Institute of Technology

September 2000

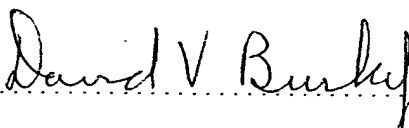
© 2000 Massachusetts Institute of Technology  
All rights reserved

Signature of Author .....  .....

Department of Ocean Engineering and the  
Department of Materials Science and Engineering  
August 4, 2000

Certified by .....  .....

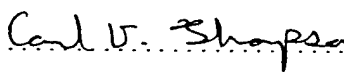
Thomas W. Eagar  
Professor of Materials Engineering  
Research Head

Certified by .....  .....

David V. Burke  
Senior Lecturer, Department of Ocean Engineering  
Thesis Supervisor

Accepted by .....  .....

Nicholas Patrikalakis  
Kawasaki Professor of Engineering  
Chairman, Departmental Committee on Graduate Studies

Accepted by .....  .....

Carl V. Thompson  
Stavros Salapatas Professor of Materials Science and Engineering  
Chairman, Departmental Committee on Graduate Students

20001027 050

**Repair of Partially Penetrated Weld Joints in Copper-Nickel Seawater  
Piping on Naval Ships**

by

Alan A. Rechel

Submitted to the Department of Ocean Engineering and the  
Department of Materials Science and Engineering  
on August 4, 2000. in partial fulfillment of the  
requirements for the Degrees of  
Master of Science in Naval Architecture and Marine Engineering  
and  
Master of Science in Materials Science and Engineering

**Abstract**

The U.S. Navy has experienced several leaks in Cu-Ni seawater piping as a result of partially penetrated welds in the ships' original construction. If it were possible to repair the welds without cutting open the pipe, the Navy could realize significant cost savings on ship repair. This investigation evaluated whether it would be possible to achieve satisfactory weld repairs by remelting the weld zone, fusing the joint through its full thickness without cleaning the interior of the pipe.

Elemental analysis of the internal deposits on pipes removed from service and manufacture of repair welds on these pipes show that it is possible to repair partially penetrated welded joints in Cu-Ni seawater pipe by remelting the weld zone. The repair weld is not likely to absorb contamination from the interior of the pipe, as shown by X-rays of the welds and elemental analysis of the weld bead, compared to the unwelded base metal.

Research Head: Thomas W. Eagar  
Title: Professor of Materials Engineering

Thesis Supervisor: David V. Burke  
Title: Senior Lecturer, Department of Ocean Engineering

# Contents

<b>1</b>	<b>Introduction</b>	<b>11</b>
<b>2</b>	<b>Background</b>	<b>13</b>
2.1	Copper-Nickel Alloy Properties . . . . .	13
2.2	Gas-shielded Tungsten Arc Welding (GTAW) . . . . .	13
2.3	Copper-Nickel Weldability . . . . .	15
<b>3</b>	<b>Analysis Methods</b>	<b>17</b>
3.1	General . . . . .	17
3.2	Material for Analysis . . . . .	18
3.3	Deposit Analysis . . . . .	18
3.4	Welding . . . . .	19
<b>4</b>	<b>Results</b>	<b>21</b>
4.1	Internal Deposit Analysis . . . . .	21
4.2	Welding Practice . . . . .	24
4.3	Weld Results . . . . .	26
4.3.1	X-ray Results . . . . .	26
4.3.2	SEM Results . . . . .	50
<b>5</b>	<b>Conclusion</b>	<b>59</b>
5.1	Specific Conclusions . . . . .	59
5.2	Recommendations . . . . .	60

<b>A X-Rays of Pipe Segments A1, A2, A3, and A4</b>	<b>61</b>
<b>B SEM and EDS Operation</b>	<b>66</b>
B.1 SEM Operation . . . . .	66
B.2 EDS Operation . . . . .	68
<b>C EDS Spectra: Internal Deposits</b>	<b>70</b>
<b>D EDS Spectra: Weldment Coupons</b>	<b>117</b>

# List of Tables

2.1	Cu-Ni Alloy Composition . . . . .	13
2.2	Cu Alloy Properties . . . . .	14
2.3	GTAW Parameters for Cu-Ni . . . . .	15
3.1	Pipe Segment Description . . . . .	18
4.1	Internal Deposit Analysis . . . . .	22
4.2	Internal Deposit Analysis . . . . .	23
4.3	Test Weld Descriptions . . . . .	25
4.4	X-ray Evaluations . . . . .	49
4.5	EDS Analysis of Weld Root Face . . . . .	50

# List of Figures

1-1	Schematic of a Partially Penetrated Weld Joint . . . . .	12
4-1	Weld A1, Section 0-1 . . . . .	28
4-2	Weld A1, Section 1-2 . . . . .	29
4-3	Weld A1, Section 2-0 . . . . .	30
4-4	Weld A2, Section 0-1 . . . . .	31
4-5	Weld A2, Section 1-2 . . . . .	32
4-6	Weld A2, Section 2-0 . . . . .	33
4-7	Weld A3, Section 0-1 . . . . .	34
4-8	Weld A3, Section 1-2 . . . . .	35
4-9	Weld A3, Section 2-0 . . . . .	36
4-10	Weld A4, Section 0-1 . . . . .	37
4-11	Weld A4, Section 1-2 . . . . .	38
4-12	Weld A4, Section 2-0 . . . . .	39
4-13	Welds C1, C2-A, C2-B . . . . .	40
4-14	Welds C3-A, C3-B, C3-C . . . . .	41
4-15	Welds C4-A, C4-B . . . . .	42
4-16	Welds C5-A, C5-B, C5-C, C5-D, C5-E . . . . .	43
4-17	Welds C6-A, C6-B . . . . .	44
4-18	Welds C6-C, C6-D . . . . .	45
4-19	Welds C7-A, C7-B, C7-C . . . . .	46
4-20	Welds C8-A, C8-B, C8-C . . . . .	47
4-21	Close-up of Weld A2, Section 1-2 . . . . .	51

4-22 Close-up of Weld A3, Section 1-2 . . . . .	52
4-23 Close-up of Weld A3, Section 2-0 . . . . .	53
4-24 Close-up of Weld A4, Section 1-2 . . . . .	54
4-25 Root Face of Weld A2, Section 1-2 . . . . .	55
4-26 Root Face of Weld A3, Section 2-0 . . . . .	56
4-27 Root Face of Weld A4, Section 1-2 . . . . .	57
A-1 Weld A1 Before Repair . . . . .	62
A-2 Weld A2 Before Repair . . . . .	63
A-3 Weld A3 Before Repair . . . . .	64
A-4 Weld A4 Before Repair . . . . .	65
B-1 SEM Cross-section . . . . .	67
B-2 Bohr Model of the Atom Showing the Origin of Emitted X-rays . . . . .	69
C-1 EDS Spectrum A11a . . . . .	71
C-2 EDS Spectrum A11b . . . . .	72
C-3 EDS Spectrum A11c . . . . .	73
C-4 EDS Spectrum A12a . . . . .	74
C-5 EDS Spectrum A12b . . . . .	75
C-6 EDS Spectrum A13a . . . . .	76
C-7 EDS Spectrum A21a . . . . .	77
C-8 EDS Spectrum A21b . . . . .	78
C-9 EDS Spectrum A21c . . . . .	79
C-10 EDS Spectrum A22a . . . . .	80
C-11 EDS Spectrum A22b . . . . .	81
C-12 EDS Spectrum A22c . . . . .	82
C-13 EDS Spectrum A23a . . . . .	83
C-14 EDS Spectrum A23b . . . . .	84
C-15 EDS Spectrum A23c . . . . .	85
C-16 EDS Spectrum A31a . . . . .	86
C-17 EDS Spectrum A31b . . . . .	87

C-18 EDS Spectrum A31c . . . . .	88
C-19 EDS Spectrum A32a . . . . .	89
C-20 EDS Spectrum A32b . . . . .	90
C-21 EDS Spectrum A32c . . . . .	91
C-22 EDS Spectrum A33a . . . . .	92
C-23 EDS Spectrum A33b . . . . .	93
C-24 EDS Spectrum A33c . . . . .	94
C-25 EDS Spectrum A41a . . . . .	95
C-26 EDS Spectrum A41b . . . . .	96
C-27 EDS Spectrum A41c . . . . .	97
C-28 EDS Spectrum A42a . . . . .	98
C-29 EDS Spectrum A42b . . . . .	99
C-30 EDS Spectrum A42c . . . . .	100
C-31 EDS Spectrum A43a . . . . .	101
C-32 EDS Spectrum A43b . . . . .	102
C-33 EDS Spectrum A43c . . . . .	103
C-34 EDS Spectrum C31 . . . . .	104
C-35 EDS Spectrum C32 . . . . .	105
C-36 EDS Spectrum C33 . . . . .	106
C-37 EDS Spectrum C41 . . . . .	107
C-38 EDS Spectrum C42 . . . . .	108
C-39 EDS Spectrum C43 . . . . .	109
C-40 EDS Spectrum C51 . . . . .	110
C-41 EDS Spectrum C52 . . . . .	111
C-42 EDS Spectrum C53 . . . . .	112
C-43 EDS Spectrum C61 . . . . .	113
C-44 EDS Spectrum C62 . . . . .	114
C-45 EDS Spectrum C63 . . . . .	115
C-46 EDS Spectrum Al Stub . . . . .	116
D-1 EDS Spectrum Weld A2, Section 0-1, Base Metal . . . . .	118

D-2	EDS Spectrum Weld A2, Section 0-1, Weld Bead . . . . .	119
D-3	EDS Spectrum Weld A3, Section 0-1, Base Metal . . . . .	120
D-4	EDS Spectrum Weld A3, Section 0-1, Weld Bead . . . . .	121
D-5	EDS Spectrum Weld A4, Section 0-1, Base Metal . . . . .	122
D-6	EDS Spectrum Weld A4, Section 0-1, Weld Bead . . . . .	123
D-7	EDS Spectrum Weld C4-A Base Metal . . . . .	124
D-8	EDS Spectrum Weld C4-A Weld Bead . . . . .	125
D-9	EDS Spectrum Weld C6-A Base Metal . . . . .	126
D-10	EDS Spectrum Weld C6-A Weld Bead . . . . .	127
D-11	EDS Spectrum Weld C6-C Base Metal . . . . .	128
D-12	EDS Spectrum Weld C6-C Weld Bead . . . . .	129
D-13	EDS Spectrum Weld C6-D Base Metal . . . . .	130
D-14	EDS Spectrum Weld C6-D Weld Bead . . . . .	131

## Acknowledgments

This thesis would not have been possible without assistance from several individuals. Of special notice are Mr. Barry Cole of Naval Sea Systems Command, who suggested this question, Professors Eagar and Burke, who provided valuable guidance, Mr. Don Galler of MIT, who provided instruction and assistance, Mr. Mike Balmforth of MIT, who made the welds, Mr. Karl Rusnak of Norfolk Naval Shipyard and Mr. Ed Jakawich of Puget Sound Naval Shipyard, who provided information and pipe samples, Mr. Harvey Castner of the Navy Joining Center and Dr. Matt Johnson of the Edison Welding Institute, who provided advice and welding flux.

# Chapter 1

## Introduction

Navy ships use seawater for cooling of other systems and for fire fighting. The piping for these seawater systems is generally copper-nickel (Cu-Ni) alloy. Cu-Ni has good corrosion resistance in seawater and has sufficient strength and toughness for these applications. Also, copper is toxic to sea life, so it resists biological fouling, such as barnacles and sea grass. The systems are assembled by gas-shielded tungsten arc welding (GTAW), also known as tungsten-inert gas (TIG) welding. After several years in service, some of these joints develop leaks, necessitating repair. It has been found that these leaks are often the result of partial penetration in the original weld. That is, when the joint was originally formed, the weld did not fully penetrate the thickness of the pipe wall. This creates a notch that weakens the pipe and can serve as a stress raiser or fatigue crack initiation site. Figure 1-1 shows a schematic of the cross-section of a partial penetration joint. This is potentially very dangerous since the weakened joint may be susceptible to rupture after a shock load, such as might occur in combat. After battle damage, of course, is when it is most important that the firemain system should function. The current method of repairing these joints is to cut open the pipe, remove the weld, prepare the inside and outside of the pipe wall, and make a new weld. As the piping system is still installed in the ship, this usually entails cutting out a short section of pipe containing the faulty weld and welding in a new piece of pipe, bridging the gap. This replaces one weld with two. It is also expensive and time-consuming. If it were possible to create a satisfactory repair by welding over the joint from the outside of the pipe, without cutting it open, the Navy could save a great deal of money on repairs, and could preemptively repair joints before they leak.

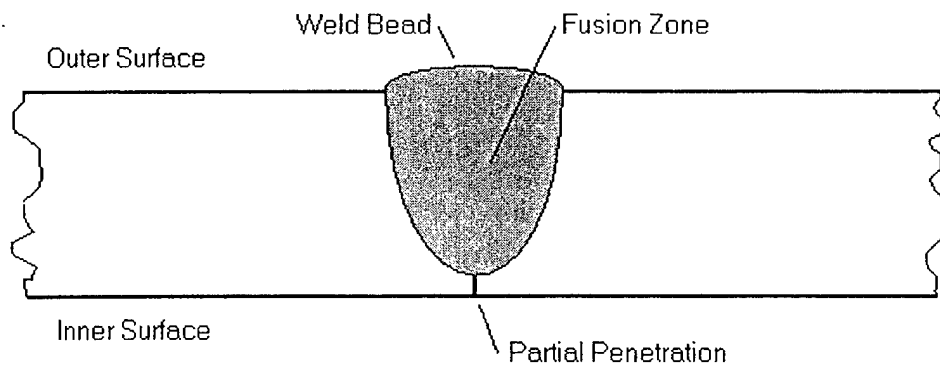


Figure 1-1: Schematic of a Partially Penetrated Weld Joint

The goal of this investigation is to determine whether such a repair method is possible. The course of the investigation will include elemental analysis of the interior surface of several pipes that have been removed from service followed by the manufacture of repair welds in them. This will include repairs of actual faulty welds. The investigation will determine whether these welds would make satisfactory repairs, considering the effects of fouling and environment and the characteristics of Cu-Ni.

# Chapter 2

## Background

### 2.1 Copper-Nickel Alloy Properties

Copper and nickel form a complete set of solid solutions, from pure copper to pure nickel [5]. Commercial Cu-Ni alloys occupy the copper-rich end of this spectrum from 10% to 30% nickel, the balance copper. Welded Cu-Ni pipe is either nominally 10% nickel or 30 % nickel, alloys C70600 and C71500, respectively. Table 2.1 [1] lists these alloys and their chemical composition. Copper is a relatively noble metal, resistant to corrosion in aqueous environments, as is nickel. The addition of nickel to the copper increases the strength of the copper and improves resistance to erosion [12]. Table 2.2 [5][11] lists the strength and elongation of Cu-Ni relative to pure copper, designated C11000.

### 2.2 Gas-shielded Tungsten Arc Welding (GTAW)

GTAW produces coalescence using the heat of an arc between the work and a nonconsumable tungsten electrode. Shielding comes from a gas or gas mixture and filler metal may or may

Table 2.1: Cu-Ni Alloy Composition

Alloy Number	Composition, %							
	Cu	Ni	Pb, max	Fe	Zn, max	Mn, max	S, max	P, max
C70600	remainder	9.0-11.0	0.05	1.0-1.8	1.0	1.0	0.02	0.02
C71500	remainder	29.0-33.0	0.05	0.40-1.0	1.0	1.0	0.02	0.02

Table 2.2: Cu Alloy Properties

Alloy Number	Tensile Strength (ksi)	Yield Strength (ksi)	Elongation in 2", %
C11000	32-50	10-40	45-6
C70600	44-60	16-57	42-10
C71500	54-75	20-70	45-15

not be used. The intense heat of the arc melts the surface of the metal. Thinner materials or edge joints do not need filler metal, a form of welding known as "autogenous." Thicker materials require filler metal, usually a rod or wire fed externally into the weld pool. The shielding gas flows through a nozzle surrounding the electrode. This displaces air from around the tungsten electrode and from the surface of the work, preventing undesirable reactions and porosity. Coalescence and joining occur as the metal cools and solidifies.

GTAW has several features that make it desirable for many applications [3]:

1. It produces high-quality welds in nearly all metals and alloys.
2. It requires little or no post-weld cleaning.
3. The arc and weld pool remain visible to the welder throughout the process.
4. The filler metal is not carried across the arc, so it produces very little spatter.
5. It can be performed in all positions.
6. It produces no slag that could become trapped in the weld.

The equipment required for GTAW includes a power supply, a supply of inert gas, a welding torch, and possibly filler metal. The power supply is a constant-current power source so that changes in arc length do not significantly change the welding current. A typical power supply can operate from 3 to 200A and 10 to 35V. The shielding gas is either argon or helium; the other inert gases are too expensive. Argon is more common. It is heavier than air so it can provide efficient shielding at lower flow rates. It also operates at a lower voltage and improves the arc starting. Helium is much lighter than air so higher flow is necessary for satisfactory shielding. It does provide a hotter arc, allowing a higher weld speed than argon. Some applications specify a mixture of argon and helium. The filler metal should be the same composition as the base metal and can be added to the weld pool manually or automatically. [3]

Table 2.3: GTAW Parameters for Cu-Ni

Alloy Number	Method	Current (A)	Travel Speed (ipm)
C70600	automatic	310 - 320	15 - 18
C70600	manual	300 - 310	5 - 6
C71500	manual	270 - 290	5 - 6

The welding torch holds the tungsten electrode and connects it to the power supply. It also directs the flow of shielding gas around the arc. It may have a handle for manual welding or be designed to clamp in an automatic welding machine. It may also include water cooling for high current applications. The electrode is tungsten, which has the highest melting temperature of any metal (6170°F), or an alloy of tungsten with thorium or zirconium. The thorium or zirconium improves electron emission and increases current capacity. These elements also stabilize the arc and improve arc starting. The size of the electrode depends on the amount and direction of the welding current. [3]

### 2.3 Copper-Nickel Weldability

Cu-Ni is readily welded with a well-controlled gas-shielded arc welding system, and GTAW is preferred, with argon shielding gas, straight polarity direct current, and thoriated tungsten. Table 2.3 [11] lists the nominal conditions for GTAW of butt joints with square and single-V groove joints. Alloy C70600 has higher thermal conductivity than C71500 so it requires higher current or lower weld speed. Preheating is not required for either alloy. Backing rings should be copper or copper-nickel, when used. The only filler metal commonly used is RCuNi. This filler contains 1.00% max Mn, 0.40-0.70% Fe, 29.0-32.0 % Ni+Co, 0.20-0.50 % Ti, remainder Cu+Ag. The titanium is a deoxidizer to prevent porosity and oxygen embrittlement. [11]

However, Cu-Ni is susceptible to cracking in the fusion and the heat-affected zones, particularly in restrained welds. These cracks have two causes: solidification of low-melting segregates and ductility dip. The first effect occurs in the fusion line and reflects the different melting temperatures of the constituent materials. As the weld metal cools after melting, certain elements solidify first, if they have not adequately diffused into the surrounding material. As more metal cools, it solidifies in dendrites that have varying composition. The core of the dendrite will be nickel-rich, surrounded by copper-rich regions and finally trace elements. Thus

the grain boundaries, where the dendrites grow into contact with each other, can have significantly different composition than the grain centers. This effect can be exacerbated in the weld zone if the weld employs filler metal of significantly different composition from the base metal. The quick heating and cooling inherent in welding may not allow sufficient diffusion of the constituents, creating large pockets of distinct composition and mechanical properties. The presence of trace elements and impurities can also aggravate solidification cracking. [13]

The second mode of cracking is the result of the ductility dip or trough that Cu-Ni exhibits at elevated temperature. When Cu-Ni cools from a temperature above its nil-ductility temperature of 1900 to 1940°F it displays a significant loss of ductility in the range from 1470 to 2010°F. Tensile tests of a range of Cu-Ni alloys at progressively lower temperatures when cooling from 1940°F illustrate this by showing less than 20% reduction in area at fracture in this temperature range. When cooled from 1920°F, the samples show increased ductility, fracturing with 40 to 90% reduction in area. All the tested alloys show consistently high ductility while heating through the range from 1470 to 2010°F, fracturing with 60 to 90% reduction in area. This indicates the ductility trough is a result of microstructure changes as the metal heats through its nil-ductility temperature. Trace elements and impurities also affect a specific alloy's susceptibility to ductility dip cracking. In particular, phosphorus, sulfur, silicon, titanium, and zirconium have been shown to increase weld metal crack susceptibility, while carbon inhibits cracking when present with phosphorus or zirconium. Titanium and zirconium are common additives in commercial alloys, and titanium is a standard deoxidizer in welding filler metal, so limiting the proportions is important. [7]

## Chapter 3

# Analysis Methods

### 3.1 General

The current method of repairing leaking joints is to cut out a short section of pipe containing the joint, clean the inside and outside of the pipe to bare metal for a distance of at least one inch from the joint edge, and weld in a short segment of pipe to replace the discarded piece, replacing one joint with two [9]. Some joints may allow movement of the pipe ends to allow remaking the joint without an additional piece of pipe and its second welded joint. Ships often have a premium on space so piping systems, cabling, pumps, motors, and other equipment often intertwine and interfere with ready access. Each individual process in a repair, such as cutting, joint preparation, and welding, requires access to the potentially tight space surrounding the joint. Any process that can be simplified or eliminated reduces the time devoted to the repair, thus reducing the cost of the repair.

One potential approach to simplifying this repair would be to weld over the faulty joint, essentially remelting the weld zone to create a full penetration weld. This method has a number of problems. First is the treatment of the outer surface of the pipe. Thick sections generally require a V-groove to make a new joint, with filler. Thin sections can be welded autogenously with no groove. Oxides, scale, paint, and other coatings should certainly be removed before welding. The second concern is the effect of the inside surface on the quality of the weld. A pipe system that has been in service will have at least a layer of oxides on its inside surface. It may also be host to biological creatures such as barnacles, despite copper's

Table 3.1: Pipe Segment Description

Pipe No.	Alloy	SPS (in)	OD (in)	Thickness (in)	Internal Condition
A1	90-10	8	8.66	0.157	Oxide film
A2	90-10	8	8.57	0.159	Oxide film
A3	90-10	8	8.59	0.152	Thick scale, barnacles
A4	90-10	8	8.64	0.158	Thick scale, barnacles
C1	70-30	1 $\frac{1}{2}$	1.90	0.120	Verdigris
C2	70-30	1 $\frac{1}{2}$	1.90	0.120	Verdigris
C3	70-30	4	4.5	0.220	Verdigris, brown scale
C4	70-30	3	3.5	0.180	Thick scale
C5	70-30	3	3.5	0.180	Very thick, black scale
C6	70-30	4	4.5	0.220	Brown scale, thick biologic growth
C7	70-30	2	2.38	0.125	Verdigris
C8	70-30	2	2.38	0.125	Verdigris

anti-fouling properties, and other deposits, depending on the system. These deposits could create inclusions or porosity in the weld, and the particular elements could contribute to the cracking phenomena described above. Cu-Ni is also very susceptible to oxygen absorption and attendant porosity, so the atmosphere inside the pipe is important to the quality of the weld.

### 3.2 Material for Analysis

For this investigation, Norfolk Naval Shipyard and Puget Sound Naval Shipyard provided sections of Cu-Ni pipe that had been removed from ships during maintenance. Table 3.1 lists the dimensions of all the pieces. The first four pieces, A1, A2, A3 and A4, came from the USS THOMAS S. GATES (CG 51) and each contains a partial penetration joint that was removed because it leaked. The other pieces came from deactivated submarines; they do not contain a faulty weld and just provide additional Cu-Ni pipe for analysis. All pieces have varying degrees of internal deposits. Appendix A shows X-rays of the joints in pieces A1, A2, A3 and A4. The black line through the white welded zone is the area of partial penetration.

### 3.3 Deposit Analysis

The internal deposit on the pipe was evaluated with a scanning electron microscope (SEM) with an energy-dispersive spectroscope (EDS). The SEM is an imaging device that uses electrons

to form the image much as a light microscope uses light to form the image. Electrons have much shorter wavelengths than photons,  $0.5\text{\AA}$  vice  $2000\text{\AA}$ , so the SEM can provide much higher magnification than the light microscope. The theoretical limit of the SEM is more than  $800,000\times$ ; practical limitations of the instrument itself limit magnification to  $\sim 75,000\times$ , with a resolution of  $40\text{\AA}$ . This compares to the light microscope's limits on magnification and resolution of  $2000\times$  and  $2000\text{\AA}$ . An EDS evaluates X-rays that are emitted by a specimen in a SEM to give information about the elemental composition of the sample. Appendix B contains more information on SEM and EDS operation. [6]

The EDS can only identify elements, not compounds or ionic states. So, a sample of rust would indicate iron and oxygen, but would not indicate ferric or ferrous oxide. The sample must be somewhat electrically conductive, to prevent accumulation of negative charge. To analyze the deposits on the inside of the pipe samples for this evaluation, the walls were scraped to yield a selection of the material. This was attached to aluminum specimen mounts with adhesive carbon tape. In some cases, segments of the pipe wall were cut small enough to fit inside the SEM chamber.

### 3.4 Welding

The selection of pipes available provided a range of wall thickness, which is a key variable in the welding method. Thin walls can be welded through the full thickness autogenously. Thicker walls need to be grooved and welded with filler metal. A recent development at the Edison Welding Institute (EWI), in response to a Navy Joining Center (NJC) project, provides another alternative. They have developed a number of fluxes for GTAW of austenitic stainless steel, carbon-manganese steel, and copper-nickel. These are not fluxes in the traditional sense of the word, since their purpose is not to remove oxides and surface contamination, or provide shielding and arc stabilization. Instead, their purpose is to increase weld penetration by up to 300%. This reduces the number of passes necessary to complete a weld, and allows single-pass full penetration in much thicker metal, compared to traditional methods. The EWI development follows introduction of GTAW fluxes by the Paton Welding Institute in the former Soviet Union. The stainless steel flux has been patented and is commercially available. Each

flux is a mixture of inorganic powders that is suspended in a volatile liquid medium, such as acetone or methanol. This is applied to the surface of the metal, in a layer less than 0.005in thick. After the liquid evaporates, the weld proceeds through the flux using conventional methods and practices, including shielding and backing gases and filler metal, if necessary. [8]

EWI developed two effective fluxes for copper-nickel, designated CN357 and CN426. This evaluation of pipe repair used both on all sizes of pipe, as well as welding without flux. On the thicker sections it was necessary to grind a groove to obtain full penetration with the first pass, followed by filler passes. Each weld was made in the 1G position, or flat. The evaluation considered one longitudinal and one circumferential weld for each flux and pipe size combination. The circumferential welds were performed by welding across the top of the pipe, then rolling it, welding across the top, and repeating all the way around the pipe. This removed the additional variable of weld position and the effect of gravity on the weld pool. In practice, actual repair welds would require all positions of welding. All welds for this evaluation were performed by a qualified welder and used argon backing gas inside the pipe.

# Chapter 4

## Results

### 4.1 Internal Deposit Analysis

Tables 4.1 and 4.2 present the results of the elemental analysis of the deposits from the pipe interiors. Appendix C contains the spectra for all samples. Each spectrum shows number of counts versus X-ray energy in keV. Each pipe yielded three samples, indicated by the second Arabic numeral in each designation: A11, A12 and A13 for pipe A1, for example. In addition, each sample from pipes A1, A2, A3 and A4 was evaluated two or three times at different spots, indicated by the trailing letter: A11a and A11b, for example. The sample labeled "subpipe" is from a pipe very similar to C1 and C2, so those pipes do not have samples. The sample labeled "Al stub" is an aluminum specimen mount with carbon tape on it, to provide a control for the other analyses. The asterisks indicate no presence of that element.

The wide variation in carbon content is partially an experimental artifact. If the volume of sample is small, it does not completely cover the carbon tape, so the EDS measures that carbon. Additionally, since the EDS measures the X-rays originating some distance below the surface, it could detect carbon under a very thin layer. Also, carbon is the lightest element the EDS can detect, so it represents the very end of the detected spectrum. The evaluation of the spectra used some averaging and noise reduction to clarify element peaks. Averaging the carbon peak with the zero response immediately adjacent can erroneously reduce the carbon indication. Also, the lowest energy noise is also the most plentiful, so a peak may appear at the lower bound of detection on a sample containing no carbon, purely due to noise. The variation

Table 4.1: Internal Deposit Analysis

Sample	Concentration, wt.%												
Label	C	O	Mg	Al	Si	S	Cl	K	Ca	Fe	Ni	Cu	Other
A11a	46.10	34.41	*	0.25	0.32	0.20	0.45	*	12.02	0.72	0.80	4.72	
A11b	56.62	25.10	*	0.15	0.44	0.21	0.69	*	4.14	1.32	1.38	9.94	
A11c	9.52	44.82	*	0.30	1.60	0.69	1.88	0.18	11.36	2.45	3.12	21.52	
A12a	6.27	26.75	*	0.77	0.92	0.63	2.06	*	2.34	3.83	3.83	55.54	
A12b	0.00	36.56	*	0.88	0.89	0.55	3.74	*	0.71	2.24	4.04	50.38	
A13a	4.53	36.54	0.25	0.84	1.33	1.03	3.15	0.29	1.14	4.70	10.09	36.12	
A21a	0.00	39.19	*	0.53	2.17	0.96	4.28	0.68	1.02	4.66	7.31	39.20	
A21b	61.26	25.31	*	0.34	0.99	0.22	0.73	0.16	0.42	1.14	1.61	7.82	
A21c	52.96	29.30	0.13	0.43	1.64	0.56	0.84	0.19	0.52	1.60	2.39	9.43	
A22a	57.35	27.76	*	0.66	1.20	0.20	0.43	0.24	0.29	1.95	2.90	7.02	
A22b	0.00	35.06	0.38	1.62	2.72	0.93	1.40	0.46	0.62	6.18	15.72	34.92	
A22c	47.29	27.86	*	0.50	0.83	0.19	0.58	0.13	0.23	2.52	5.97	13.90	
A23a	56.34	28.79	0.10	0.26	0.63	0.31	0.43	0.06	3.94	1.36	2.56	5.22	
A23b	56.49	23.57	*	0.30	0.31	0.16	0.85	*	0.32	1.26	1.90	14.85	
A23c	62.21	20.34	*	0.15	0.28	0.11	0.73	*	0.29	1.38	1.55	12.97	
A31a	0.00	46.21	0.34	4.78	16.77	0.30	1.48	1.12	1.12	6.47	7.06	14.37	
A31b	0.00	47.32	0.06	4.25	14.70	0.44	2.47	1.28	0.84	5.71	5.70	17.24	
A31c	0.00	50.56	0.36	4.97	17.87	0.57	1.39	1.26	0.89	5.65	3.31	13.16	
A32a	0.00	44.93	0.25	2.42	6.30	0.86	1.70	0.70	5.17	5.13	7.36	25.16	
A32b	0.00	41.46	0.37	2.49	7.25	0.89	2.10	0.56	3.24	4.12	5.19	32.33	
A32c	0.00	39.22	0.30	2.59	6.77	0.72	2.25	0.94	2.56	4.29	5.93	34.42	
A33a	0.00	40.31	*	1.66	3.44	0.41	2.71	*	6.44	5.32	7.18	32.55	
A33b	0.00	39.26	0.18	2.30	4.64	0.46	1.91	0.48	6.15	5.19	5.13	34.30	
A33c	62.64	25.12	0.04	0.26	0.54	0.13	0.38	0.10	1.10	1.37	2.36	5.96	
A41a	0.00	36.95	0.32	1.78	3.65	1.05	2.57	0.60	1.64	4.12	6.63	40.69	
A41b	56.61	25.78	0.06	0.55	1.02	0.19	0.64	0.20	1.12	1.20	1.13	11.52	
A41c	0.00	36.86	0.25	3.77	5.45	0.68	1.71	0.62	3.21	4.59	4.00	38.84	
A42a	0.00	32.88	*	2.71	4.62	0.92	1.49	0.56	0.89	5.49	4.94	45.50	
A42b	0.00	36.99	0.43	3.13	5.93	0.69	1.46	0.58	1.02	5.08	4.94	39.77	
A42c	57.12	23.04	0.04	0.47	0.81	0.24	0.35	0.14	0.16	1.35	1.30	14.98	
A43a	0.00	52.73	0.70	5.36	16.93	0.92	1.39	1.63	3.27	6.24	1.99	8.84	
A43b	0.00	55.95	0.59	4.43	12.98	0.67	0.92	1.05	9.38	3.89	1.27	8.88	
A43c	0.00	56.06	0.64	4.35	13.21	1.02	1.05	1.05	8.03	4.06	0.85	9.67	

\* = No detectable concentration

Table 4.2: Internal Deposit Analysis

Sample Label	Concentration, wt.%												
	C	O	Mg	Al	Si	S	Cl	K	Ca	Fe	Ni	Cu	Other
C31	28.01	28.45	0.58	0.42	0.51	0.37	6.05	0.12	1.04	2.42	5.08	26.95	
C32	25.30	23.28	0.27	13.21	0.31	0.42	5.00	0.09	0.44	2.04	4.08	25.36	
C33	30.78	26.54	0.37	0.51	0.41	0.40	5.77	0.12	0.35	1.68	4.93	28.15	
C41	28.98	33.41	0.40	3.28	0.06	0.27	1.40	0.08	0.51	0.44	9.16	21.85	P: 0.16
C42	15.80	23.87	0.42	16.69	0.05	0.39	1.38	0.08	0.43	0.57	9.2	30.31	P: 0.08
C43	35.26	29.27	0.12	0.16	0.09	0.15	1.72	0.20	0.78	0.36	5.34	21.84	P: 1.48, Cd: 3.24
C51	41.09	40.44	1.89	0.07	0.15	0.29	0.860	0.09	6.10	0.43	0.96	5.30	P: 2.32
C52	52.14	26.20	0.10	0.12	0.08	0.18	0.77	0.04	0.41	0.42	5.85	13.48	P: 0.19
C53	34.13	31.08	0.82	0.06	0.03	2.51	1.37	0.11	6.37	0.16	2.87	19.07	P: 1.41
C61	21.56	27.56	0.27	1.82	0.52	0.47	8.10	0.04	0.90	2.11	8.37	28.28	
C62	27.37	28.04	0.53	0.58	0.72	0.38	4.05	0.17	1.48	4.60	5.17	26.92	
C63	27.28	44.04	0.87	1.00	1.13	0.27	2.03	0.16	16.68	1.38	0.28	2.25	Na: 2.65
sub pipe	0.00	30.52	1.37	0.24	0.47	0.45	12.53	0.25	0.60	0.93	7.76	44.87	
Al stub	73.51	25.75	*	0.36	0.37	*	*	*	*	*	*	*	

\* = No detectable concentration

of the other elements reflects the variability of the composition of the internal deposit.

The copper and nickel are clearly present due to the oxidation of the base metal. The iron is part of the alloy. The oxygen would be a component of many compounds, in particular metallic oxides. The chlorine would come from the sea water, which contains on the order of 35ppt chlorides. Sodium should be present as well, but its energy peak on the spectrum falls under the very large  $L\alpha$  peak for copper, the left-hand copper peak at around 0.8keV on the spectra in Appendix B, so it is undetectable except in sample C63. The calcium, potassium, phosphorus, sulfur, and silicon could result from biological remains, or from waterborne compounds, since seawater contains a wide variety of suspended and dissolved contaminants. Similarly the magnesium, aluminum, and cadmium would come from the seawater. Some of the aluminum and silicon could also come from the specimen mount itself. The very small levels of those elements in the Al stub sample indicate that most of the detected aluminum and silicon actually come from the deposit sample.

Several of these elements could cause problems if dissolved into the pipe wall metal. The phosphorus, sulfur, and silicon could increase susceptibility to solidification cracking. If the heat of the welding causes the contamination to dissociate into its component elements, they can combine with the base metal to form compounds such as  $CaNi_5$ ,  $Cu_5Ca$ ,  $Cu_2O$ ,  $Cu_3P$ ,  $Ni_3P$ ,

$\text{Ni}_3\text{S}_2$ , and  $\text{Ni}_4\text{Si}$  [2]. Any contamination that does not dissolve can cause inclusions which would weaken the joint, if large enough.

## 4.2 Welding Practice

Table 4.3 lists the welds in each pipe segment. Several of the pipes received a number of welds, indicated by the letters following the pipe number in the weld numbers in Table 4.3. All welds were performed manually except for C1 and C2-B, which were made with an automatic welding machine. The welder sought full penetration as indicated when the surface of the weld pool slumped below the pipe surface. This left a trough in the surface of the weld. In practice, a cover pass would fill this trough to reinforce the pipe wall and fill any thickness reduction due to the slump of the weld bead. The first test welds were in the C-series of samples. It was possible to obtain full penetration autogenous welds in these pipes up to 0.125" thick with no flux or joint preparation. However, the weld pool was very wide and was difficult to control, tending to flow down the side of the pipe in the circumferential welds. It was also more susceptible to burning through. The EWI fluxes both narrowed the weld bead, by one-third to one-half, making it easier to control. This also required less current for full penetration and allowed full penetration with no joint preparation in all tested thicknesses, up to 0.220". The CN357 flux, grey in color, appeared to melt into the weld pool and at first seemed easier to work with. The CN426 flux, red in color, seemed to float on top of the pool. This initially complicated the task of observing full penetration by concealing the surface of the pool. With experience, however, the welder reported that it was easier to control the weld pool with the CN426 flux than with the CN357. Welds without flux in the thickest pipes, C3, C5, and C6, were accomplished by first grinding a groove in the surface of the pipe. This groove was 0.08 to 0.09" deep and 0.15" wide, in a U-shape. This groove provided a thinner section for the root pass and provided mechanical containment for the weld pool, making it easier to control. Each of these welds also received a filler pass over part of its length.

Table 4.3: Test Weld Descriptions

Weld No.	Joint Prep.	Weld Direction
A1	Ground bead, 0.02" proud, CN357 flux	Circumferential
A2	Ground bead, flush, no flux	Circumferential
A3	Ground bead, 0.02" proud, CN426 flux	Circumferential
A4	Unground bead, CN426 flux	Circumferential
C1	CN426 flux	Longitudinal
C2-A	No flux	Longitudinal
C2-B	CN357 flux	Longitudinal
C3-A	CN426 flux	Longitudinal
C3-B	U-groove, no flux	Longitudinal
C3-C	CN357 flux	Longitudinal
C4-A	CN357 flux	Circumferential
C4-B	CN426 flux	Circumferential
C5-A	CN357 flux	Longitudinal
C5-B	No flux	Longitudinal
C5-C	U-groove, no flux	Longitudinal
C5-D	CN426 flux	Longitudinal
C5-E	U-groove, no flux	Circumferential
C6-A	CN426 flux	Circumferential
C6-C	U-groove, no flux	Circumferential
C6-D	CN357 flux	Circumferential
C7-A	No flux	Circumferential
C7-B	CN357 flux	Circumferential
C7-C	CN426 flux	Circumferential
C8-A	CN426 flux	Longitudinal
C8-B	No flux	Longitudinal
C8-C	CN357 flux	Longitudinal

The welds on the A-series of pipes were over the old welds in those pipes, attempting to repair them. Each pipe was cleaned on the outside and the existing weld bead modified in one of two ways. On pipe A2 the weld bead was ground flush with the pipe surface, to reduce the thickness to be penetrated. On pipes A1 and A3 the weld bead was ground down flat, but not flush. It was left standing about 0.02" proud of the pipe surface, to determine whether it was necessary to remove the whole weld bead. On pipe A4 the weld bead was not ground down at all, to determine if it was necessary to remove any of the bead. It was possible to obtain full penetration without a groove or flux on this thickness of material, but the pool was again very wide and difficult to control. Both fluxes again resulted in narrower pools that were easier to control. The exception was weld A4 where the unground weld bead caused the pool to spread out. One principal benefit of not completely removing the weld bead, illustrated by welds A1 and A3, was that it was easier to see the position of the old joint. A difficulty that arose with the fluxes was that the new weld was so narrow that it could miss the old joint entirely. Weaving the torch to purposely make a wider weld zone would reduce this problem. None of the welds showed any cracking on solidification, but the pipes were not restrained so cracking was not expected.

## 4.3 Weld Results

### 4.3.1 X-ray Results

The figures on the next several pages show X-rays of all the joints. Small dark spots are pores, larger dark patches are thin patches, usually due to concavity, dark lines are partially penetrated seams. Figures 4-1 through 4-12 show the original condition of the weld on the left and the condition after welding on the right. The numerals 0, 1 and 2 are indices around the circumference; the index 3 on the right of Figures 4-10 and 4-12 is equivalent to the index 0 on the left. Weld C1 is on the left of Figure 4-13, C2-A is in the center, C2-B is on the right. Figure 4-14 shows welds C3-A, C3-B and C3-C from left to right. Welds D and C in Figure 4-15 are continuations of welds C4-A and C4-B, respectfully, from top to bottom. The four vertical welds in Figure 4-16 are welds C5-A, C5-C, C5-D and C5-B from left to right; weld C5-E runs horizontally across the bottom. Figures 4-17 and 4-18 use circumferential indices 0,

1 and 2; weld B in Figure 4-17 was originally in the pipe and was not part of this evaluation.  
Figure 4-19 shows two views of the welds in pipe C7.



Figure 4-1: Weld A1, Section 0-1

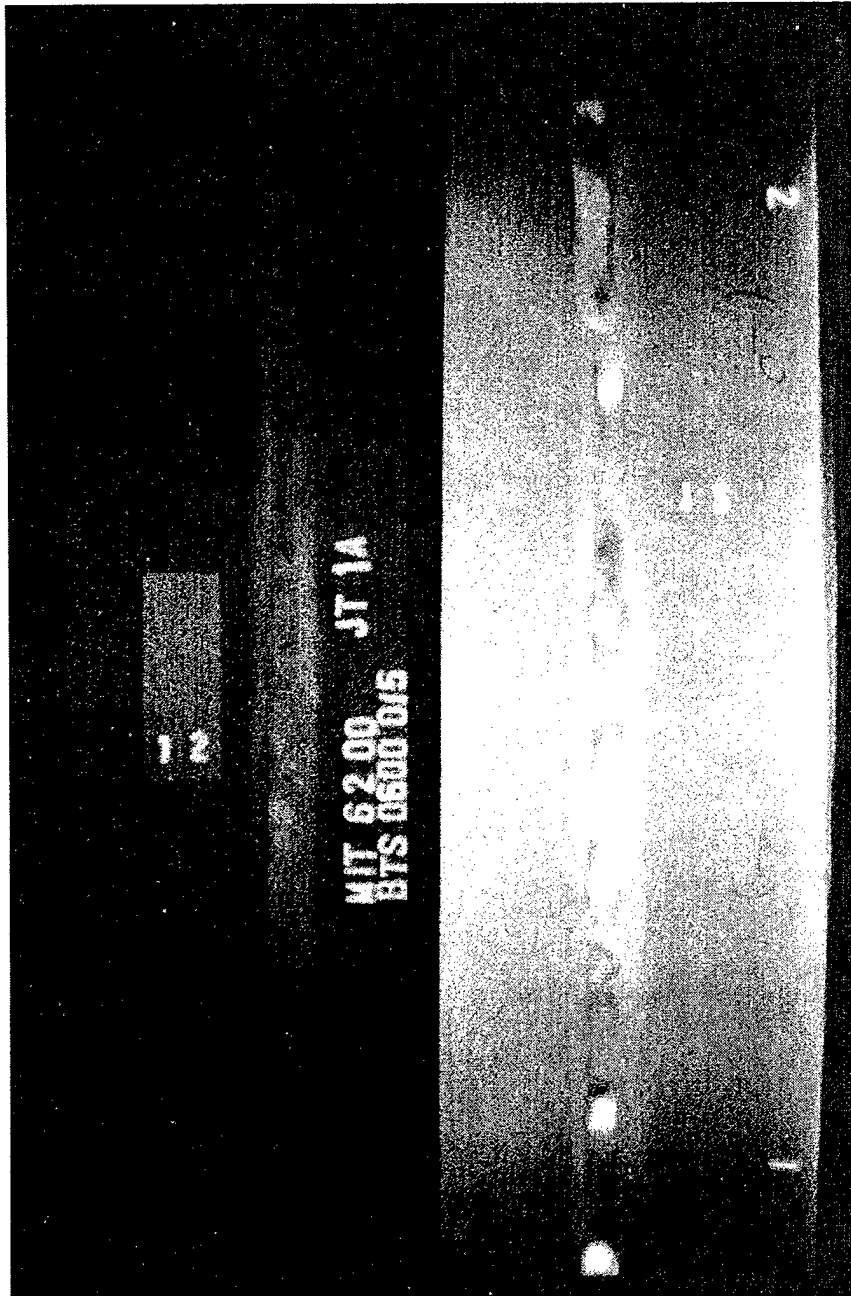


Figure 4-2: Weld A1, Section 1-2



Figure 4-3: Weld A1, Section 2-0

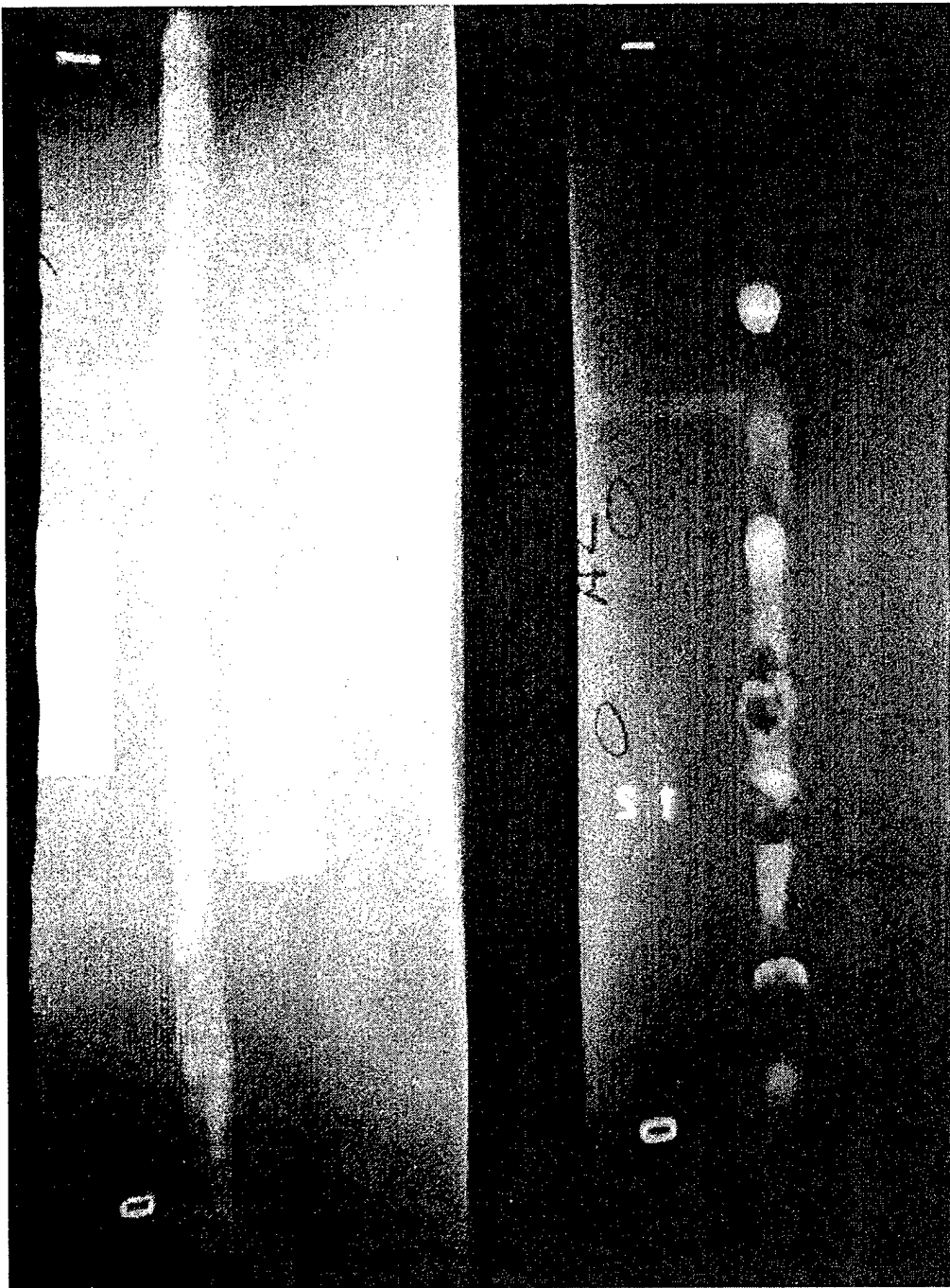


Figure 4-4: Weld A2, Section 0-1

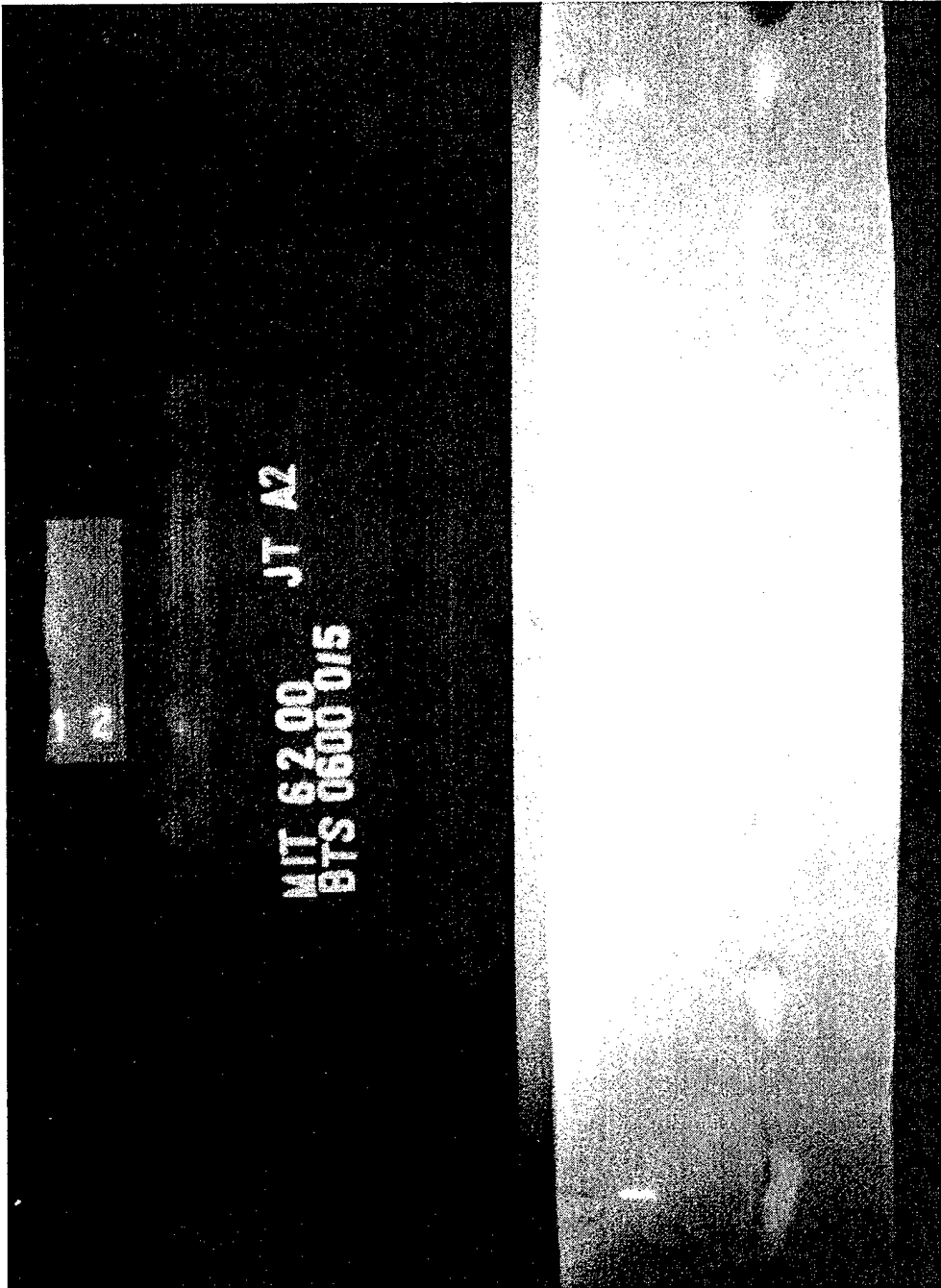


Figure 4-5: Weld A2, Section 1-2

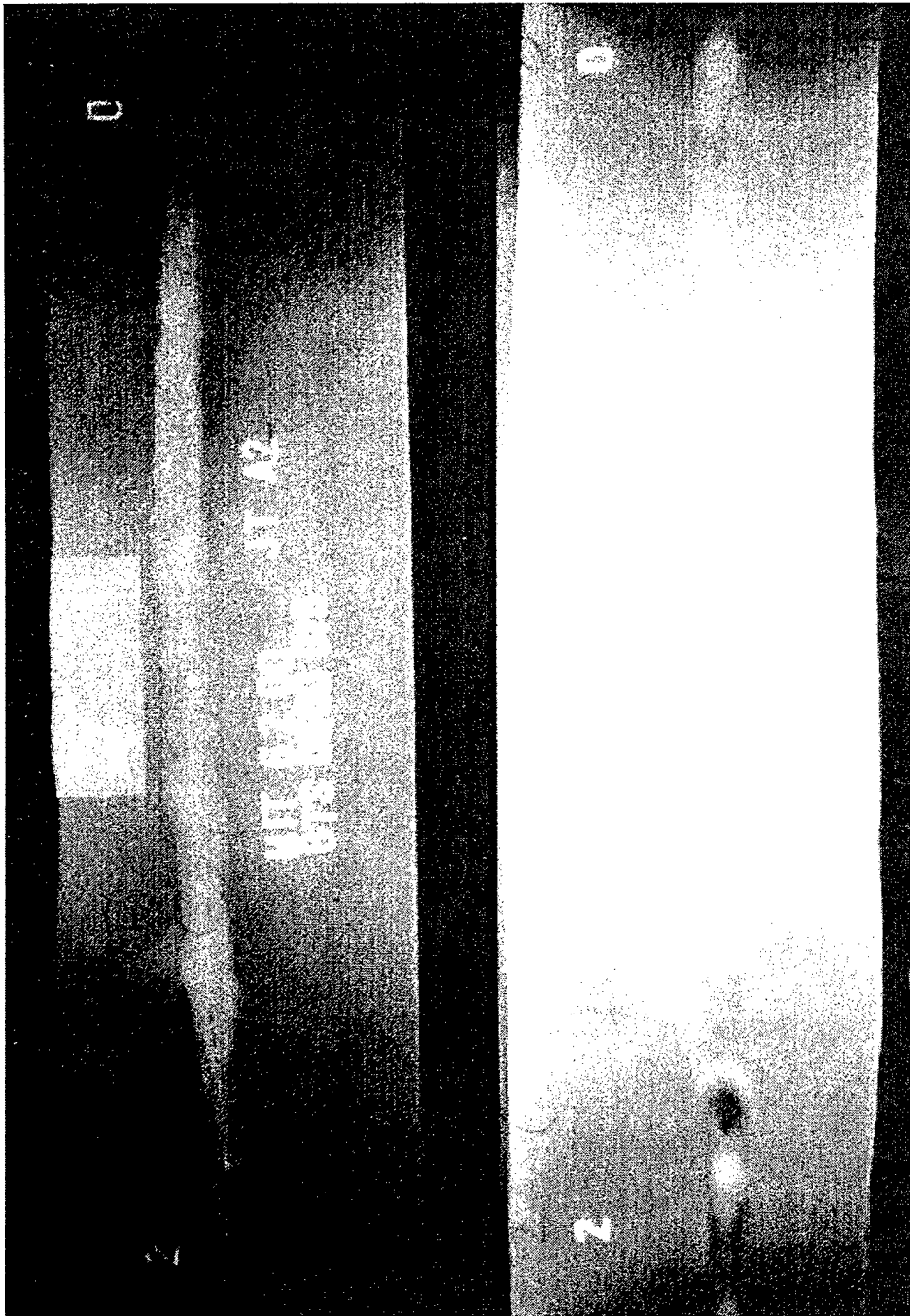


Figure 4-6: Weld A2, Section 2-0

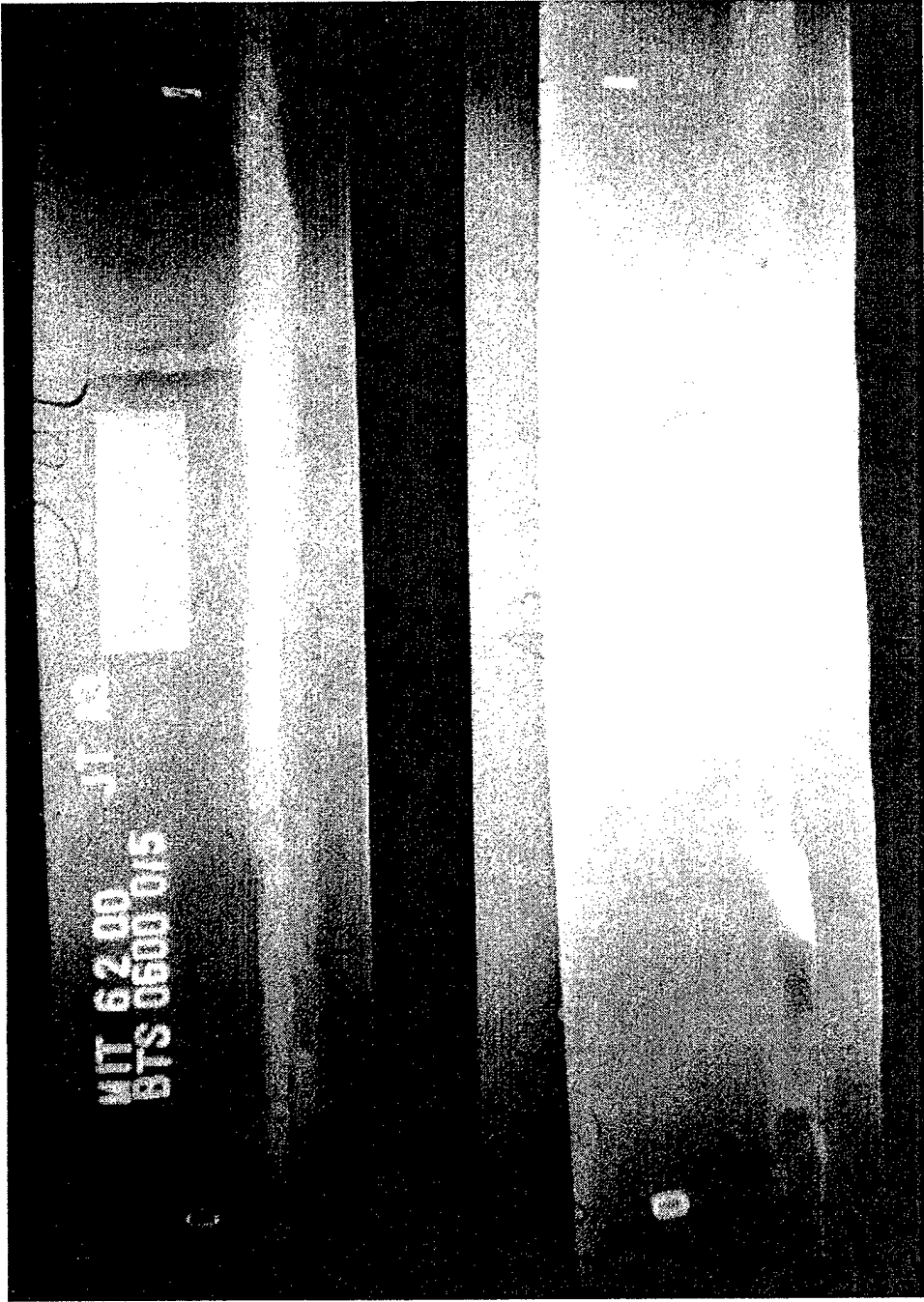


Figure 4-7: Weld A3, Section 0-1

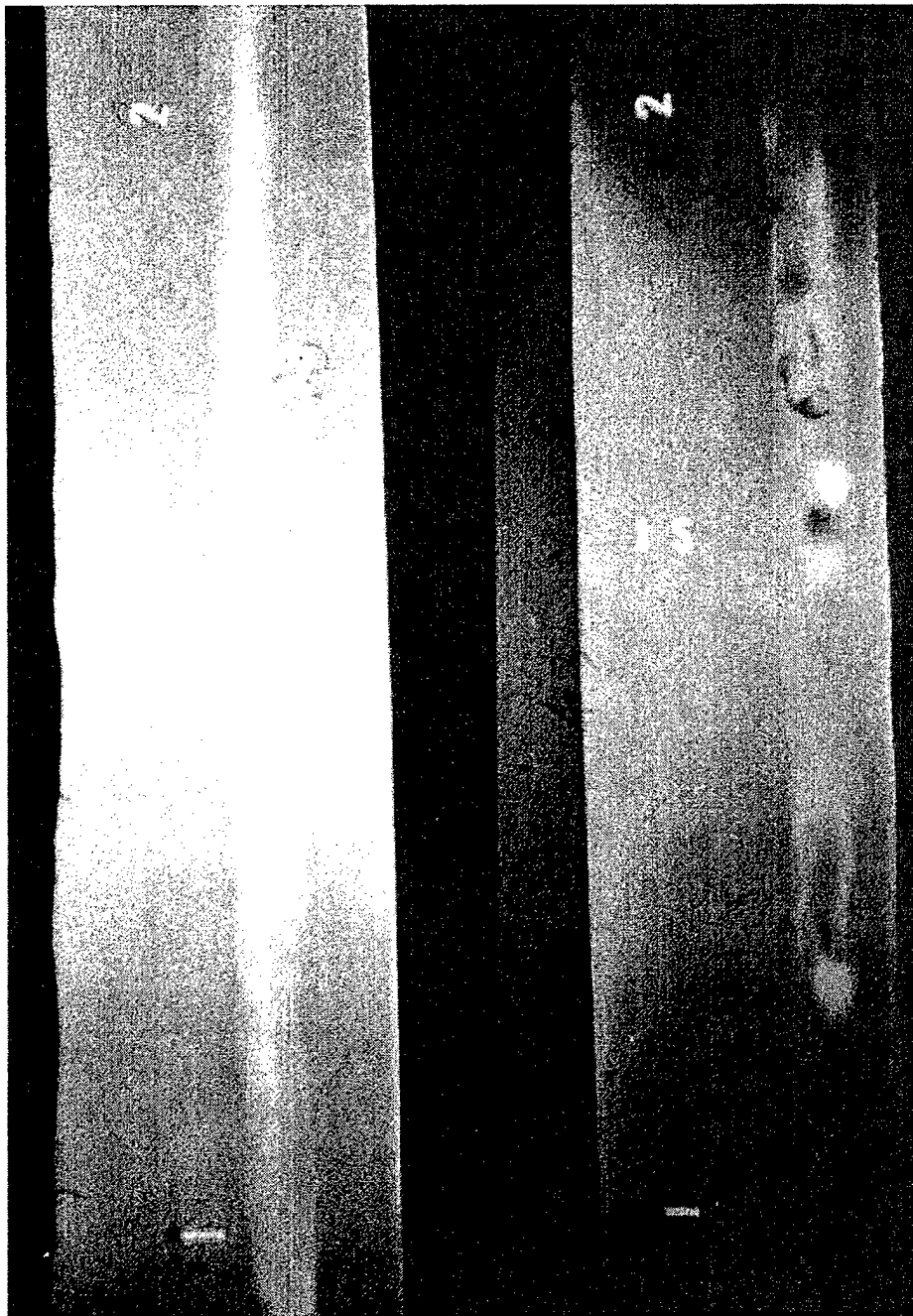


Figure 4-8: Weld A3, Section 1-2

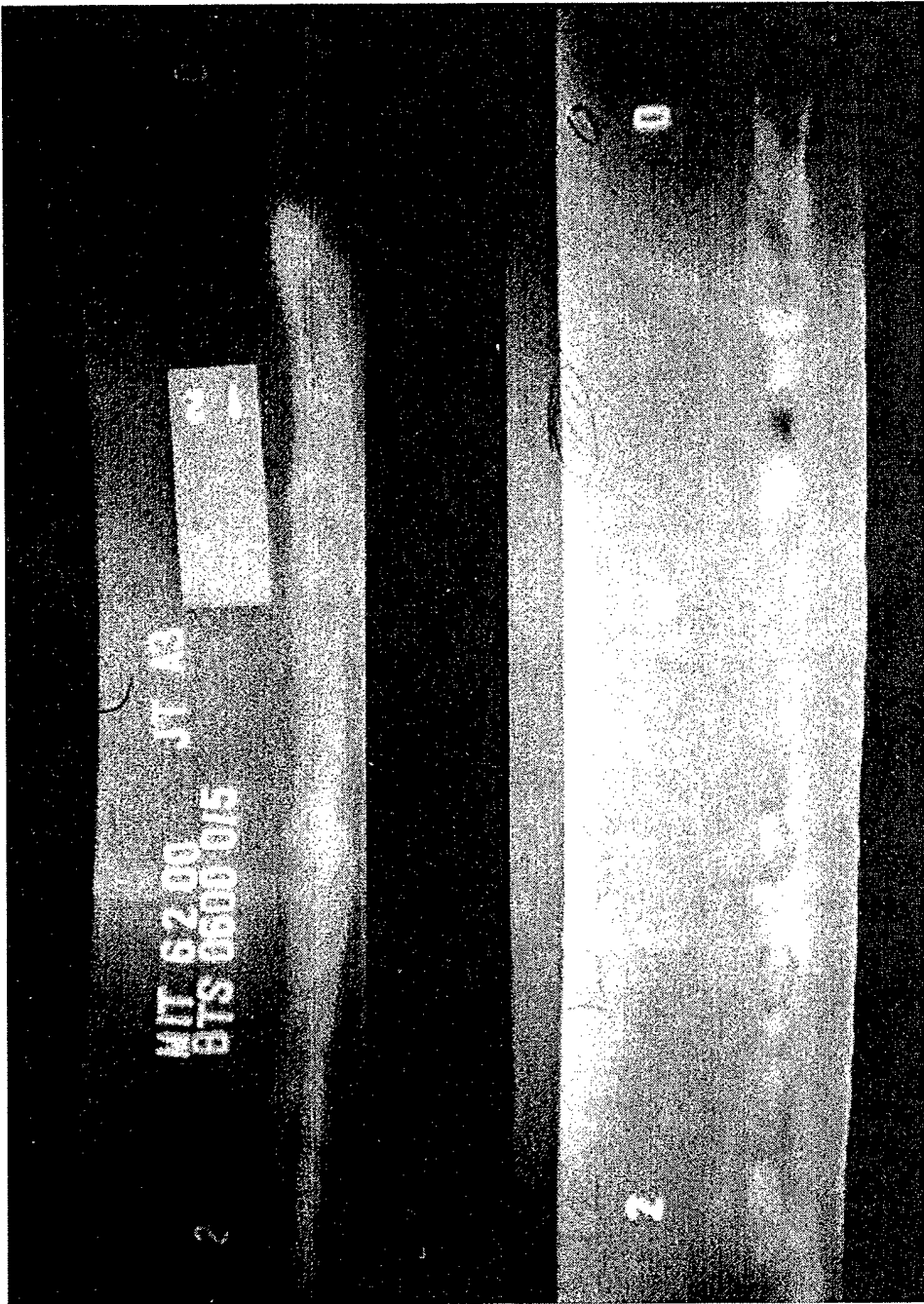


Figure 4-9: Weld A3, Section 2-0

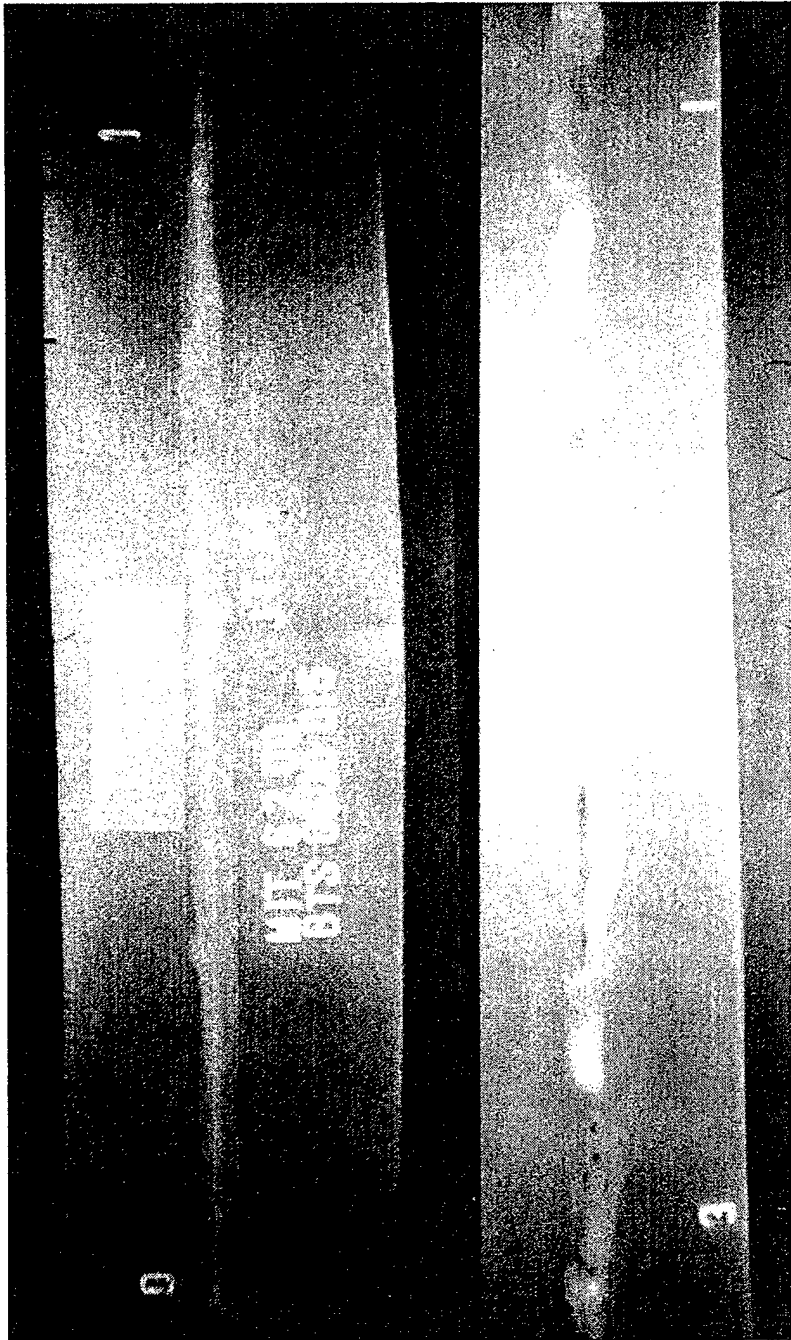


Figure 4-10: Weld A4, Section 0-1

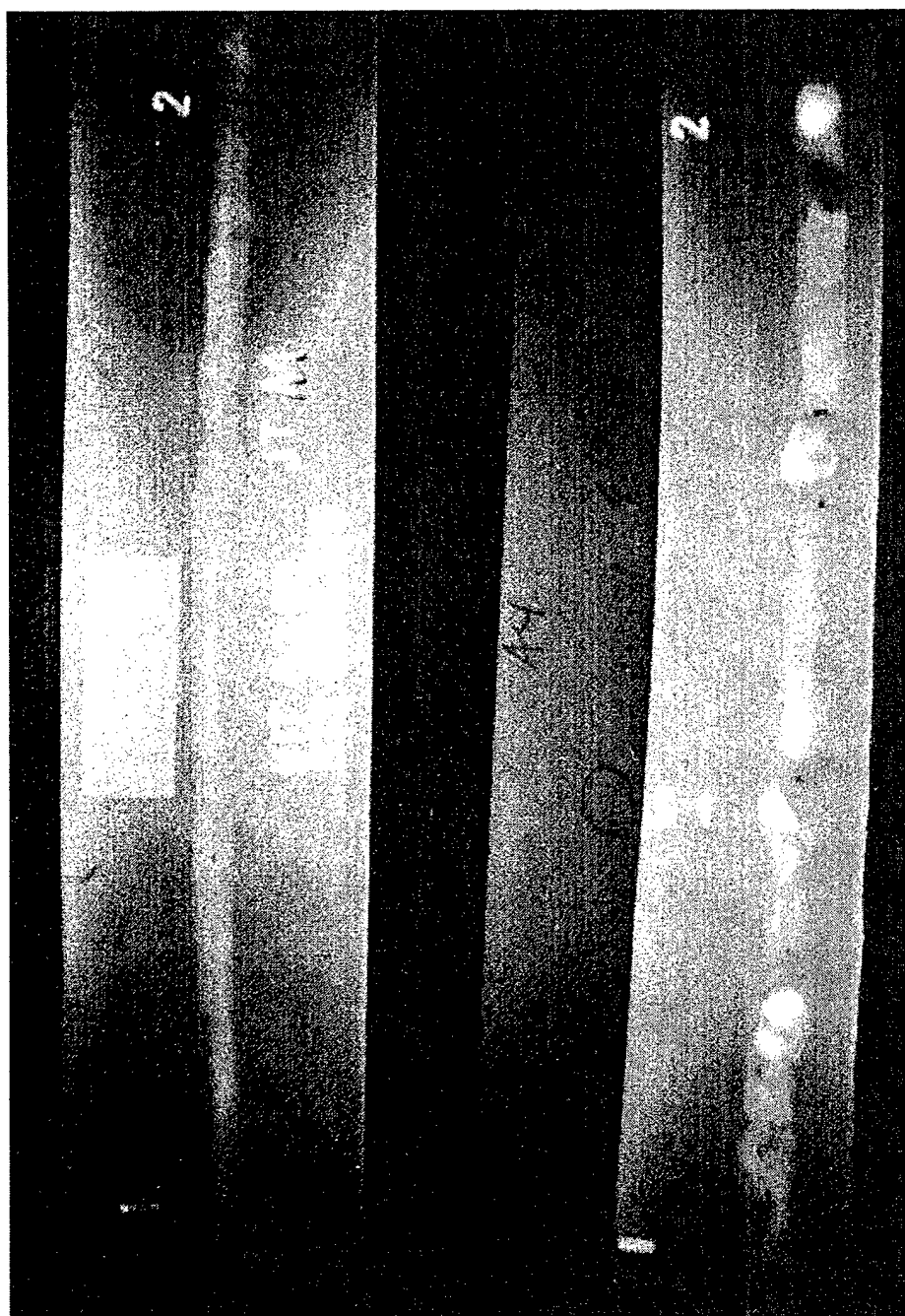


Figure 4-11: Weld A4, Section 1-2

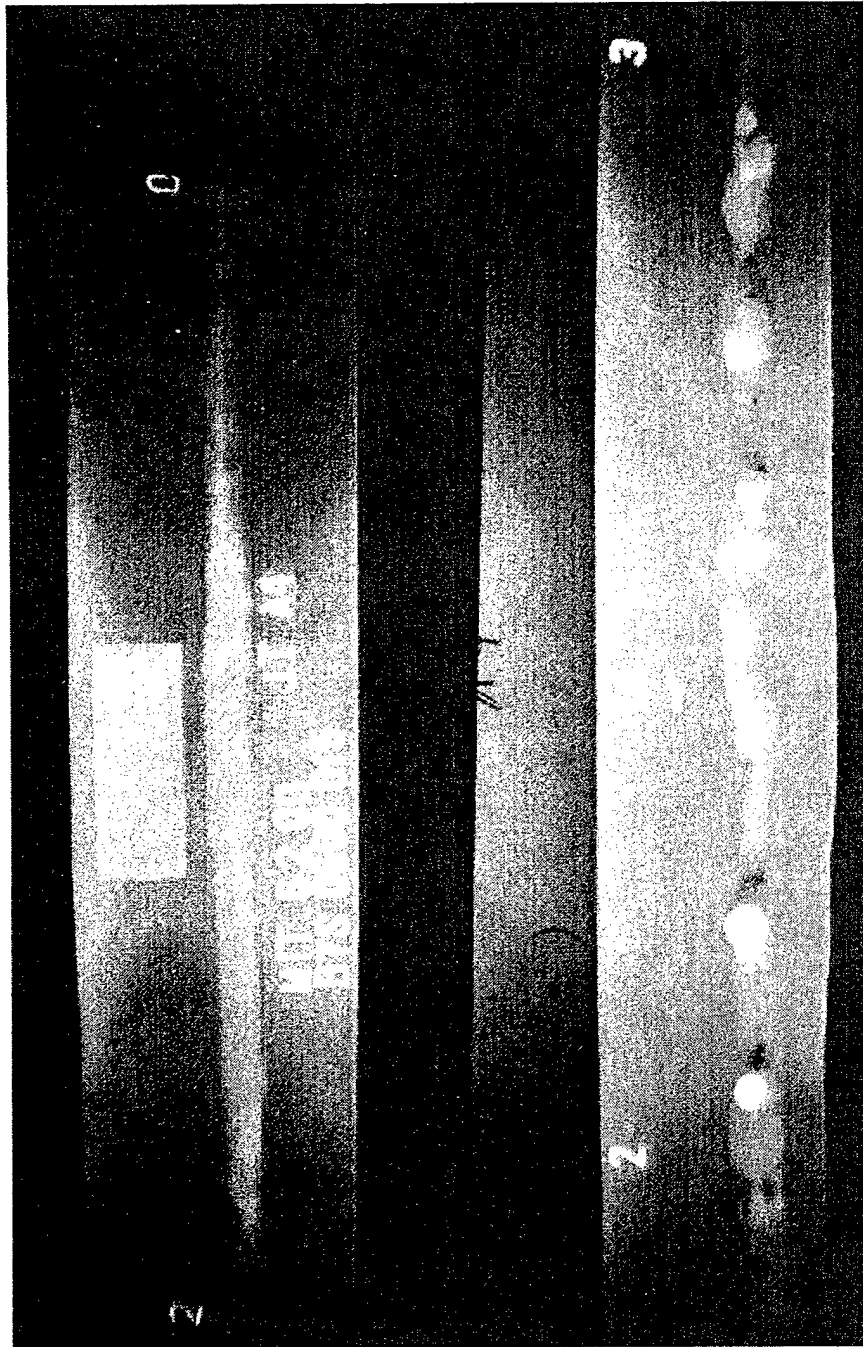


Figure 4-12: Weld A4, Section 2-0

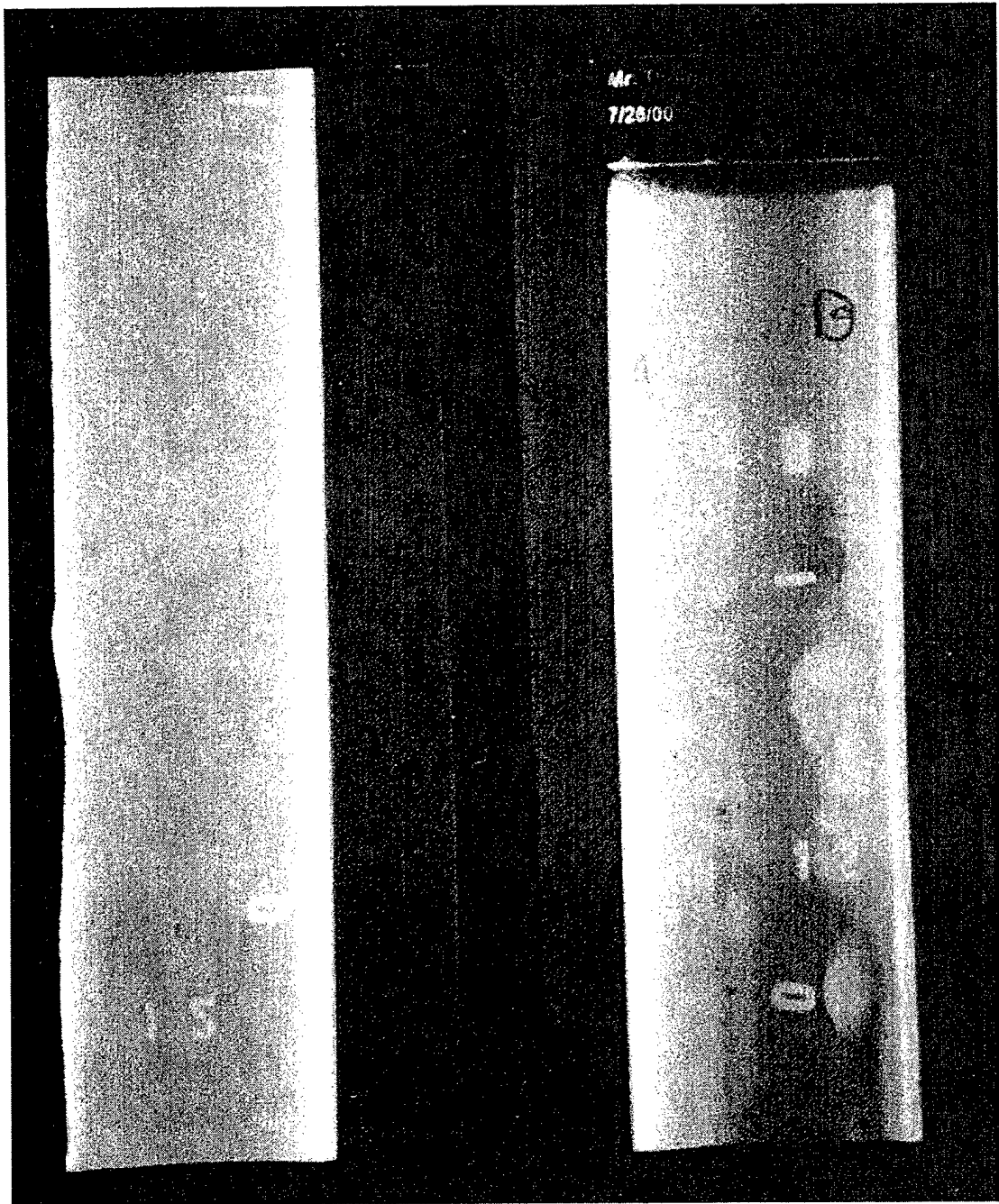


Figure 4-13: Welds C1, C2-A, C2-B

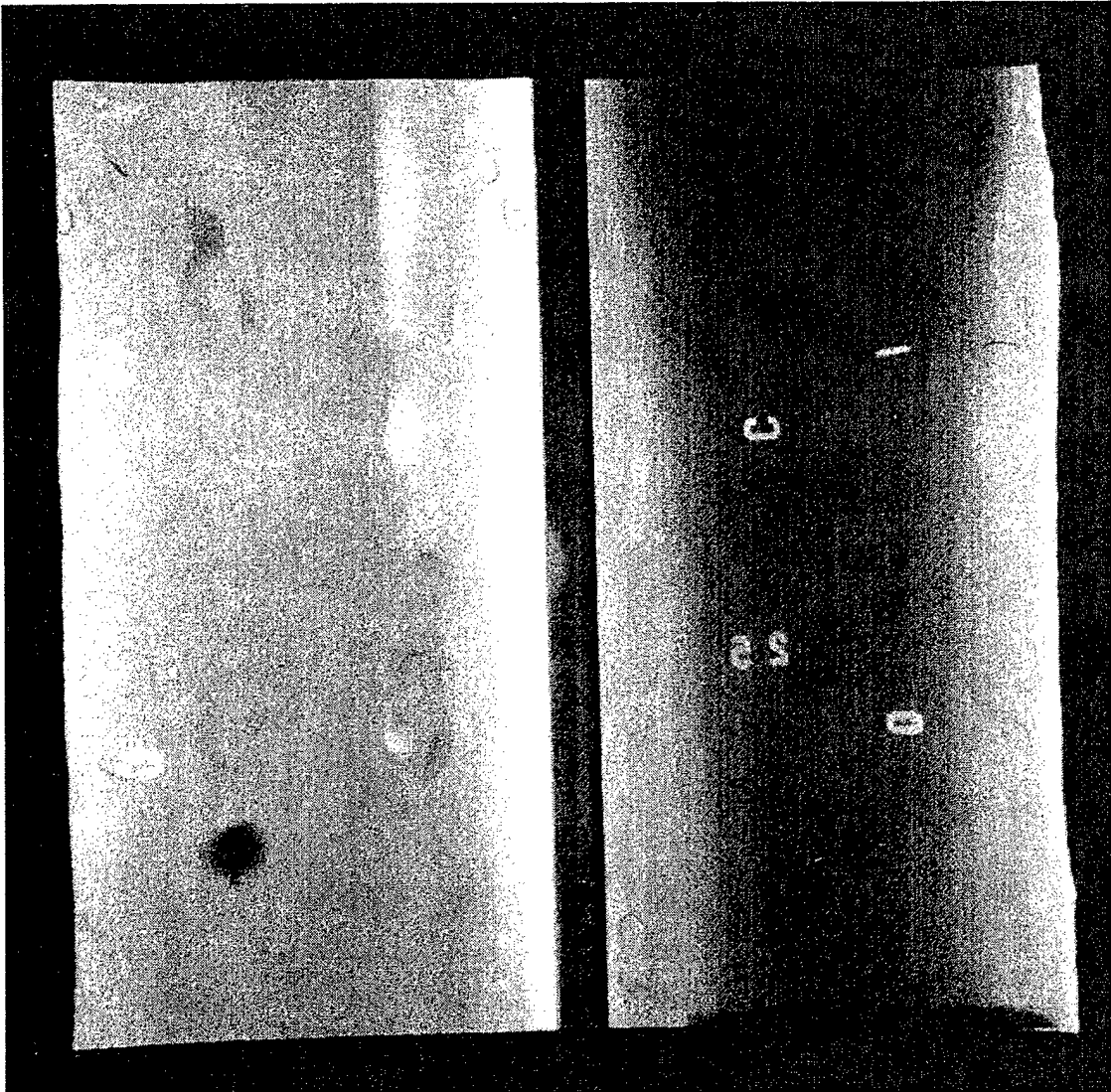


Figure 4-14: Welds C3-A, C3-B, C3-C

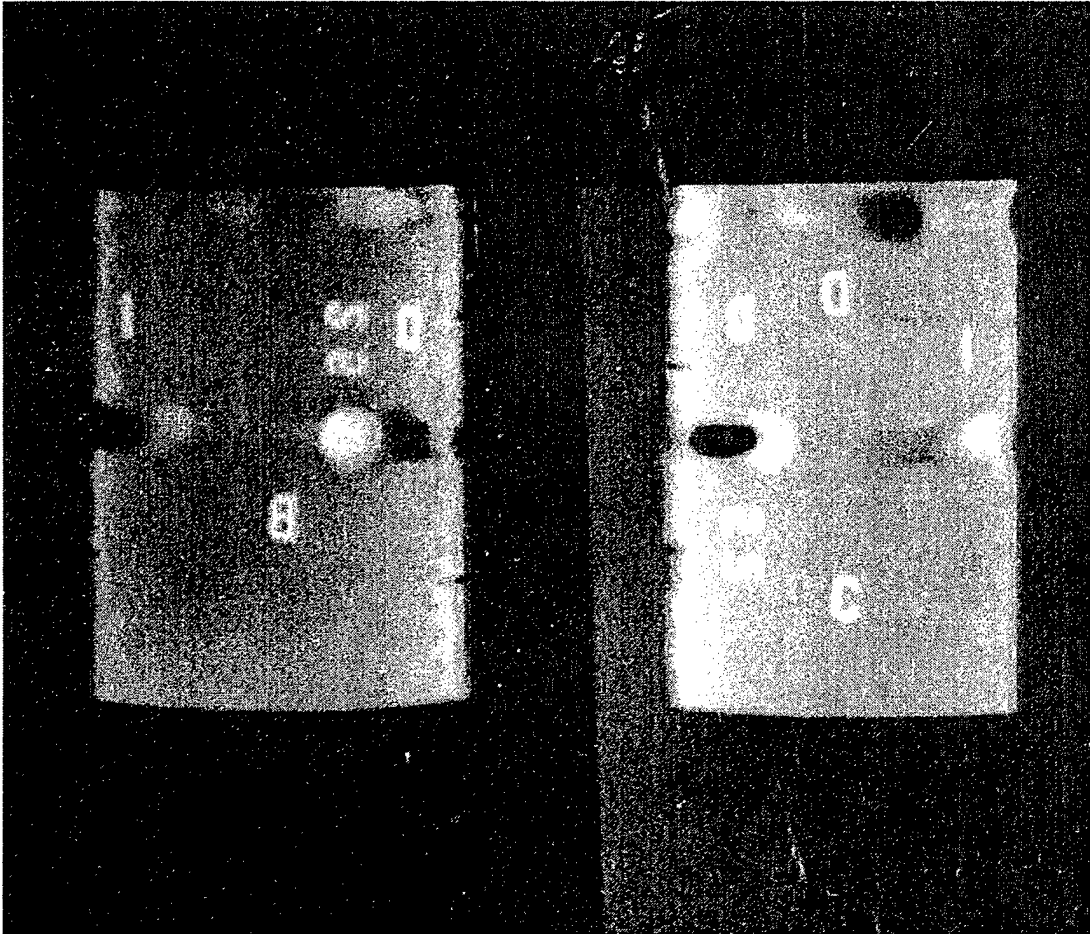


Figure 4-15: Welds C4-A, C4-B

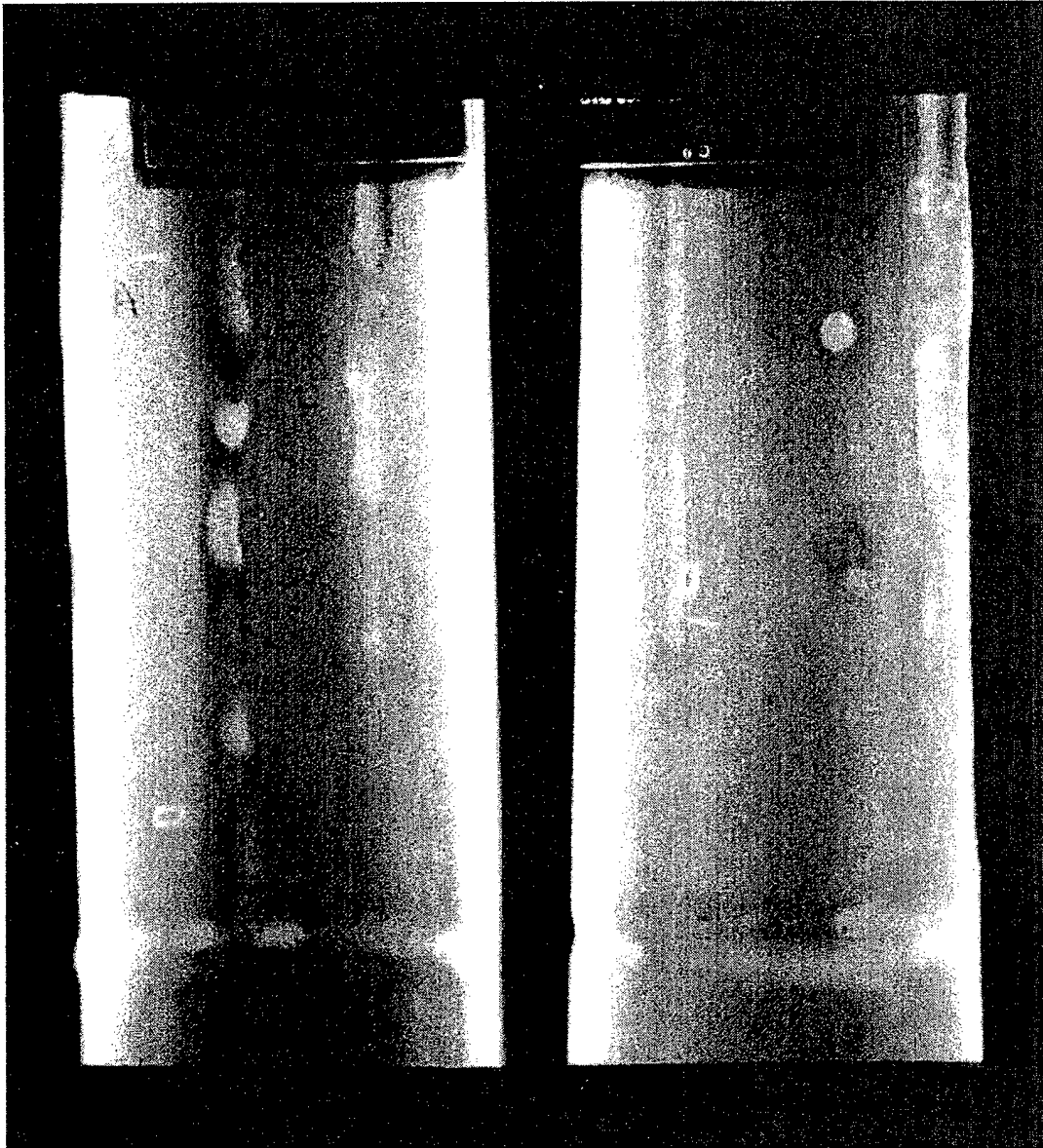


Figure 4-16: Welds C5-A, C5-B, C5-C, C5-D, C5-E

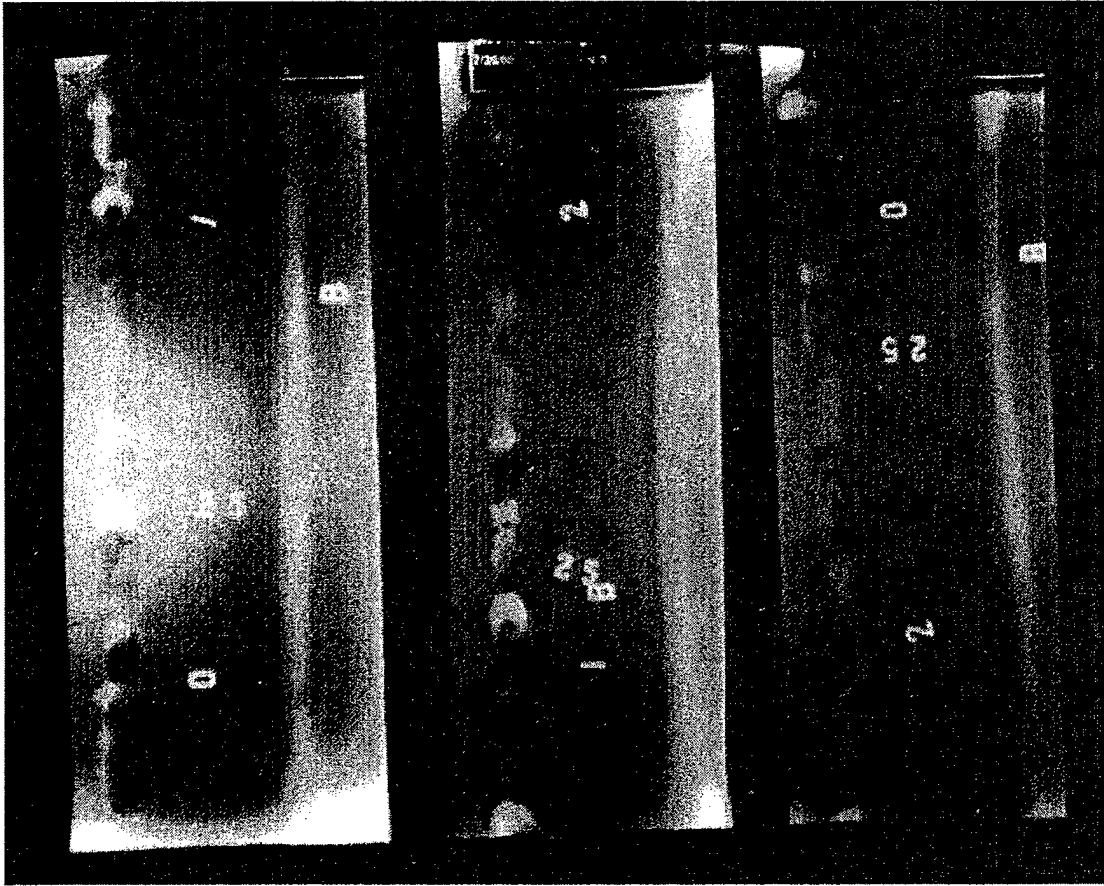


Figure 4-17: Welds C6-A, C6-B

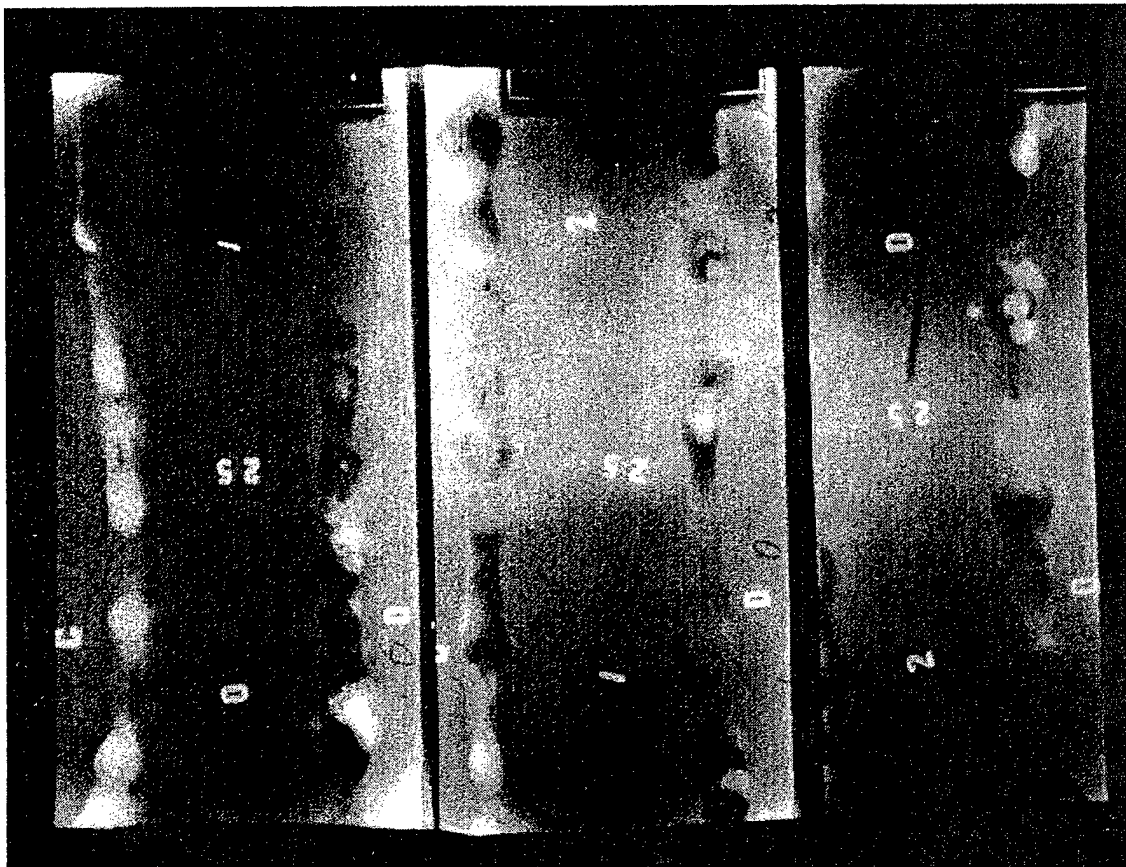


Figure 4-18: Welds C6-C, C6-D

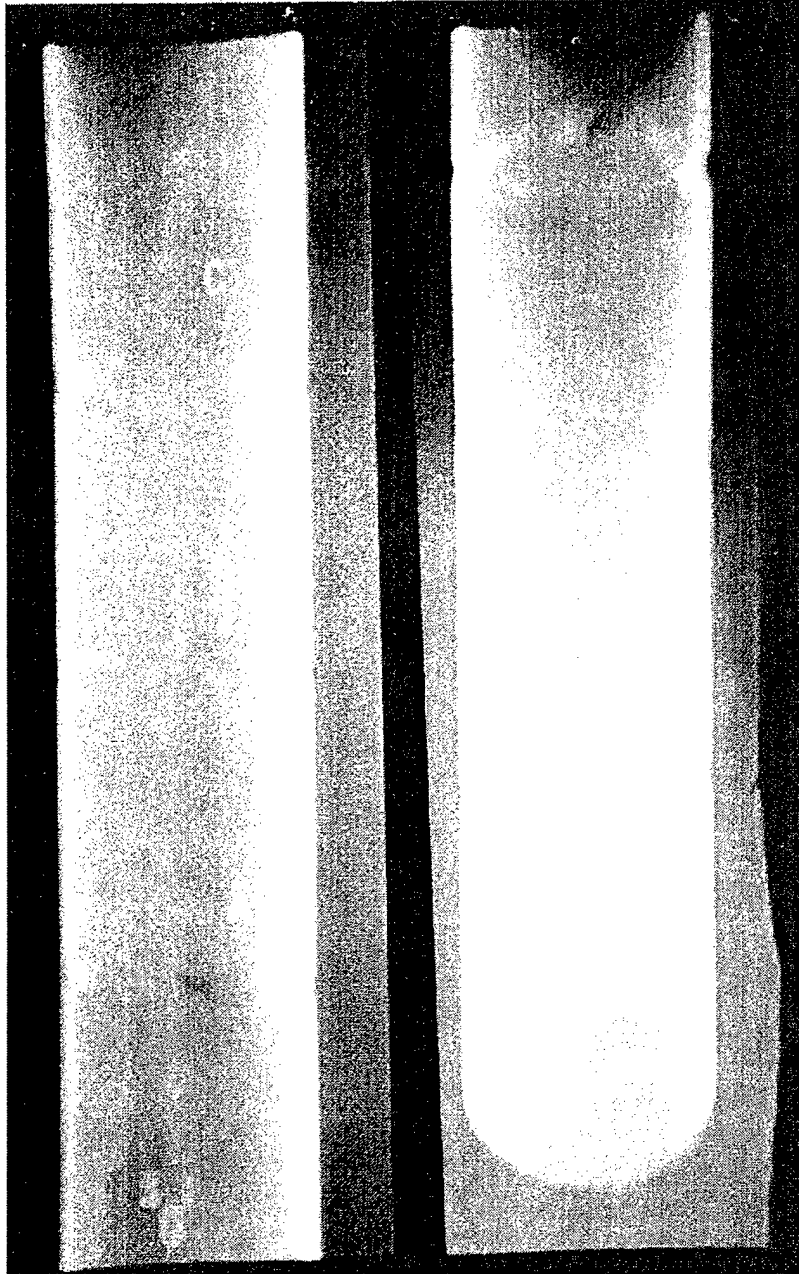


Figure 4-19: Welds C7-A, C7-B, C7-C

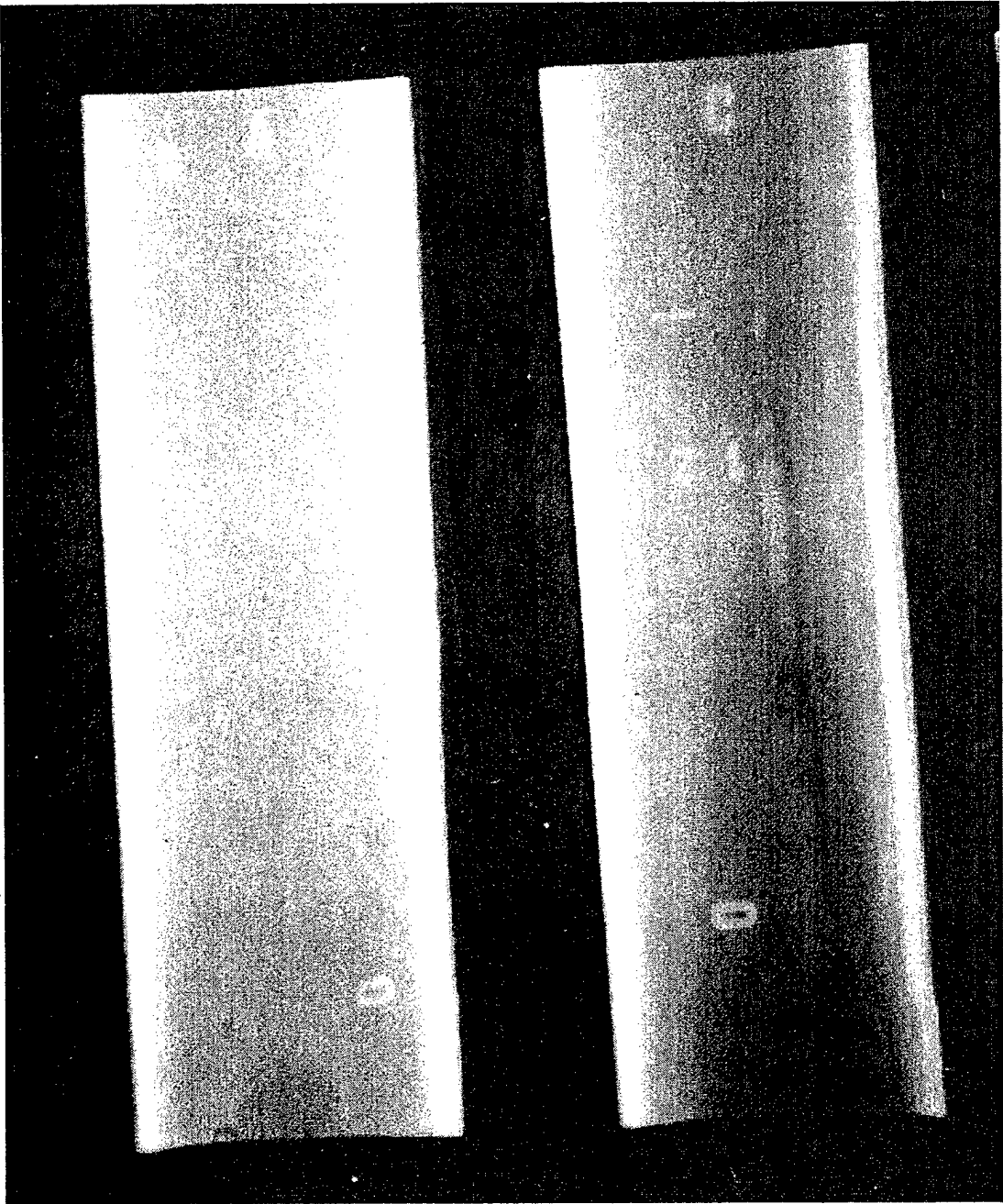


Figure 4-20: Welds C8-A, C8-B, C8-C

The testing laboratory that made the X-rays provided evaluations of the acceptability of the welds. Table 4.4 lists these evaluations. Initially, these results would appear to indicate that making welds without cleaning the root surface is not likely to yield a satisfactory weld. However, examination of the X-rays alongside the actual pipes gives a different indication.

Table 4.4 shows that the welds in pipes C1, C2, C7, and C8, the smaller pipes, are all satisfactory. These thinner sections allow easier control of the weld pool and penetration, and it does not appear that the root of the weld bead became porous due to the oxygen in the root surface. These pipes all had the least internal contamination, only light verdigris, which would help reduce the contamination of the weld. All the welds in pipes C3 and C4 were also satisfactory, though C4 showed porosity and linear indication. Examination of the pipe itself reveals that these apparent flaws are peculiarities in the surface that would be filled and covered by a cover pass. The welds in pipe C6 were unacceptable, but the flaws apparent on the X-rays were actually not serious. The porosity in weld C6-A was in the start-stop region and reflects flaws in the welder's technique. Additional proficiency would resolve this. The porosity in weld C6-C occurred in the fill material over the root pass. This probably reflects incomplete cleaning of the root pass before laying down the fill pass. The incomplete penetration and porosity in weld C6-D was in the weldment patching a burn through. Welds C5-B and C5-D were satisfactory; welds C5-A, C5-C, and C5-E were unsatisfactory due to excessive porosity. Pipes C5 and C6 had thick deposits on the interior, making these most challenging regarding inclusions and porosity.

Table 4.4 indicates that all the welds in the A-series pipes were unsatisfactory. Since these are the welds that most closely reflect the practical situation, this result would seem a conclusive condemnation of weld repair without cleaning the root surface. However, it actually shows the practical difficulty of performing this sort of repair. Examination of the X-rays in Figures 4-1 through 4-12 alongside the pipes themselves shows that whenever the repair weld lay on top of the flawed weld, and fully penetrated the pipe wall, the resultant weld is whole and not flawed. It was difficult to obtain this, however. Small misalignment was sufficient for the repair weld to miss the seam. Obtaining full penetration without burning through was a delicate matter, especially when starting the weld. Most of the incomplete penetrations are at starting points before the welder obtained full penetration. This is another facet that depends

Table 4.4: X-ray Evaluations

Weld No.	Accept	Reject	Defect Codes
A1		X	IP
A2		X	IP
A3		X	IP
A4		X	IP, P
C1	X		
C2-A	X		
C2-B	X		
C3-A	X		
C3-B	X		
C3-C	X		
C4-A	X		P
C4-B	X		LI
C5-A		X	P
C5-B	X		P
C5-C		X	P
C5-D	X		
C5-E		X	P
C6-A		X	IP, P, CV
C6-C		X	IP, P
C6-D		X	IP, P
C7-A	X		
C7-B	X		
C7-C	X		P
C8-A	X		
C8-B	X		
C8-C	X		

Defect Codes	
CV	= Concavity
IP	= Incomplete Penetration
LI	= Linear Indication
P	= Porosity

Table 4.5: EDS Analysis of Weld Root Face

Weld No	Weld/Base	Concentration, wt.%									
		O	Al	Si	Cl	K	Ca	Mn	Fe	Ni	Cu
A2, 0-1	W	23.23	1.03	1.02	0.56	*	1.45	1.64	7.32	13.40	50.35
A2, 0-1	B	18.33	1.22	0.69	1.06	*	0.84	0.47	2.14	9.81	65.45
A3, 0-1	W	8.85	1.08	1.01	*	*	*	2.05	3.52	7.96	75.54
A3, 0-1	B	15.20	1.97	*	1.60	*	0.73	*	2.97	7.81	69.72
A4, 0-1	W	20.02	1.39	1.62	*	1.36	*	1.24	3.98	8.46	61.93
A4, 0-1	B	13.02	3.78	0.32	*	0.39	*	0.70	1.79	9.62	70.39
C4-A	W	11.38	*	*	*	*	*	2.19	1.46	21.52	63.45
C4-A	B	11.86	3.00	*	*	*	*	2.01	1.87	23.58	57.68
C4-B	W	12.25	*	*	*	*	1.98	2.47	2.13	21.15	60.02
C4-B	B	11.68	*	*	*	*	2.06	2.12	2.25	24.94	56.94
C6-A	W	12.16	0.96	0.49	0.36	*	0.54	1.51	1.69	17.58	64.71
C6-A	B	20.14	2.25	0.21	1.21	*	0.36	0.54	1.42	25.19	48.69
C6-C	W	15.16	1.01	*	*	*	*	2.65	1.32	15.72	64.13
C6-C	B	15.26	1.63	*	*	*	*	0.73	1.29	25.42	55.67
C6-D	W	14.25	*	*	0.70	*	*	0.87	1.54	17.15	65.48
C6-D	B	14.08	*	*	0.91	*	*	0.72	1.56	29.31	53.42

\* = No detectable concentration

on the individual welder's proficiency. Figures 4-21 through 4-24 show close-ups of the X-rays showing locations where the repair weld did indeed fill the flawed weld. Figures 4-25 through 4-27 are photographs of the root surface of effectively repaired welds, cleaned of scale. The black lines show where the partial penetration had been; the arrows indicate the extent of the full penetration. The protruding bead has filled the crevice.

#### 4.3.2 SEM Results

The other analysis of the welds examined the composition of the root surface of the welds, the inside of the pipes. This was to determine whether the weld bead absorbed any contamination from the internal deposits. This involved SEM/EDS analysis of the surface of coupons from several welds. The evaluation took sections of the welds, cleaned them of loose scale, and analyzed the surface of the weld bead and compared it to the surface of the adjacent base metal. Table 4.5 shows these results; Appendix D contains the spectra.

Weld A2 shows little difference between the composition of the weld bead and the base metal. Weld A3 shows little difference in the common elements. The appearance of chlorine

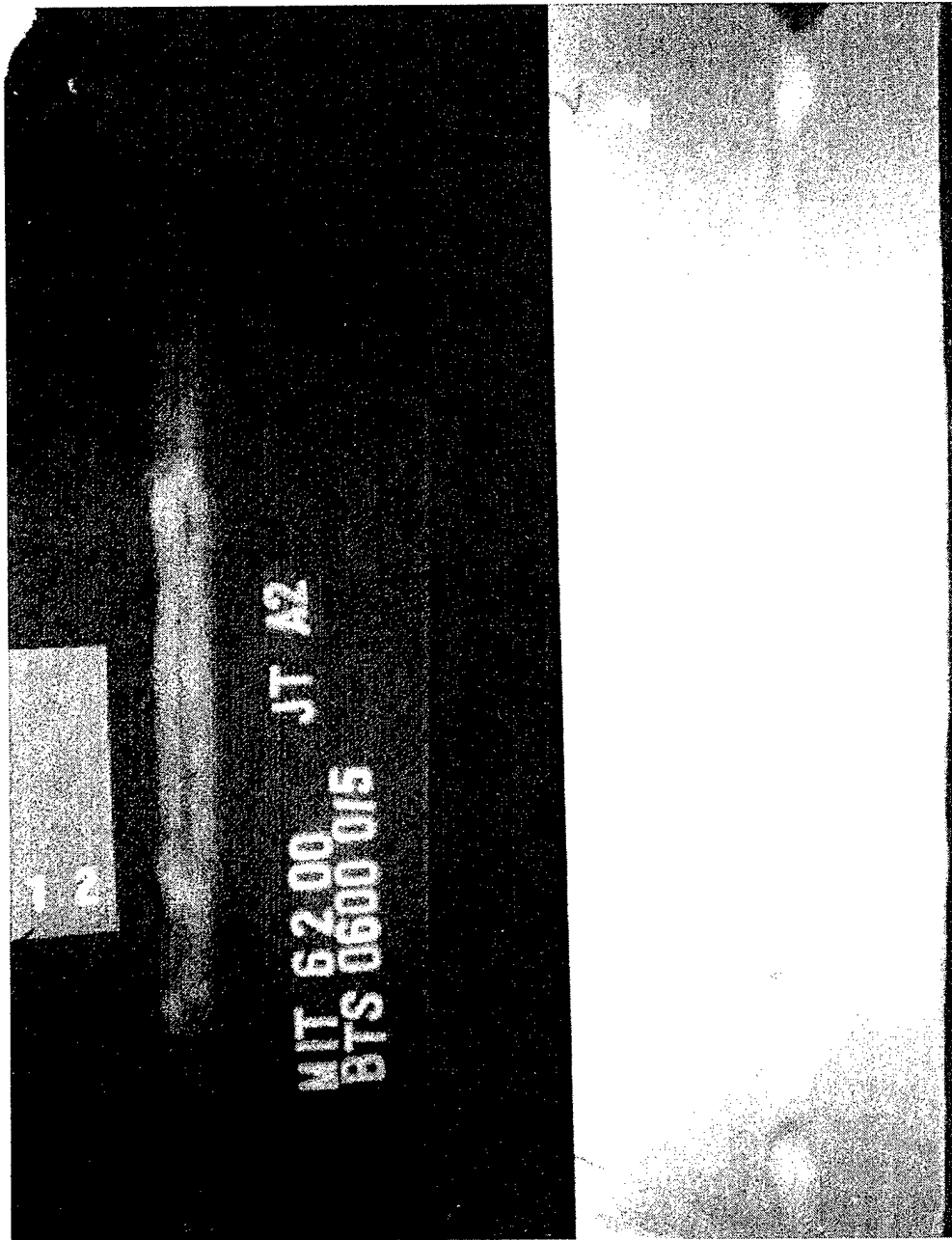


Figure 4-21: Close-up of Weld A2, Section 1-2



Figure 4-22: Close-up of Weld A3, Section 1-2

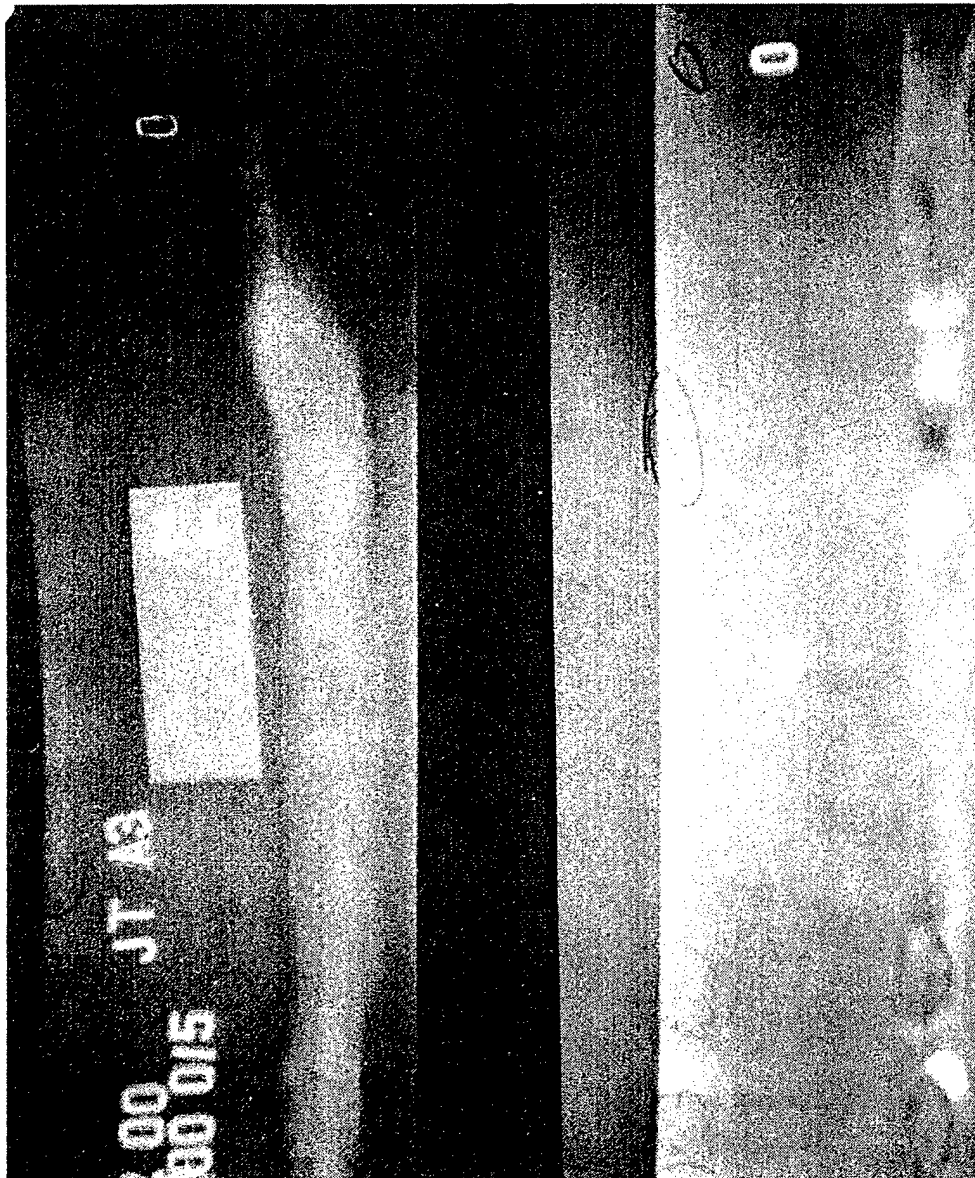


Figure 4-23: Close-up of Weld A3, Section 2-0

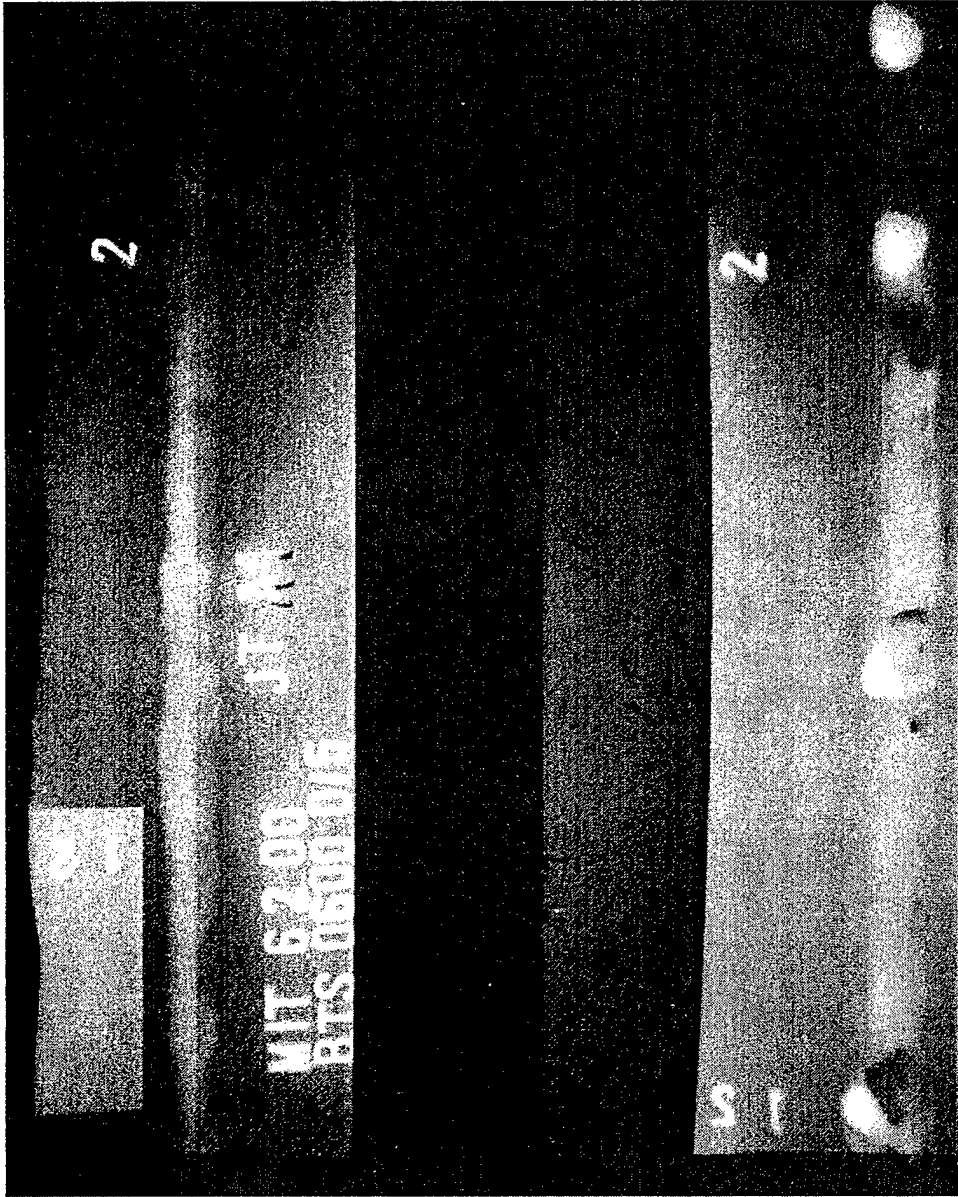


Figure 4-24: Close-up of Weld A4, Section 1-2

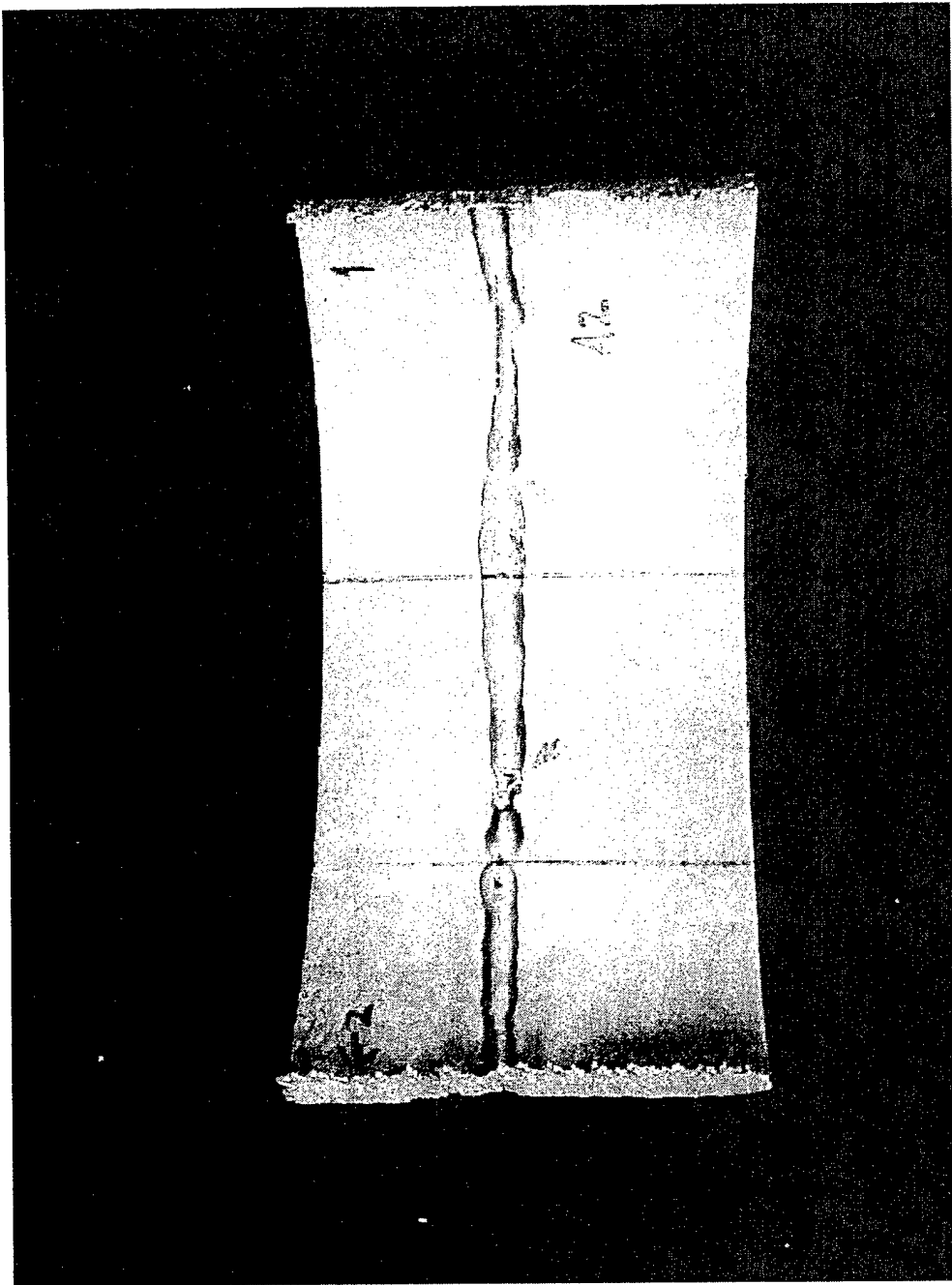


Figure 4-25: Root Face of Weld A2, Section 1-2

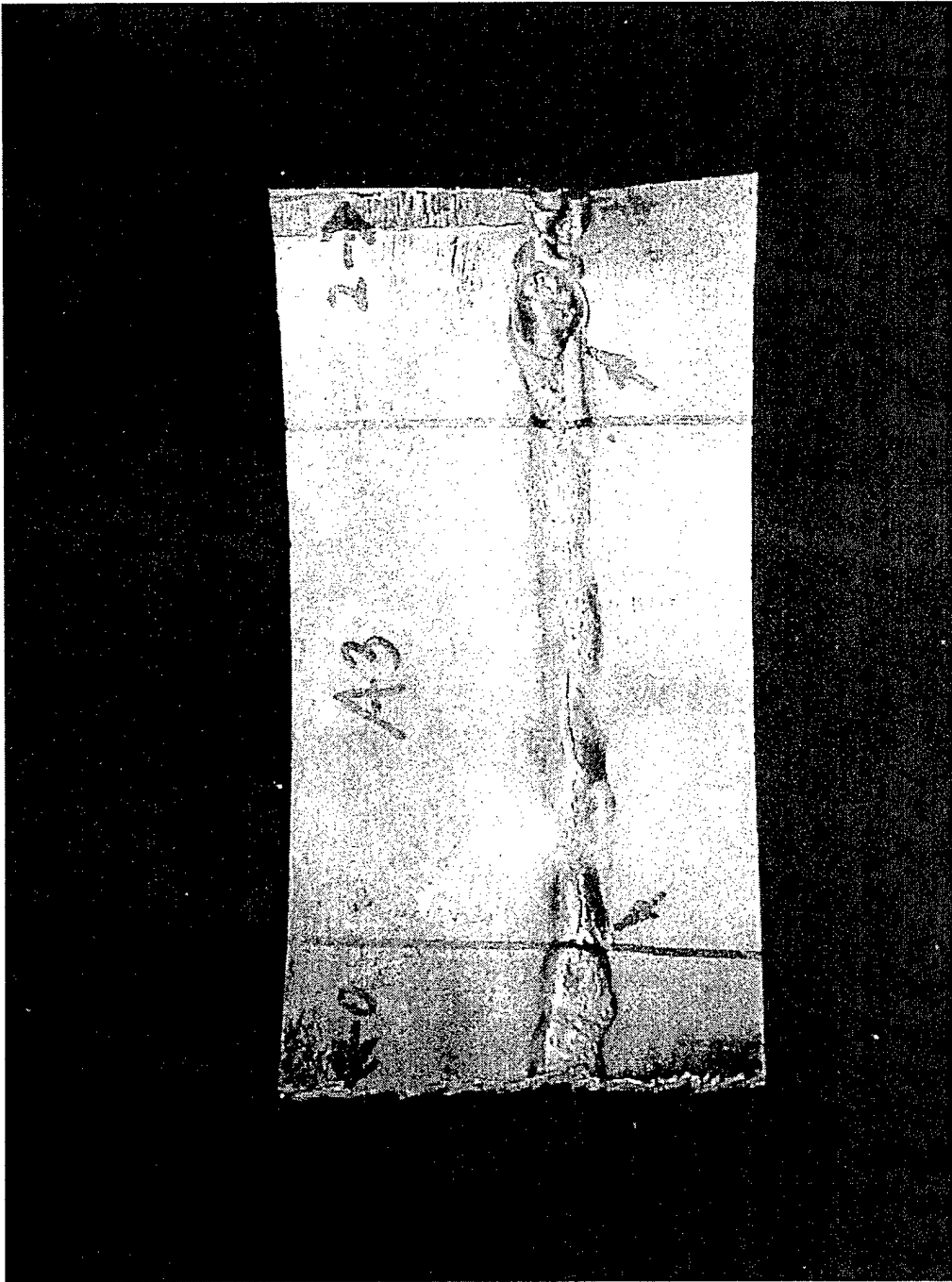


Figure 4-26: Root Face of Weld A3, Section 2-0

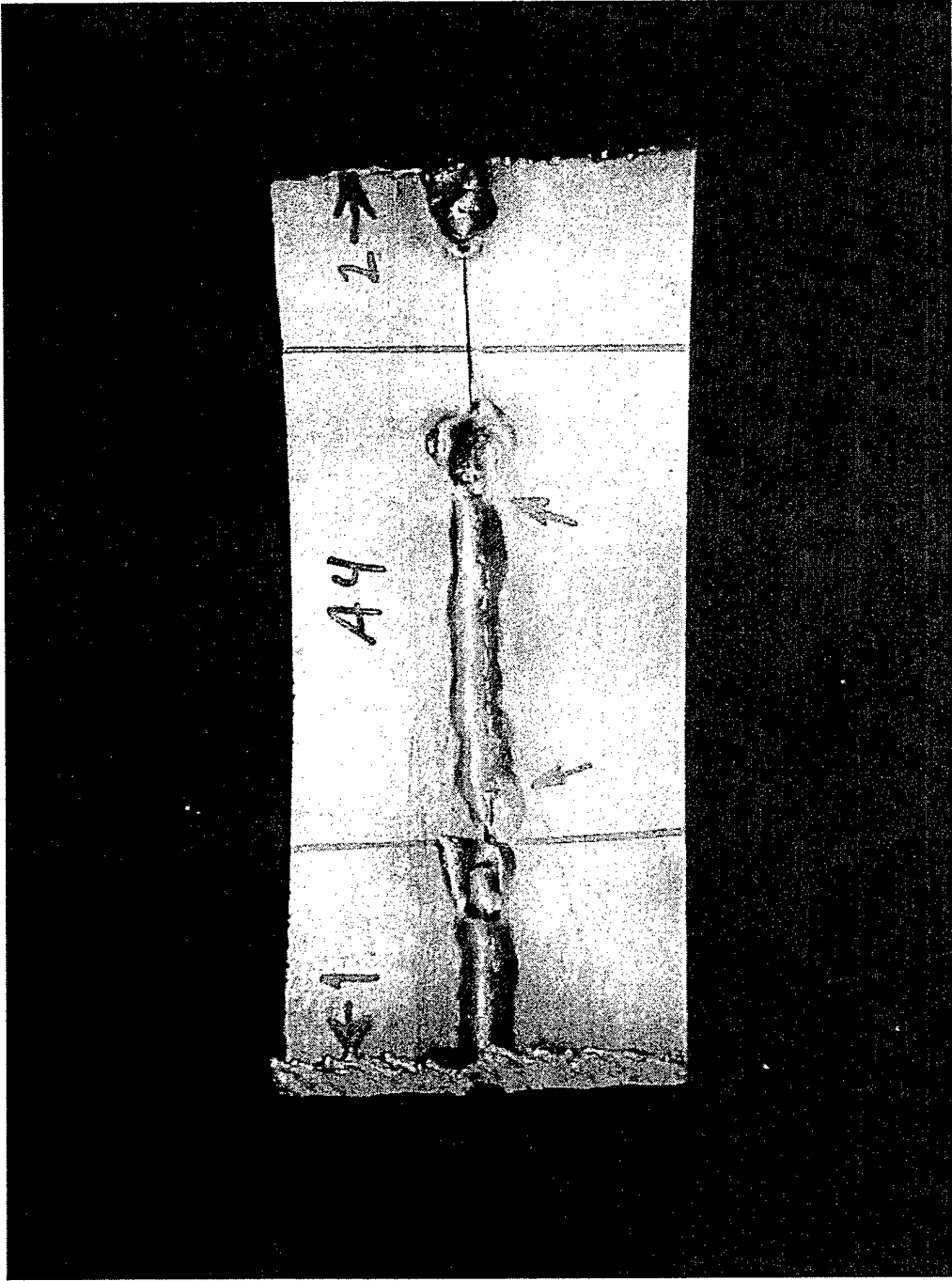


Figure 4-27: Root Face of Weld A4, Section 1-2

and calcium in the base metal is probably due to incomplete cleaning of the surface. Weld A4 shows more variation, in particular more oxygen in the weld bead, but still not significantly different. Welds C4-A and C4-B show almost no variation. Welds C6-A, C6-C and C6-D show little variation between the bead and the base metal. The most variation is in the oxygen content and manganese in weld C6-A. These results indicate that welding from a clean outside surface through an uncleaned root face does not increase the likelihood of absorbing the internal scale into the weld metal.

# Chapter 5

## Conclusion

### 5.1 Specific Conclusions

The U.S. Navy has experienced several leaks in Cu-Ni seawater piping as a result of partially penetrated welds in the ships' original construction. The current method of repairing these leaks entails cutting out the faulty weld and replacing it with new pipe, a process that is lengthy and expensive. If it were possible to repair the welds without cutting open the pipe, the Navy could realize significant cost savings on ship repair. This investigation evaluated one possible solution to this question: whether it would be possible to achieve satisfactory weld repairs by remelting the weld zone, fusing the joint through its full thickness without cleaning the interior of the pipe.

Several results were obtained:

1. The interior of the pipe carries a scale that varies in thickness and composition, consisting primarily of oxides of the pipe alloying elements and precipitated salts from the seawater, as well as biological remains. The primary elements in this scale are carbon, oxygen, magnesium, aluminum, silicon, sulfur, chlorine, potassium, calcium, iron, nickel and copper.
2. Welding through the thickness of the pipe wall, having cleaned the outer surface of the pipe, and using an inert purge inside the pipe, without cleaning the inside surface of the pipe is not more likely to cause porosity than welding into a cleaned root face.

3. EWI fluxes CN357 and CN426 increase the penetration and reduce the width of the weld pool, allowing full penetration of thicker sections in a single pass than is possible without the flux. CN426 is easier to use than CN357 and is less likely to result in porosity.
4. When the new weld pool fully penetrates the wall thickness on top of a partially penetrated joint, it is effective at sealing the joint and filling the crevice. Obtaining this result is not straightforward, since small misalignment of the repair pass can result in missing the seam, and consistent full penetration requires some skill.
5. The repair bead does not have significantly different elemental composition than the base metal, indicating that the bead is not likely to absorb the surface contamination.

These results show that it is possible to repair partially penetrated welded joints in Cu-Ni seawater pipe by remelting the weld zone. It is necessary to clean the outer surface of the pipe and provide an inert purge gas inside the pipe. Welder proficiency and skill are important in obtaining a consistent full penetration weld without burning through. Weaving the torch during the repair pass will create a wider bead that is more likely to cover the faulty joint. A full penetration pass leaves the surface of the weld bead below the surface of the surrounding metal; fill and cap passes would cover this. EWI flux CN426 can assist in the repair by making the weld pool more controllable, and by requiring lower current.

## 5.2 Recommendations

This conclusion is limited to welds made in controlled circumstances, in the 1G, or flat position. Additional investigation is necessary to determine the effect of gravity on penetration when welding in the 5G or 6G position. Practical evaluation is necessary as well to determine the importance of welder skill in satisfactory execution of this method of repair. These future investigations should make autogenous welds in various sizes of pipe in all positions, using welders with a variety of skill levels. This should encompass the probable spectrum of skill and array a pipes present in a pipe repair shop. The evaluation should lead to development of specifications for repair of partially penetrated weld joints by remelting the weld zone.

## Appendix A

# X-Rays of Pipe Segments A1, A2, A3, and A4

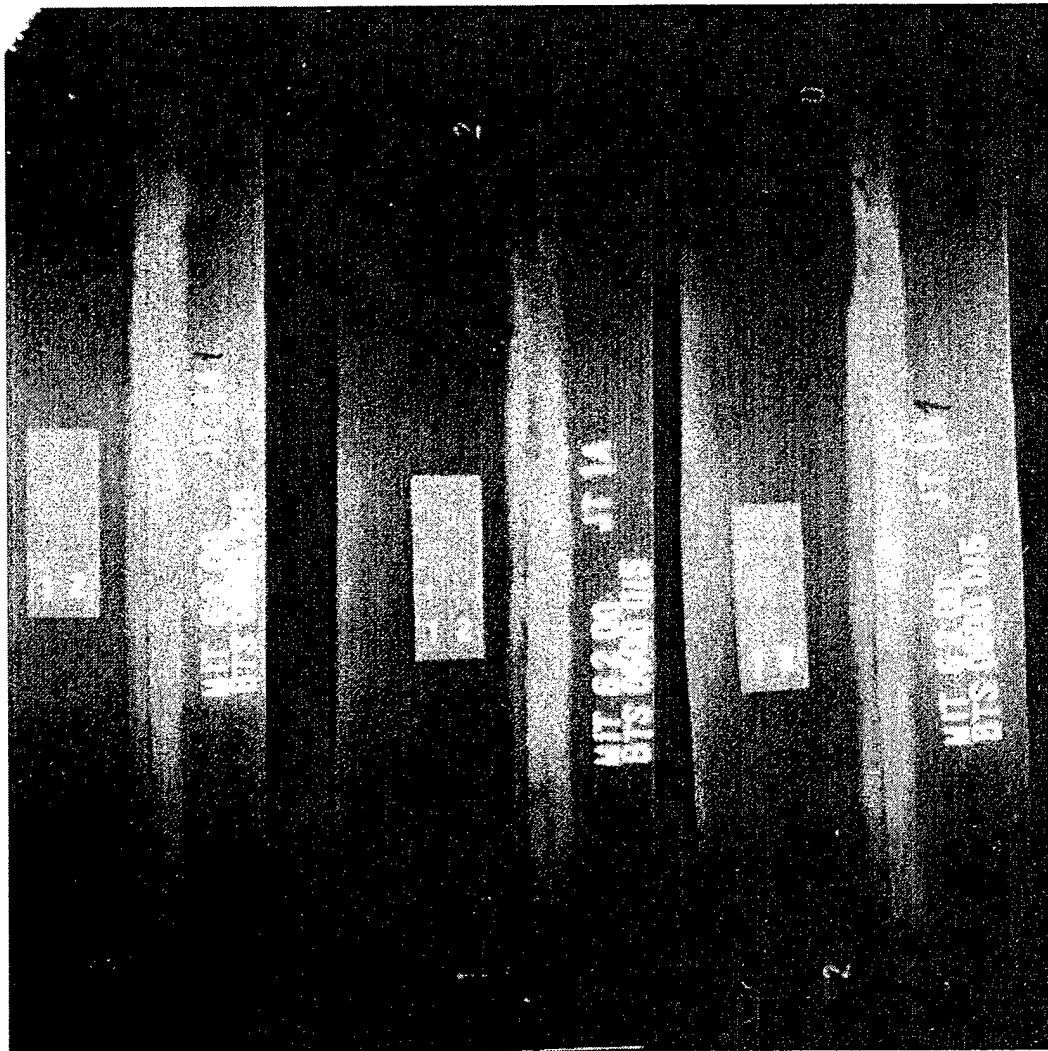


Figure A-1: Weld A1 Before Repair

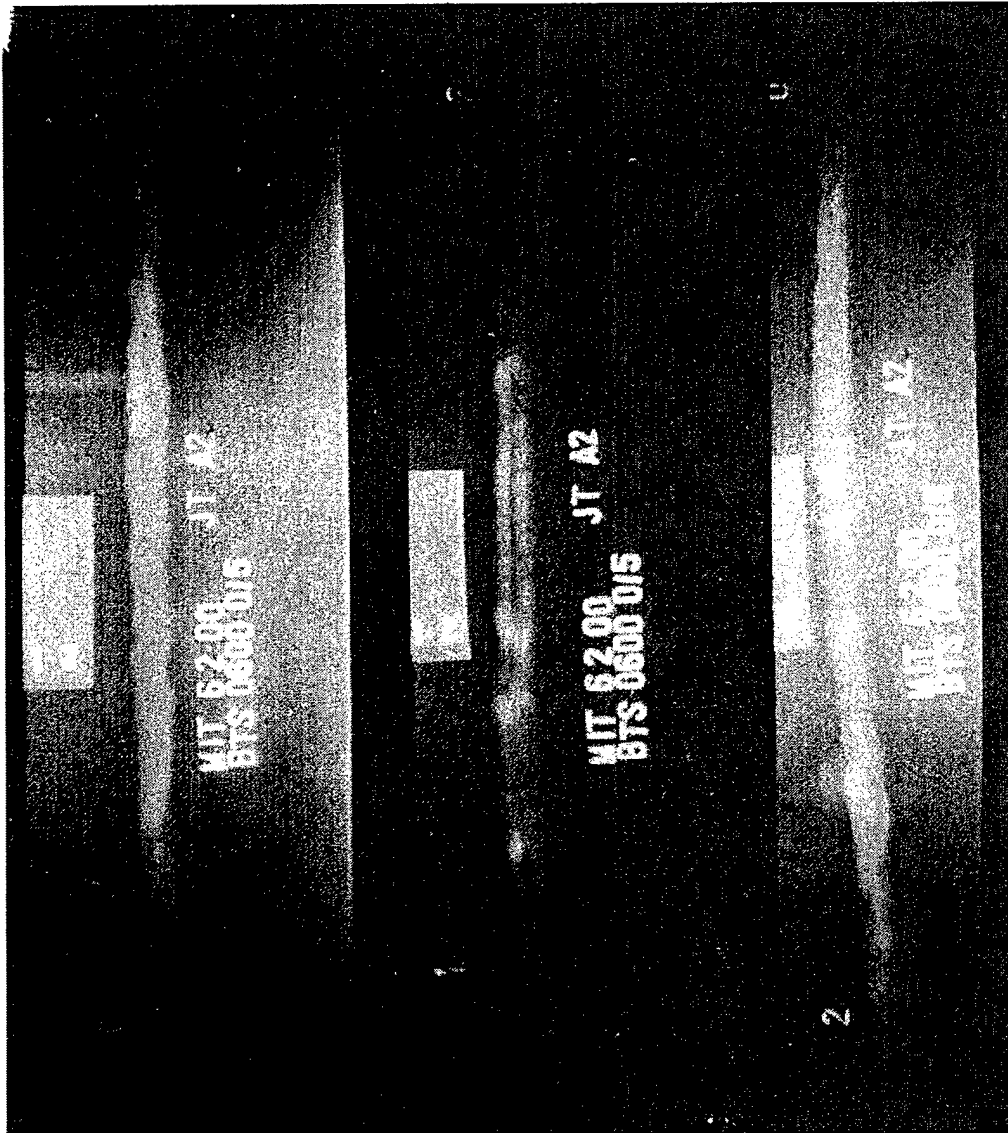


Figure A-2: Weld A2 Before Repair

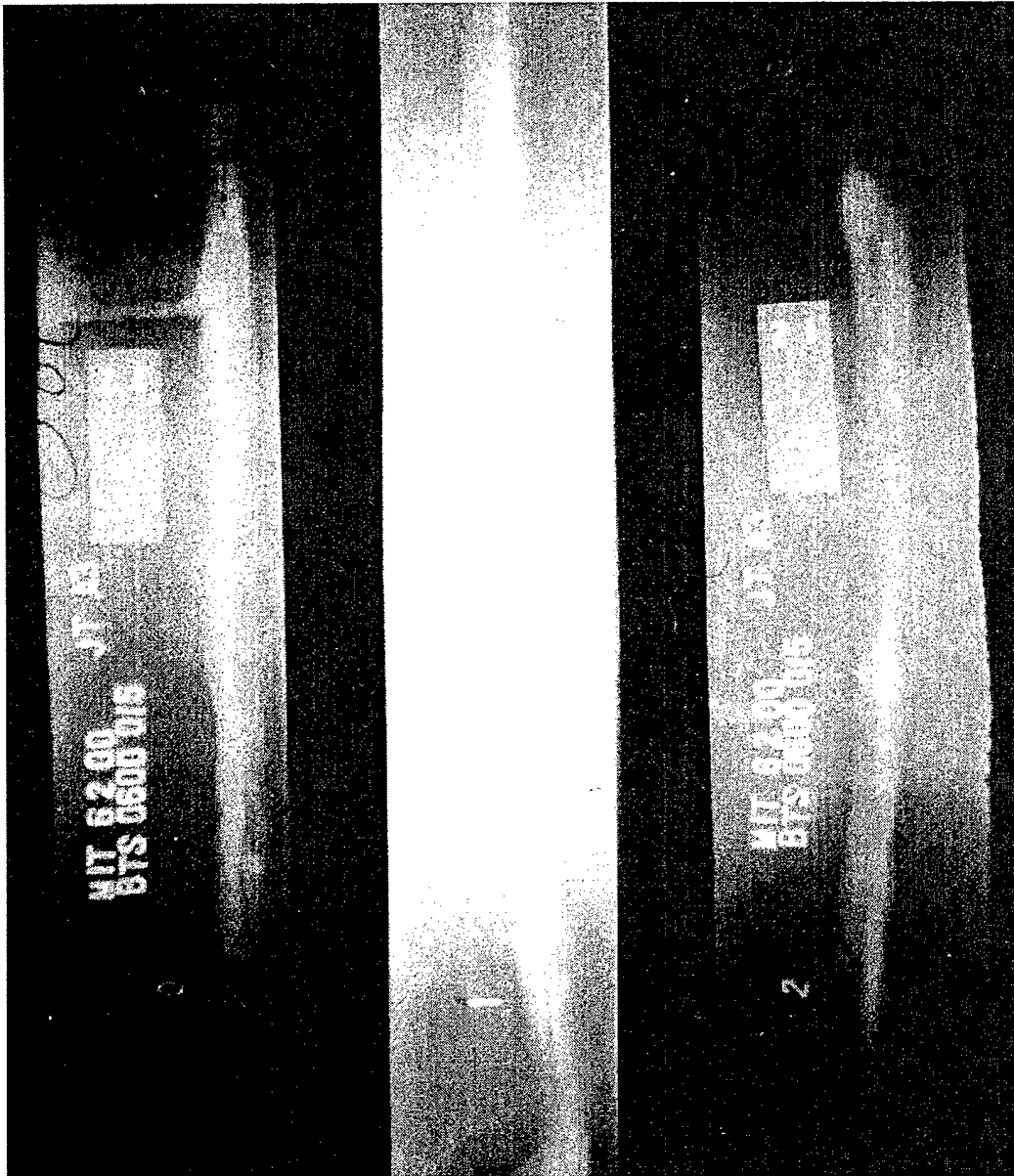


Figure A-3: Weld A3 Before Repair

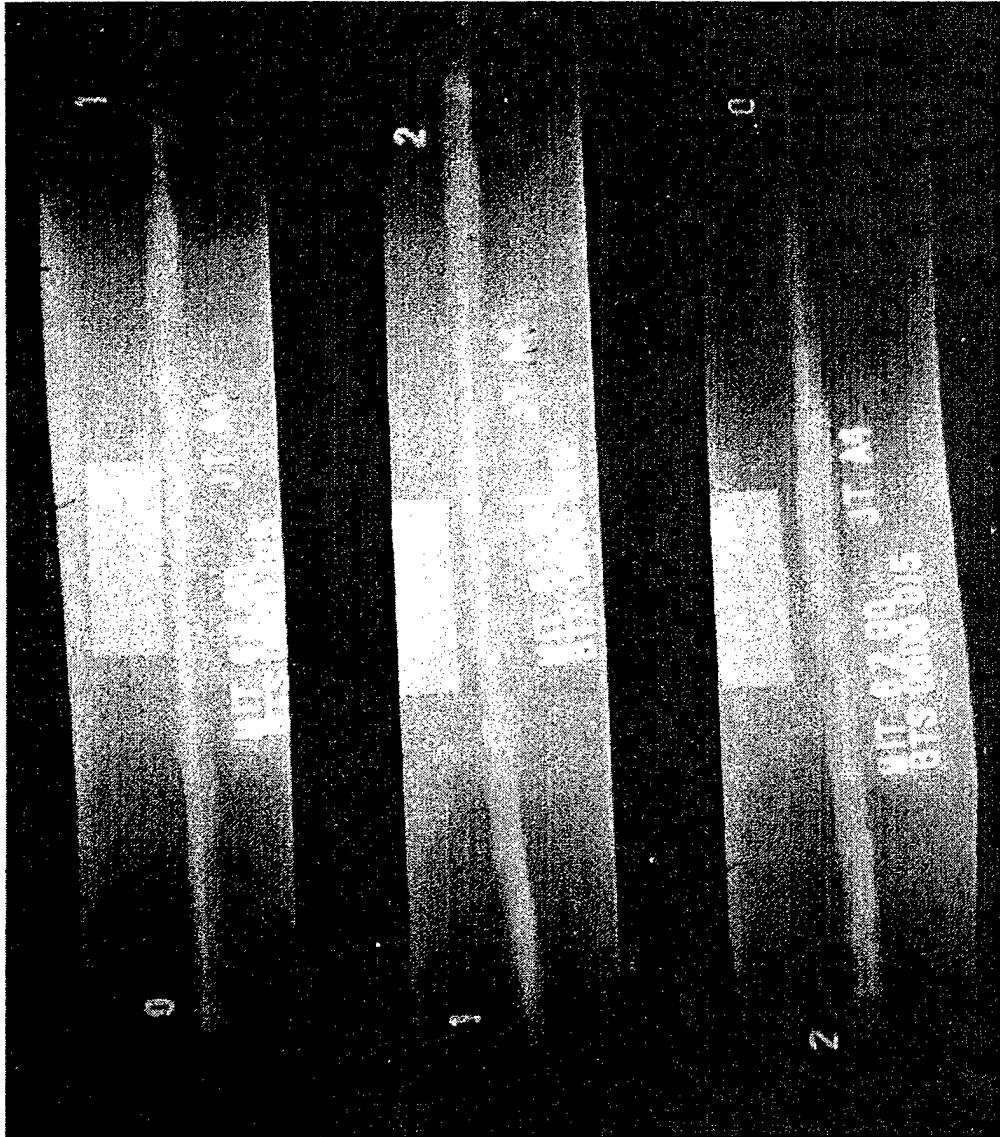


Figure A-4: Weld A4 Before Repair

## Appendix B

# SEM and EDS Operation

The SEM is an imaging device that uses electrons to form the image much as a light microscope uses light to form the image. Electrons have much shorter wavelengths than photons,  $0.5\text{\AA}$  vice  $2000\text{\AA}$ , so the SEM can provide much higher magnification than the light microscope. The theoretical limit of the SEM is more than  $800,000\times$ ; practical limitations of the instrument itself limit magnification to  $\sim 75,000\times$ , with a resolution of  $40\text{\AA}$ . This compares to the light microscope's limits on magnification and resolution of  $2000\times$  and  $2000\text{\AA}$ . An EDS evaluates X-rays that are emitted by a specimen in a SEM to give information about the elemental composition of the sample. [6]

### B.1 SEM Operation

The SEM comprises four basic subsystems:

1. An illuminating system which produces the electron beam, directing it onto the sample.
2. An information system that uses a variety of detectors to collect and analyze the information coming from the bombarded sample.
3. A display system that provides for observing and photographing the sample.
4. A vacuum system to remove gases from the SEM interior, so they do not degrade the image, contaminate the SEM components, or compromise the SEM's operation.

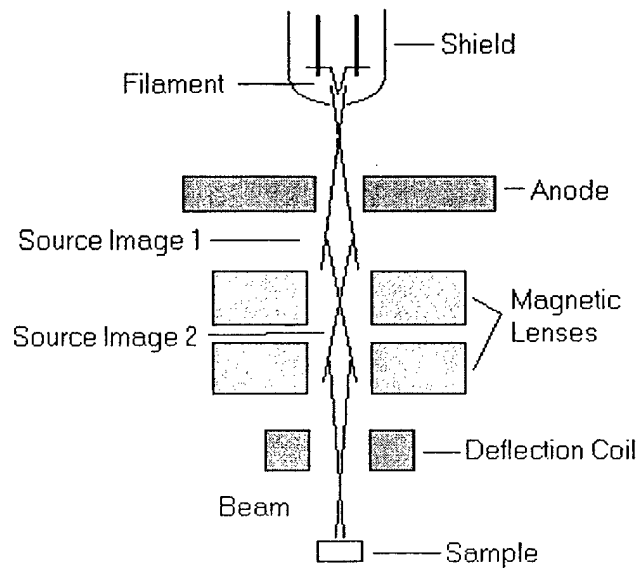


Figure B-1: SEM Cross-section

The electron beam originates from a filament, a hairpin-shaped wire of tungsten or lanthanum hexaboride which emits electrons when heated by a flowing current. A shield surrounds the filament. It is held at a positive potential relative to the filament and collimates the electrons through a hole centered over the filament tip. The electron beam passing through the shield is accelerated by the anode which is held at a very positive potential relative to the filament. The anode acts as an electrostatic lens, directing the beam to the sample. The beam passing through the anode is 25,000 to 50,000Å in diameter, too wide for effective imaging. A series of magnetic lenses below the anode compresses the beam to  $\sim 100\text{Å}$ , and focuses the image. After compression, a deflection coil moves the beam in a rectangular scanning pattern, synchronized with the display system. Figure B-1 shows the arrangement of these components.

[6]

## B.2 EDS Operation

When the electron beam hits the sample, the sample radiates several types of information depending on the interaction between the electrons and the sample atoms. Some beam electrons collide elastically with sample nuclei producing back-scattered electrons which provide topographic and compositional information. Other electrons collide inelastically with sample electrons to produce secondary electrons, which provide topographic information, and X-rays, light, and heat. Measurement of each variety of radiation requires a particular detector. The interactions occur within an excitation volume that extends 100 to 200 $\mu\text{m}$  below the surface of the sample. The depth of this volume depends on the atomic weight of the sample: higher weight means less penetration. The various signals emanate from different depths within this volume. Secondary electrons originate closest to the surface, backscattered electrons originate deeper, X-rays originate deepest. Backscattered electrons essentially rebound directly from the much more massive nucleus with nearly as much energy as before the collision, exiting with slight angular deflection from the incoming beam. The compositional information arises because the probability of a backscattering event depends on the nucleus mass. Low mass nuclei are less likely to backscatter the electrons than high mass nuclei. The resultant image will show brighter areas where heavier atoms backscatter more electrons and darker areas where lighter atoms backscatter fewer. [6]

Secondary electrons result when a sample atom absorbs the incoming electron, becoming a negative ion. It returns to neutral by emitting a secondary electron. The secondary electron has much lower energy than the incoming electron did, so it can be drawn into the detector by a positively charged cage, providing an image of the surface. Sometimes the atom returns to neutral by emitting an electron from an inner electron shell, leaving the atom in an excited state. To return to its lowest excitation level, an upper shell electron must fall into the vacancy, emitting an X-ray in the transition. The energy of this X-ray is equal to the energy difference between the two shells, which is unique to a given element. Figure B-2 portrays a Bohr model of the atom and shows the X-rays resulting from a variety of transitions. The electron shells are designated K, L, M, N, from the closest to the nucleus to the furthest. X-rays from a given shell have different energy depending on the source electron shell and the particular electron within the shell. So, a  $K\alpha$  X-ray results from an L to K transition, a  $K\beta$  X-ray

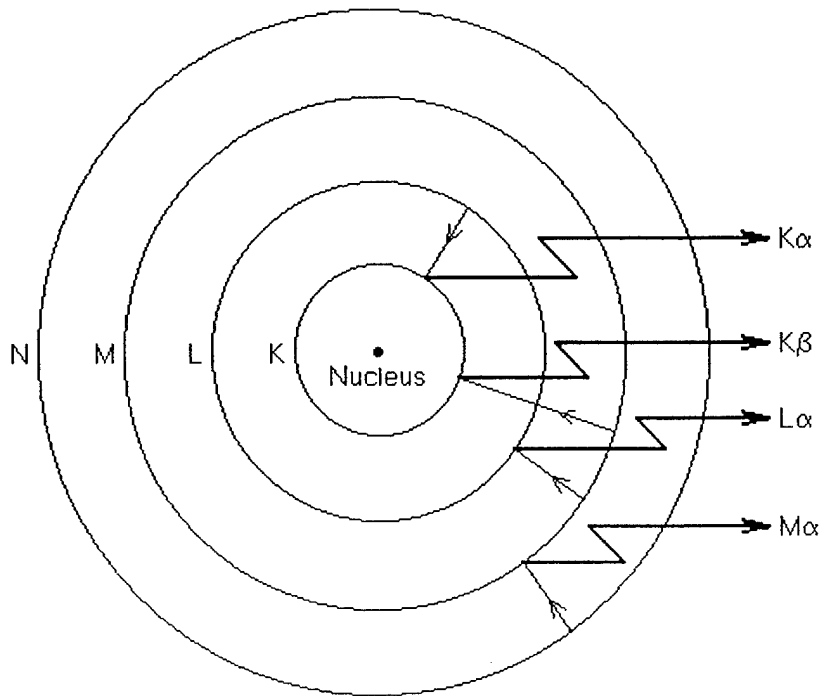


Figure B-2: Bohr Model of the Atom Showing the Origin of Emitted X-rays

results from an M to K transition, an  $L\alpha$  X-ray results from an M to L transition, and so forth. Finer energy differences are designated  $K\alpha_1$ ,  $K\alpha_2$ , and so forth. Each element has a characteristic distribution of X-rays, so measuring the wavelengths or energies of the emitted X-rays will indicate what elements are present. For example, iron uniquely emits X-rays with the following energies (keV):  $K\alpha_1$ , 6.403;  $K\alpha_2$ , 6.390;  $K\beta$ , 7.057;  $L\alpha$ , 0.704; and  $L\beta$ , 0.717. If these energies are present in the X-ray spectrum collected from the sample, the sample contains iron. [6]

## Appendix C

# EDS Spectra: Internal Deposits



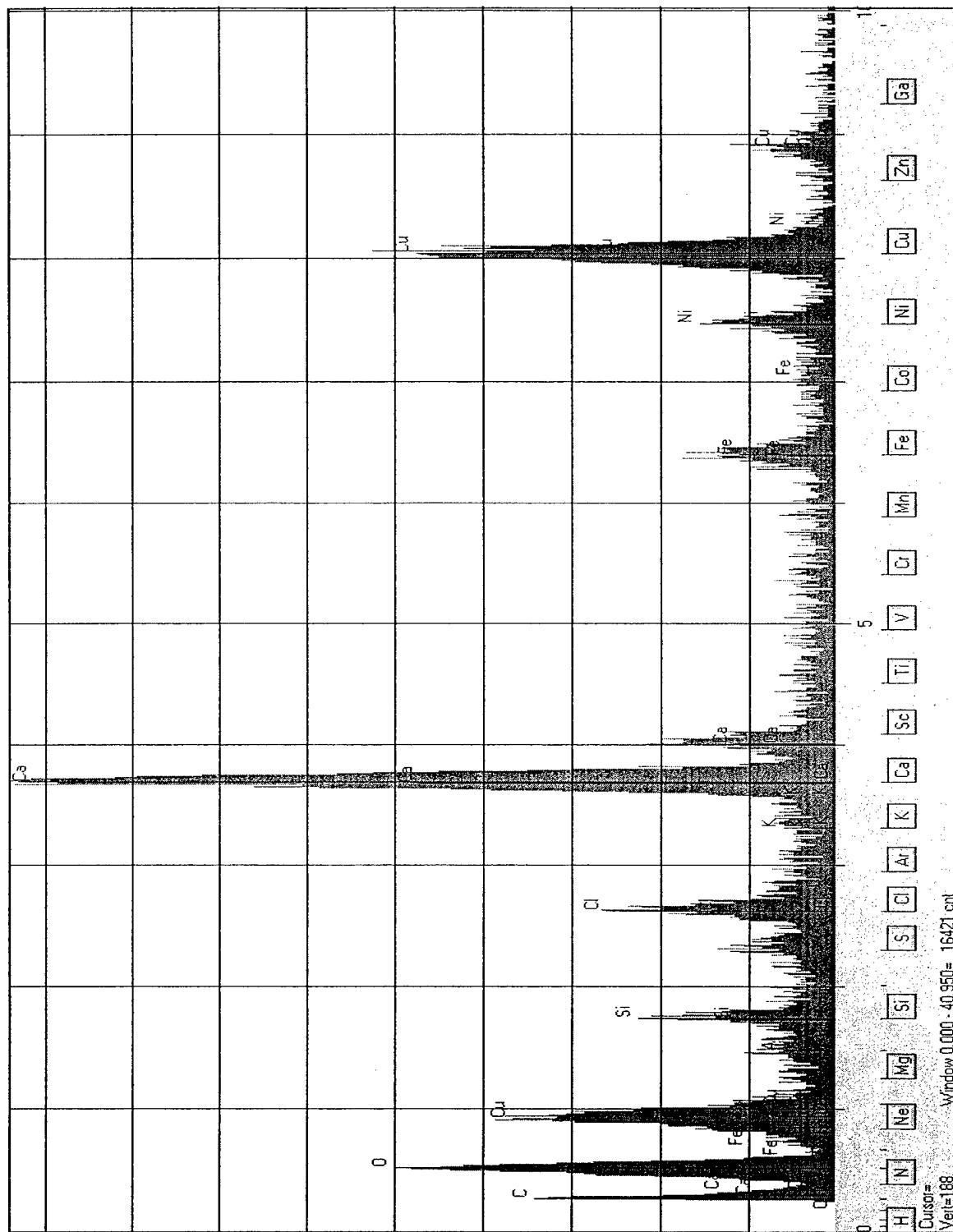


Figure C-2: EDS Spectrum A11b

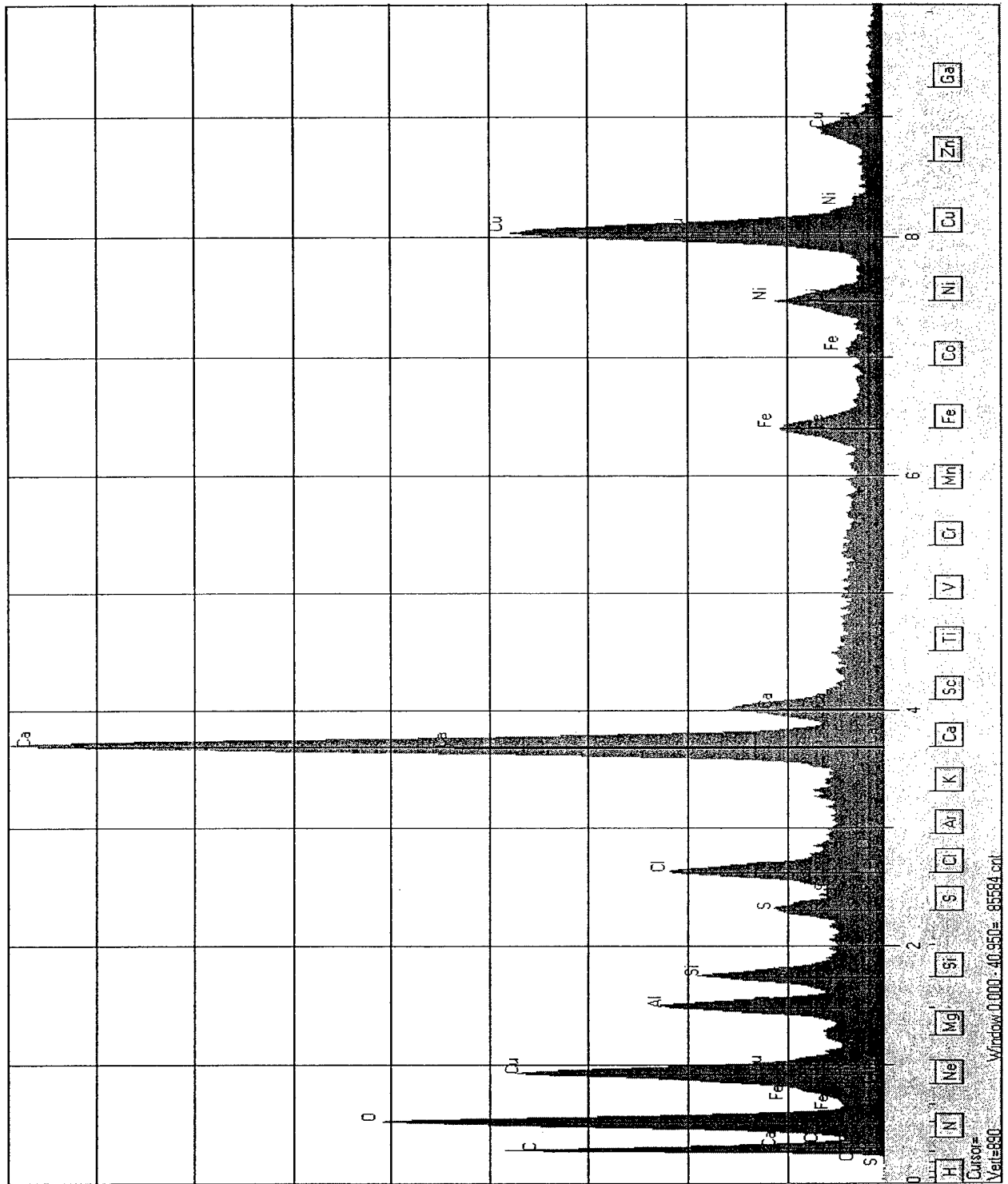


Figure C-3: EDS Spectrum A11c

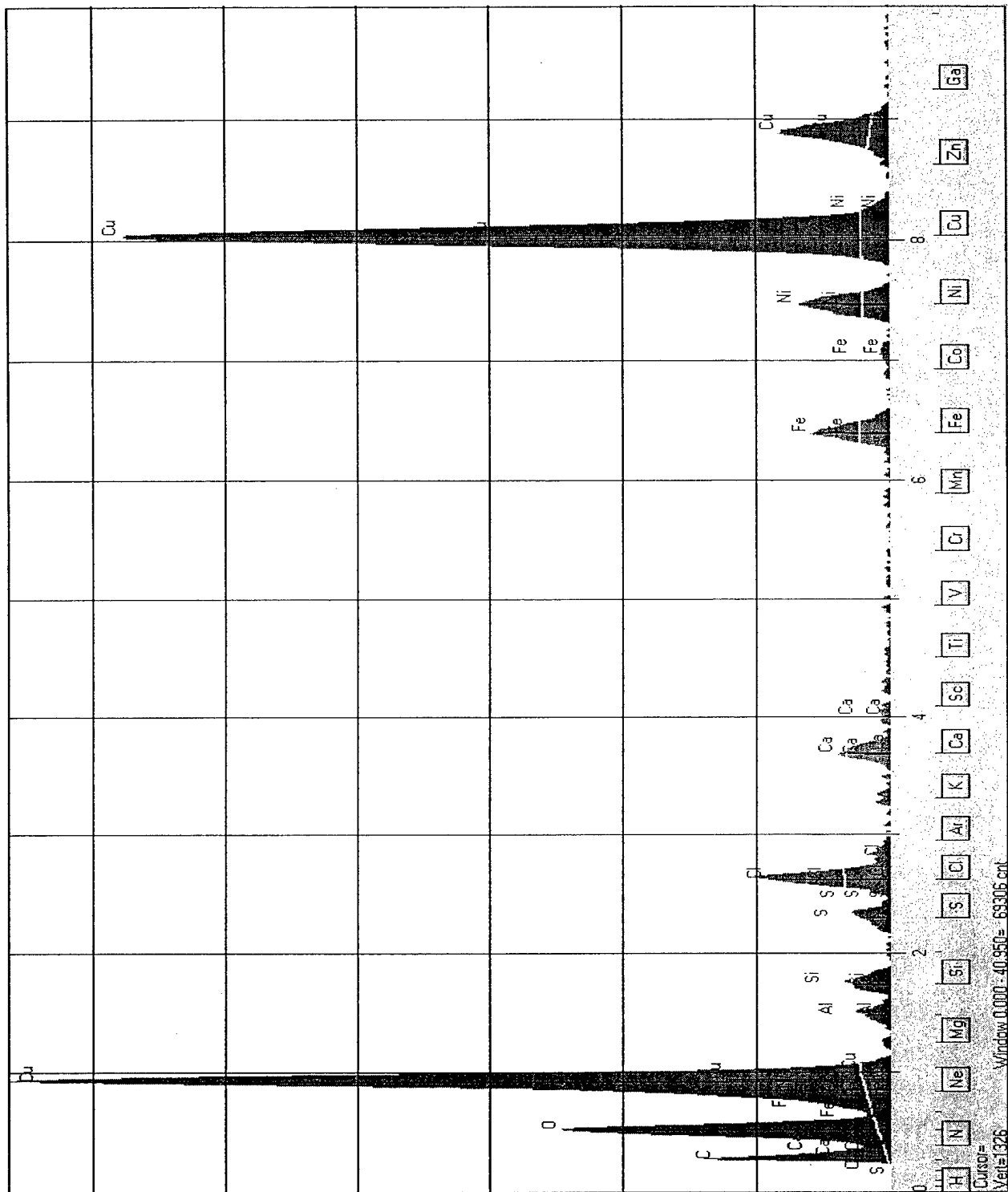


Figure C-4: EDS Spectrum A12a

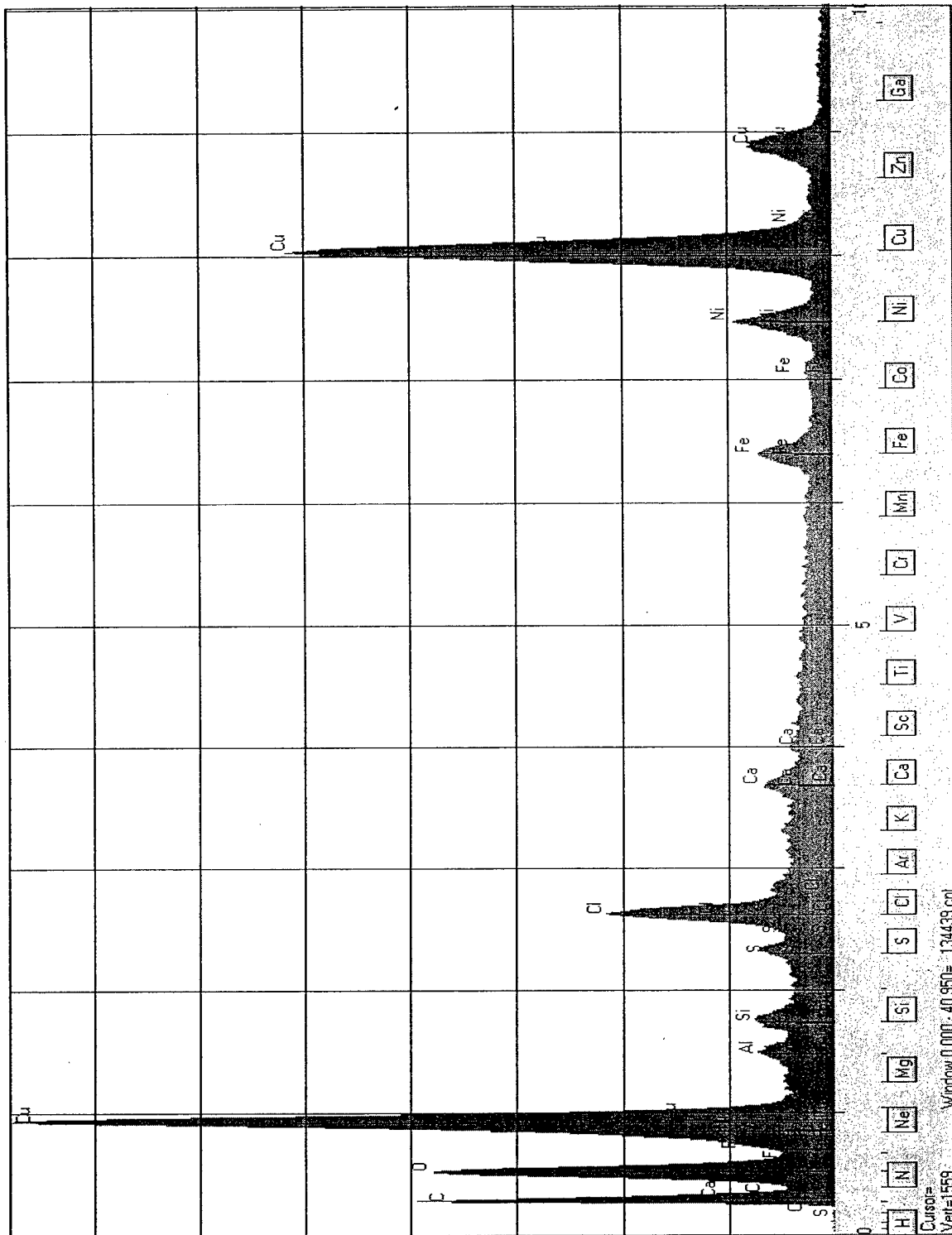


Figure C-5: EDS Spectrum A12b

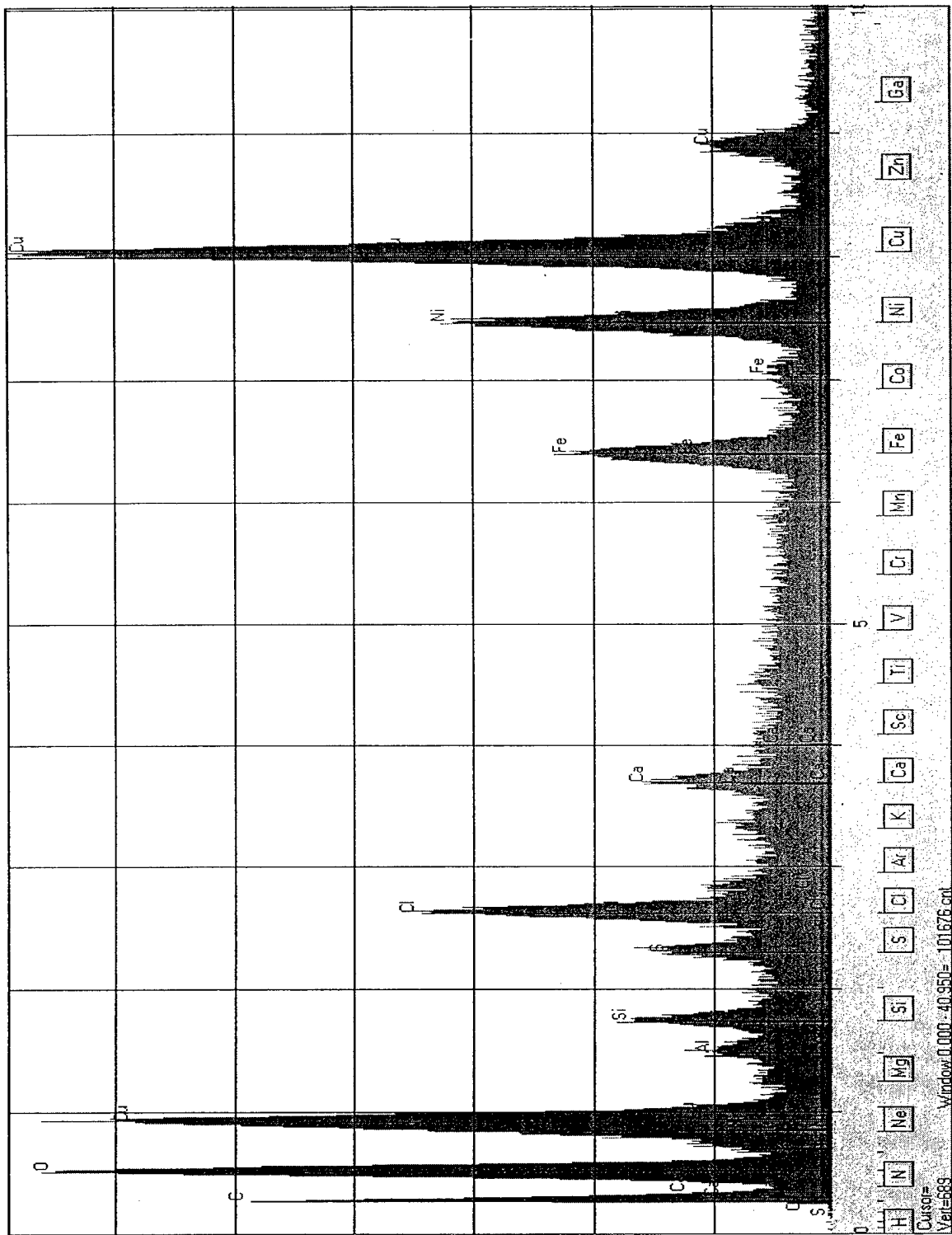


Figure C-6: EDS Spectrum A13a

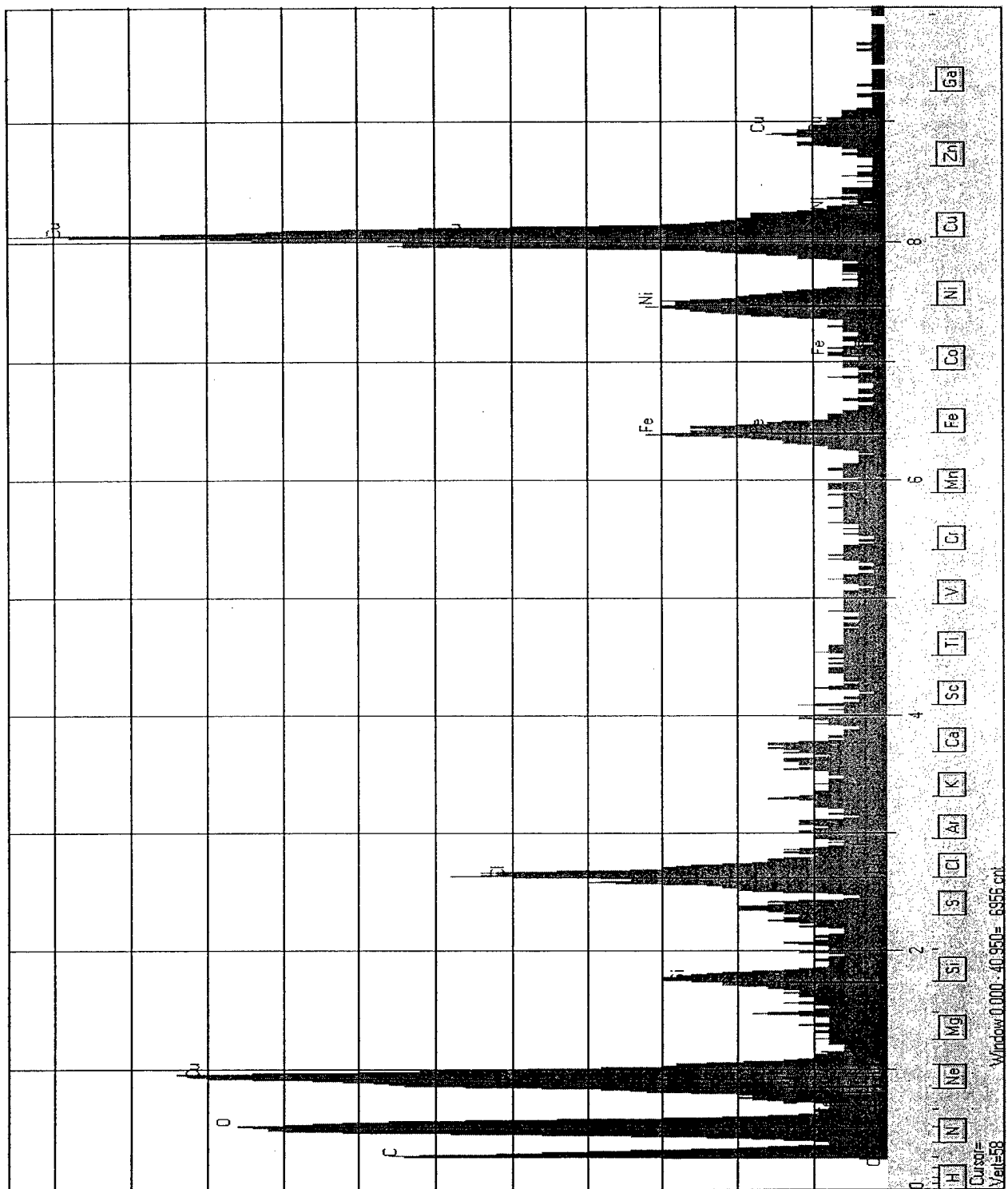


Figure C-7: EDS Spectrum A21a

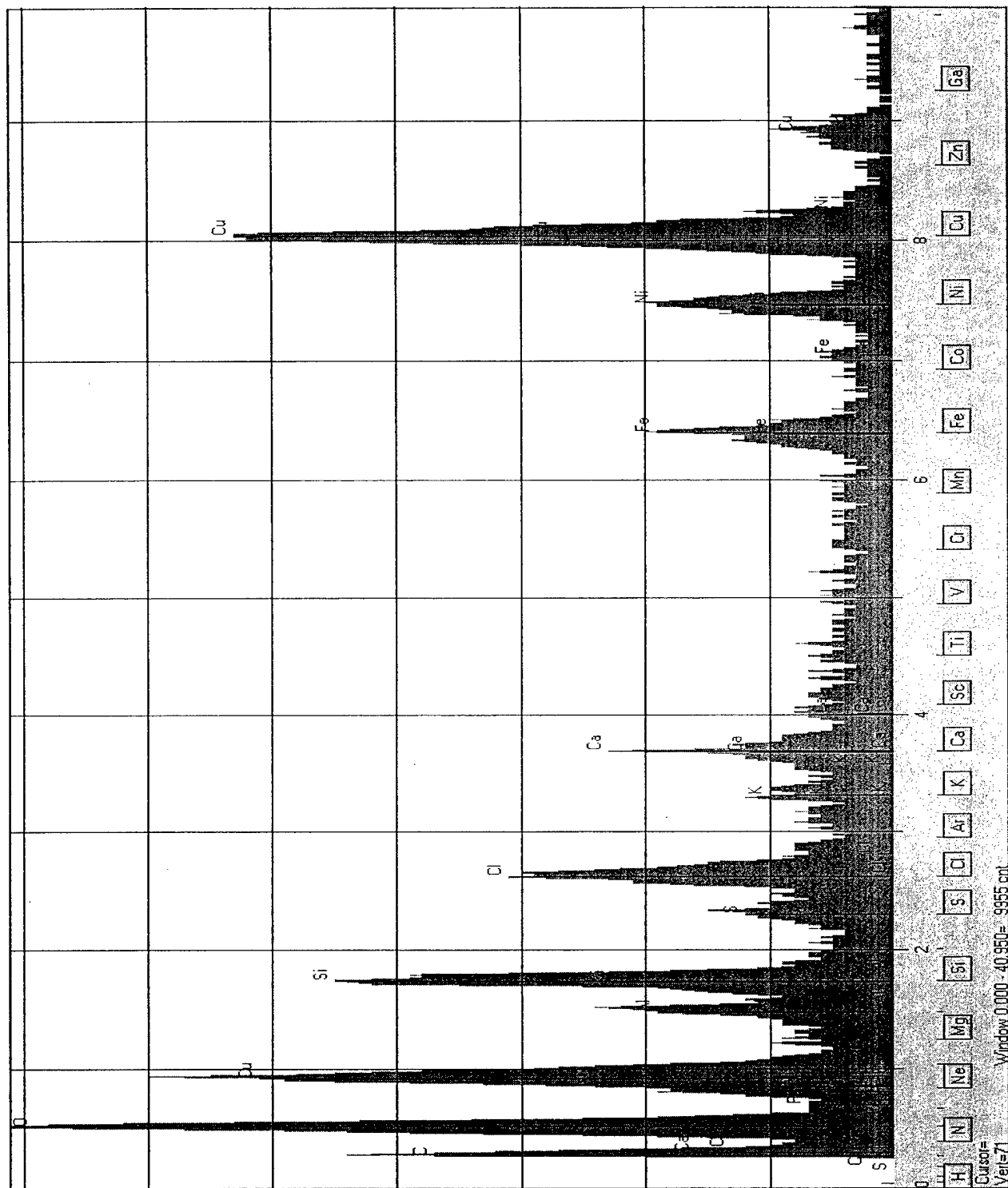


Figure C-8: EDS Spectrum A21b

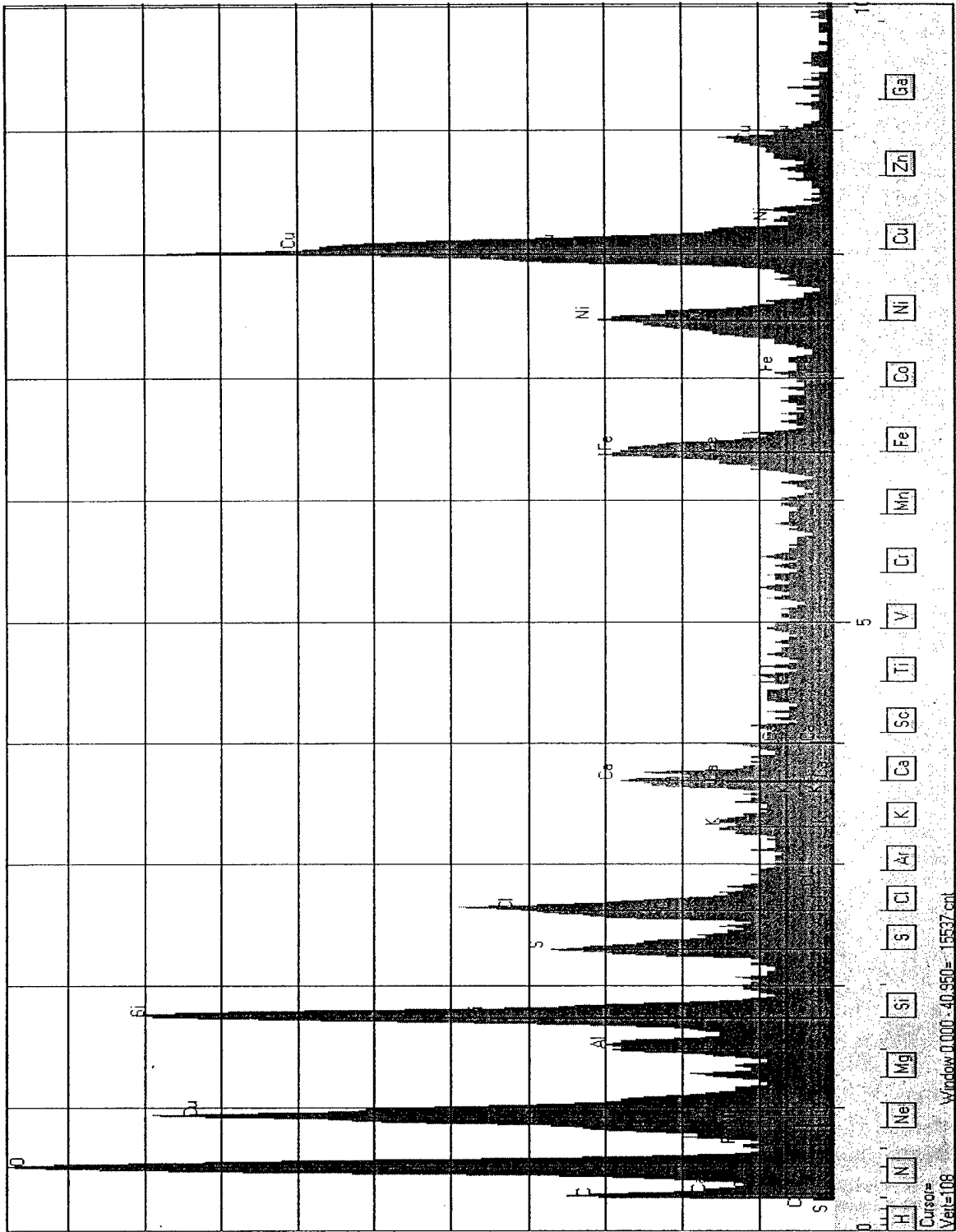


Figure C-9: EDS Spectrum A21c

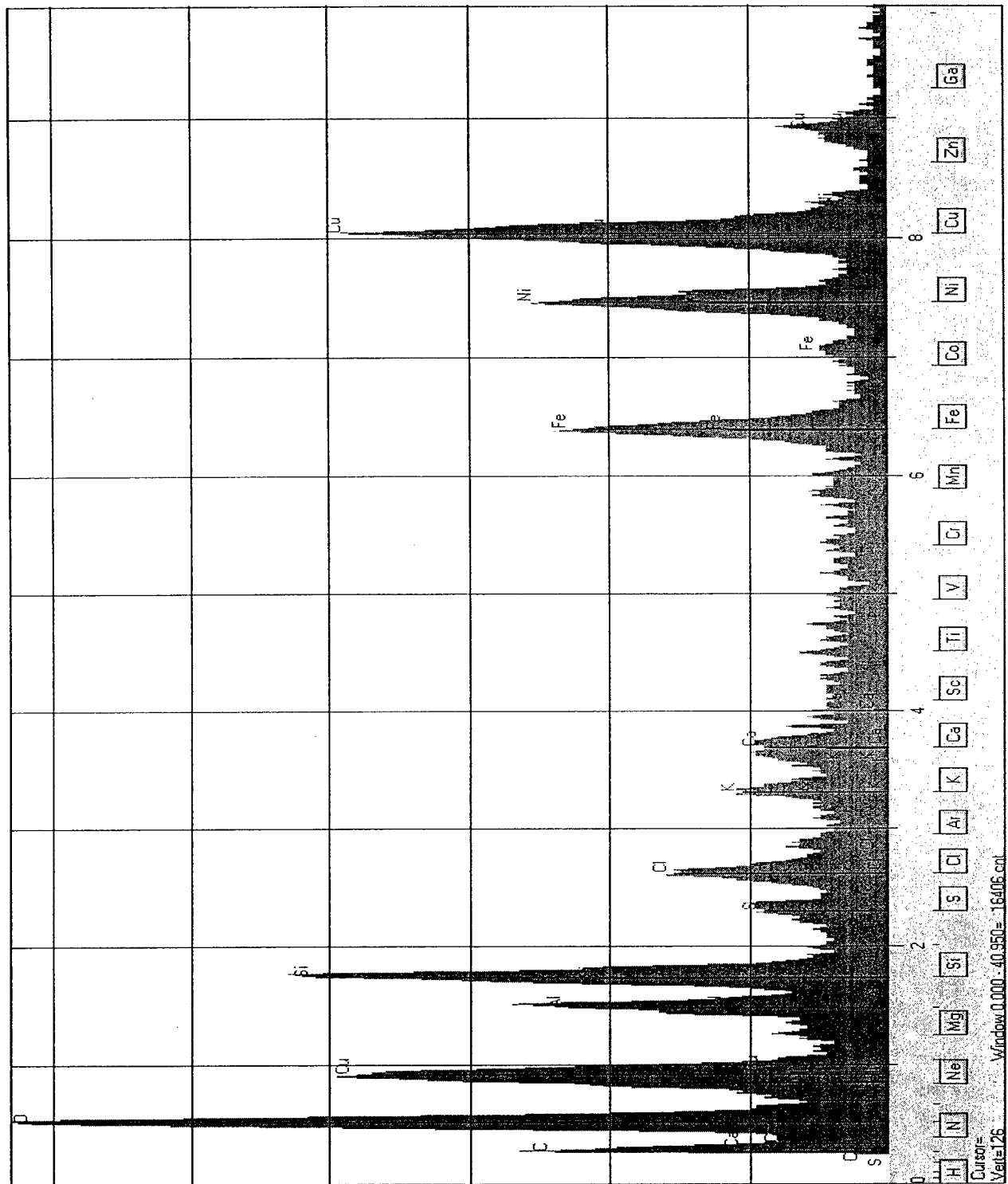


Figure C-10: EDS Spectrum A22a

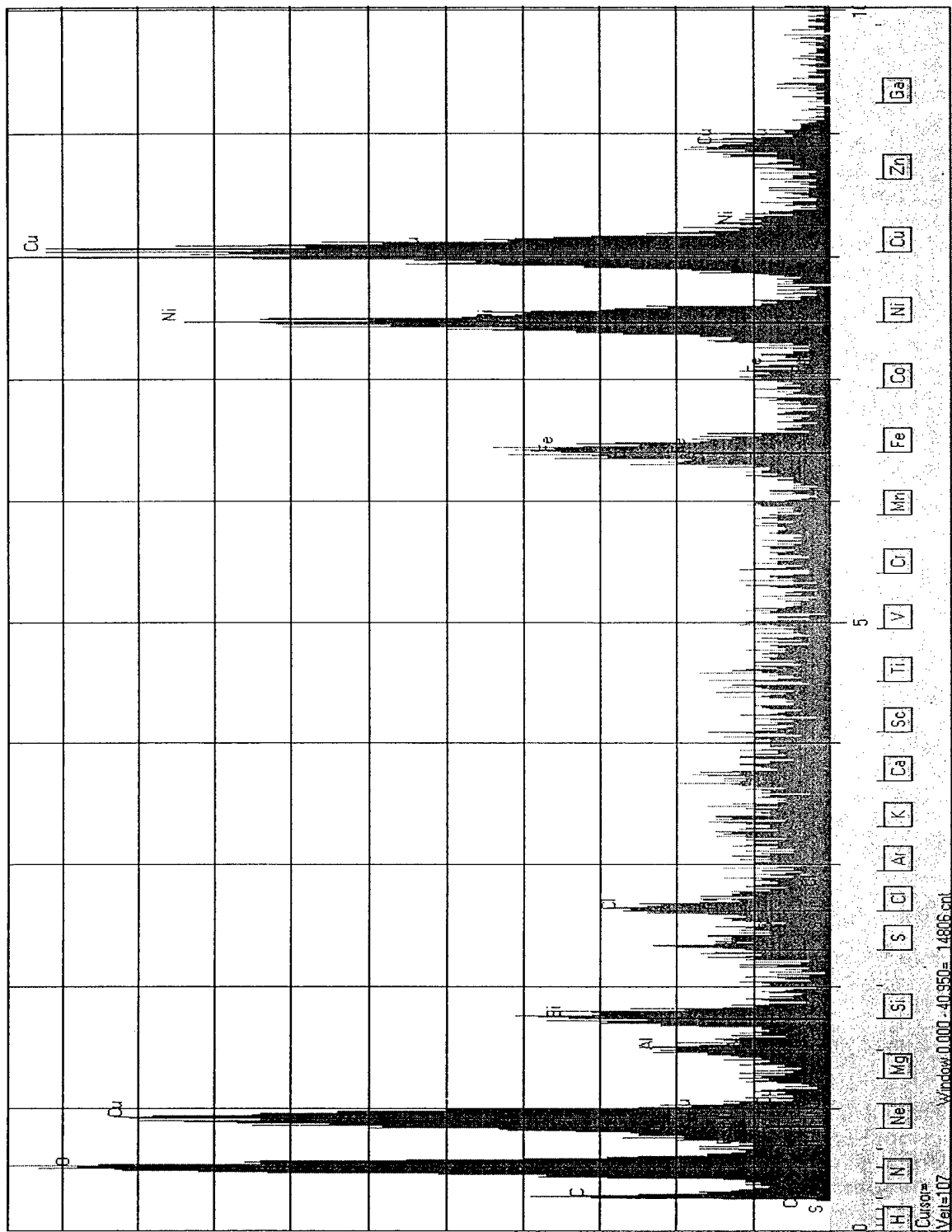


Figure C-11: EDS Spectrum A22b

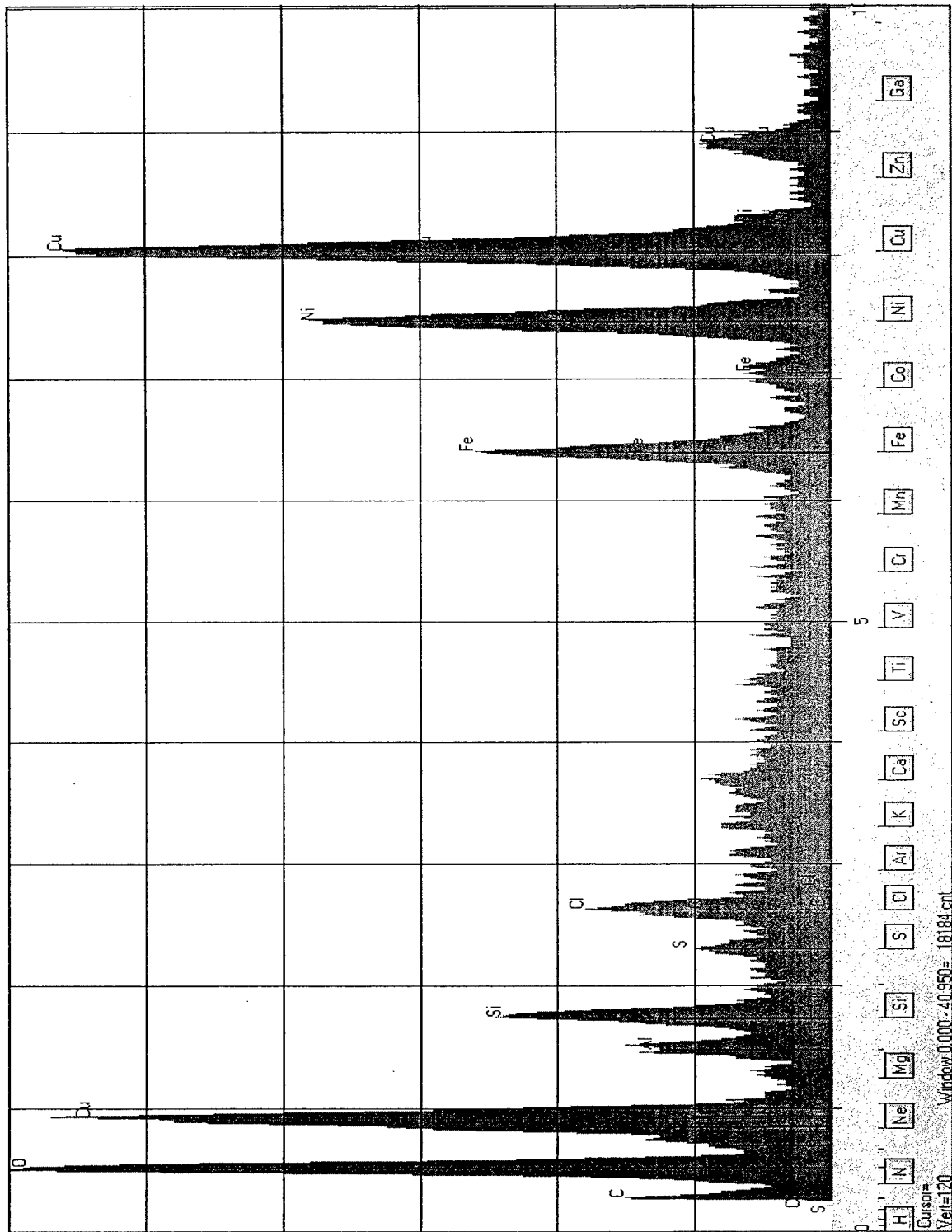


Figure C-12: EDS Spectrum A22c

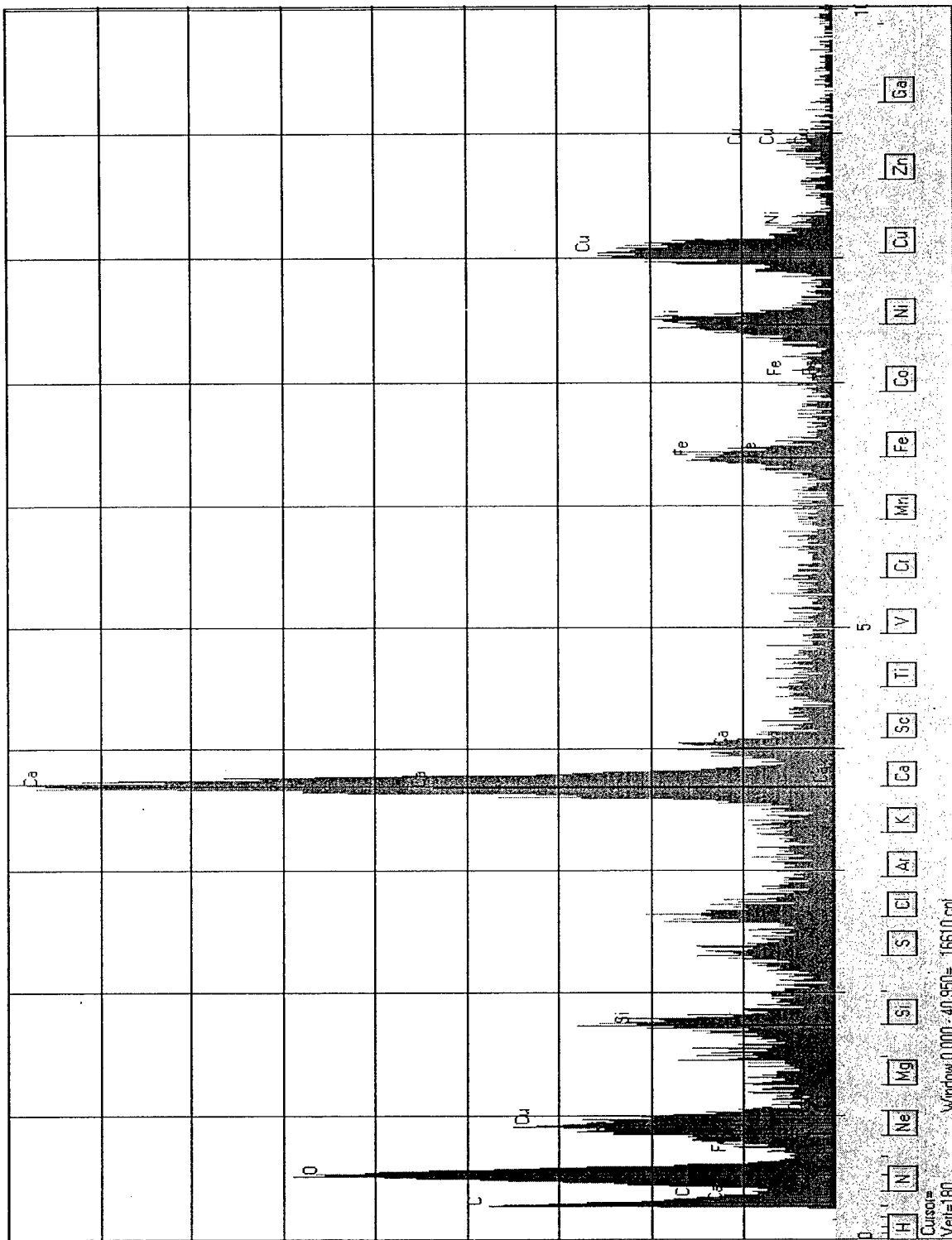


Figure C-13: EDS Spectrum A23a

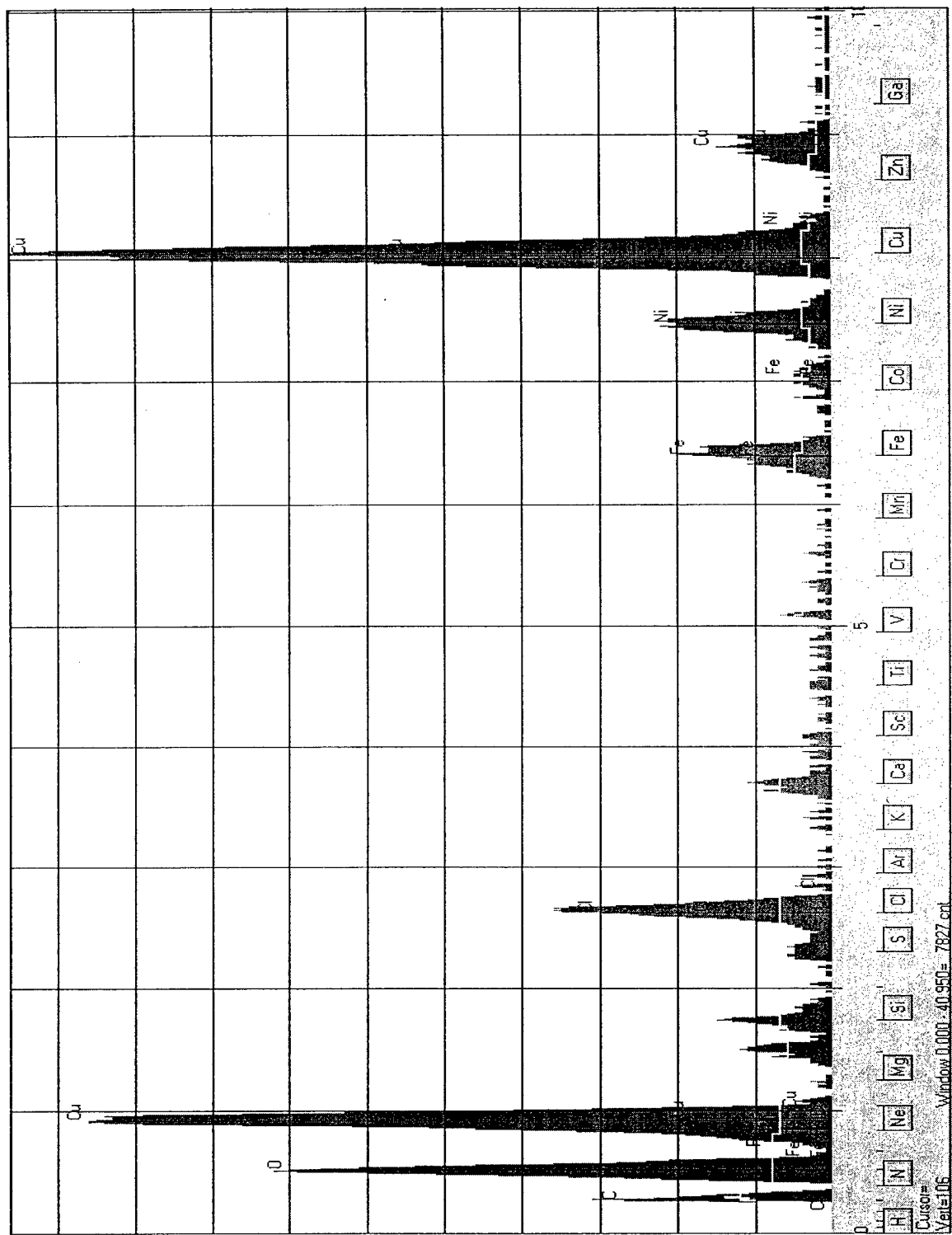


Figure C-14: EDS Spectrum A23b

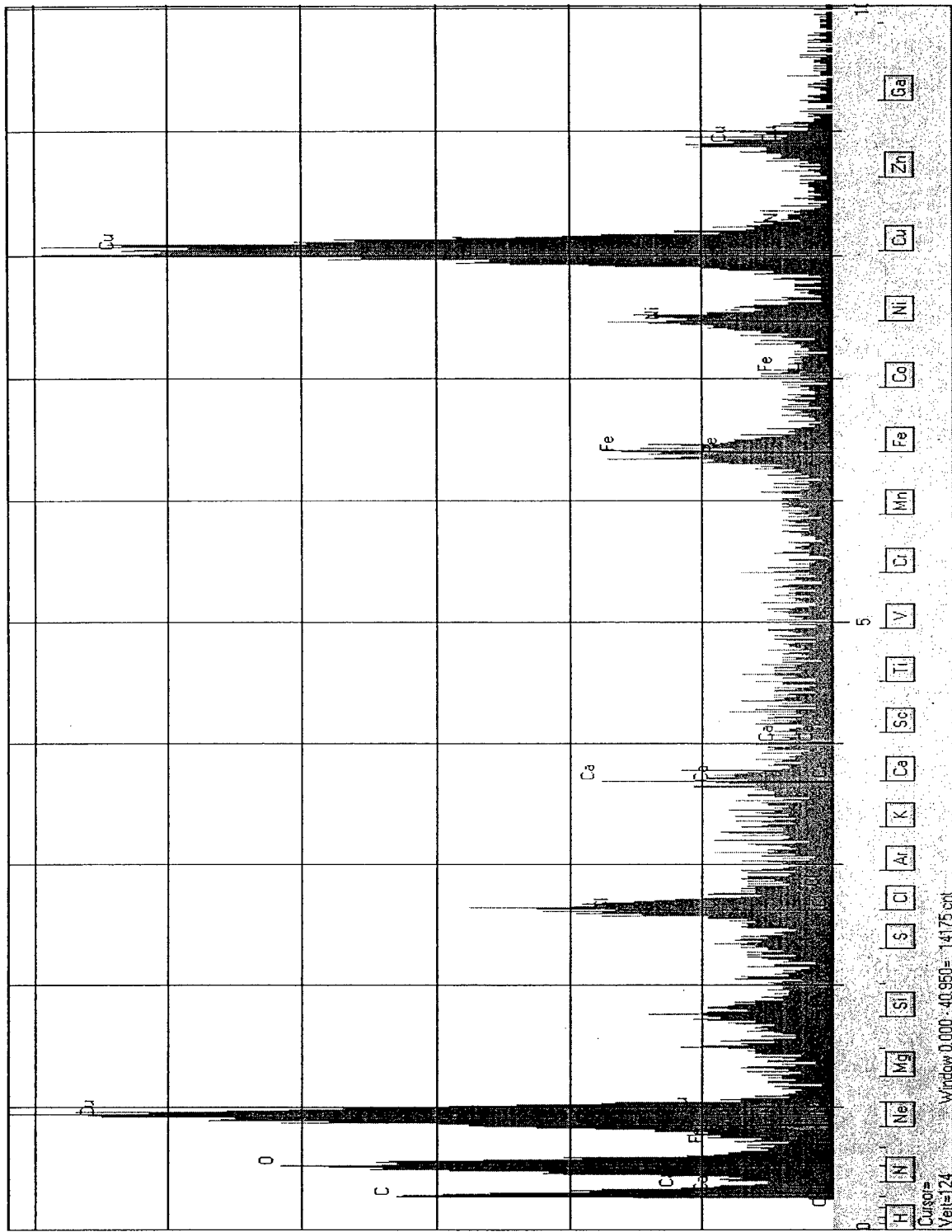


Figure C-15: EDS Spectrum A23c

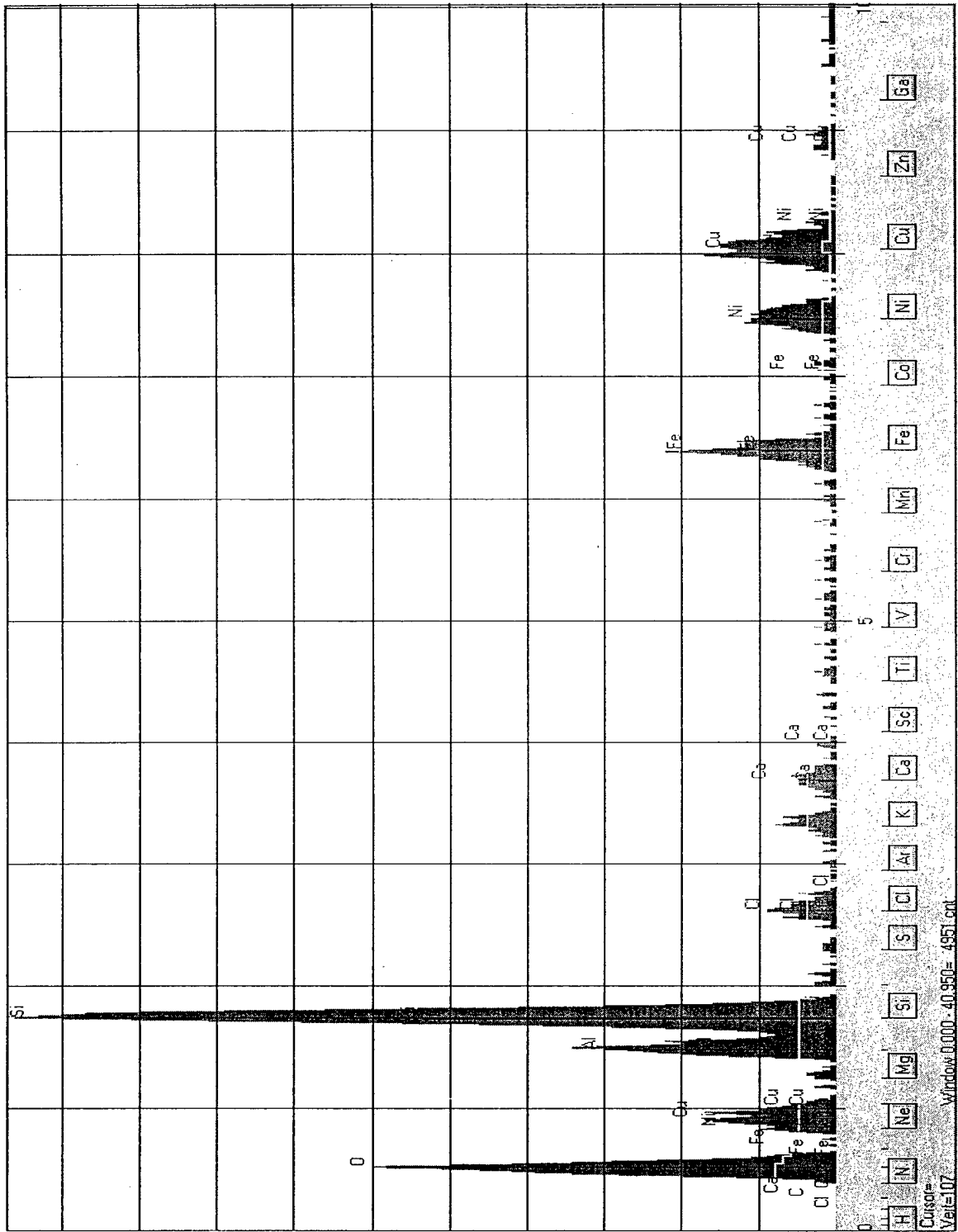


Figure C-16: EDS Spectrum A31a

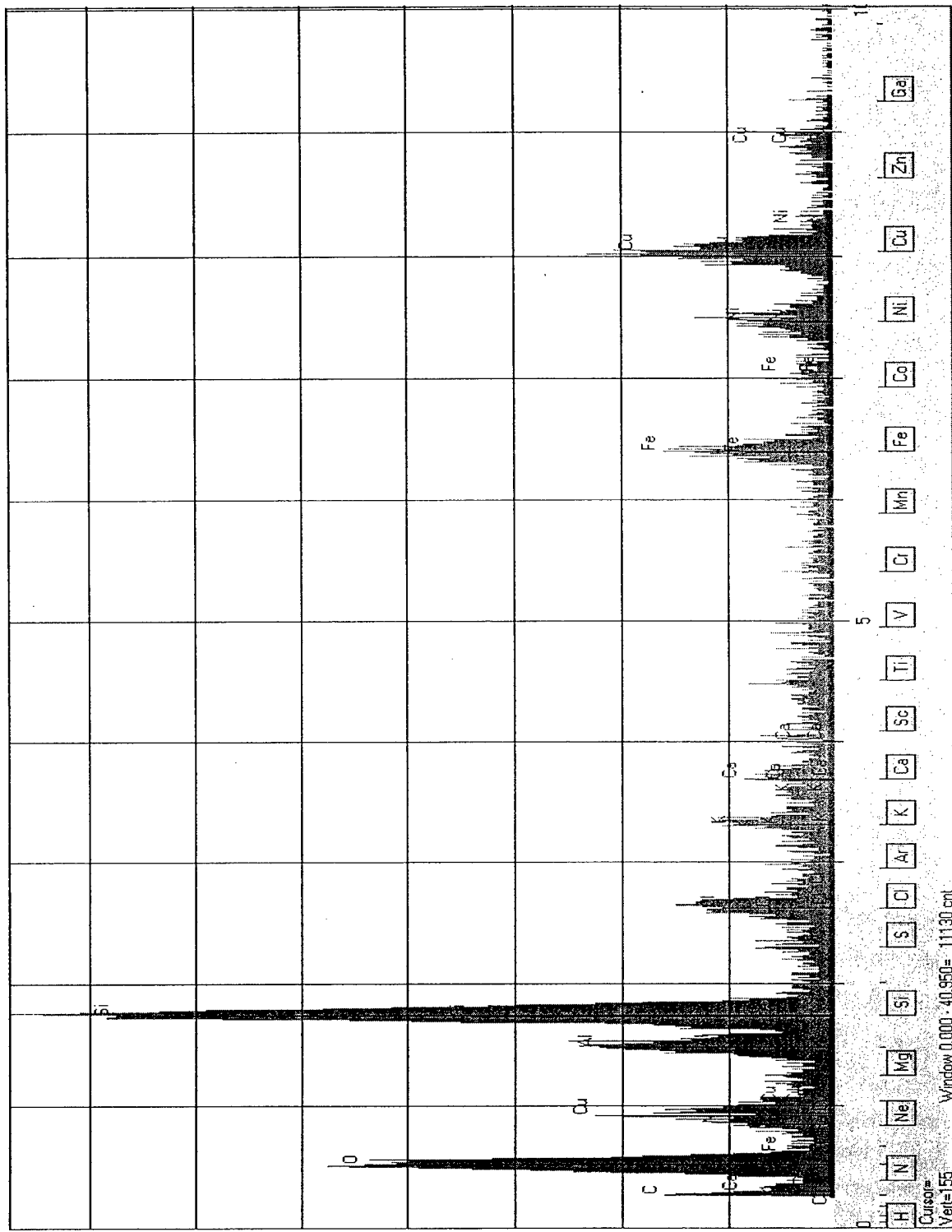


Figure C-17: EDS Spectrum A31b

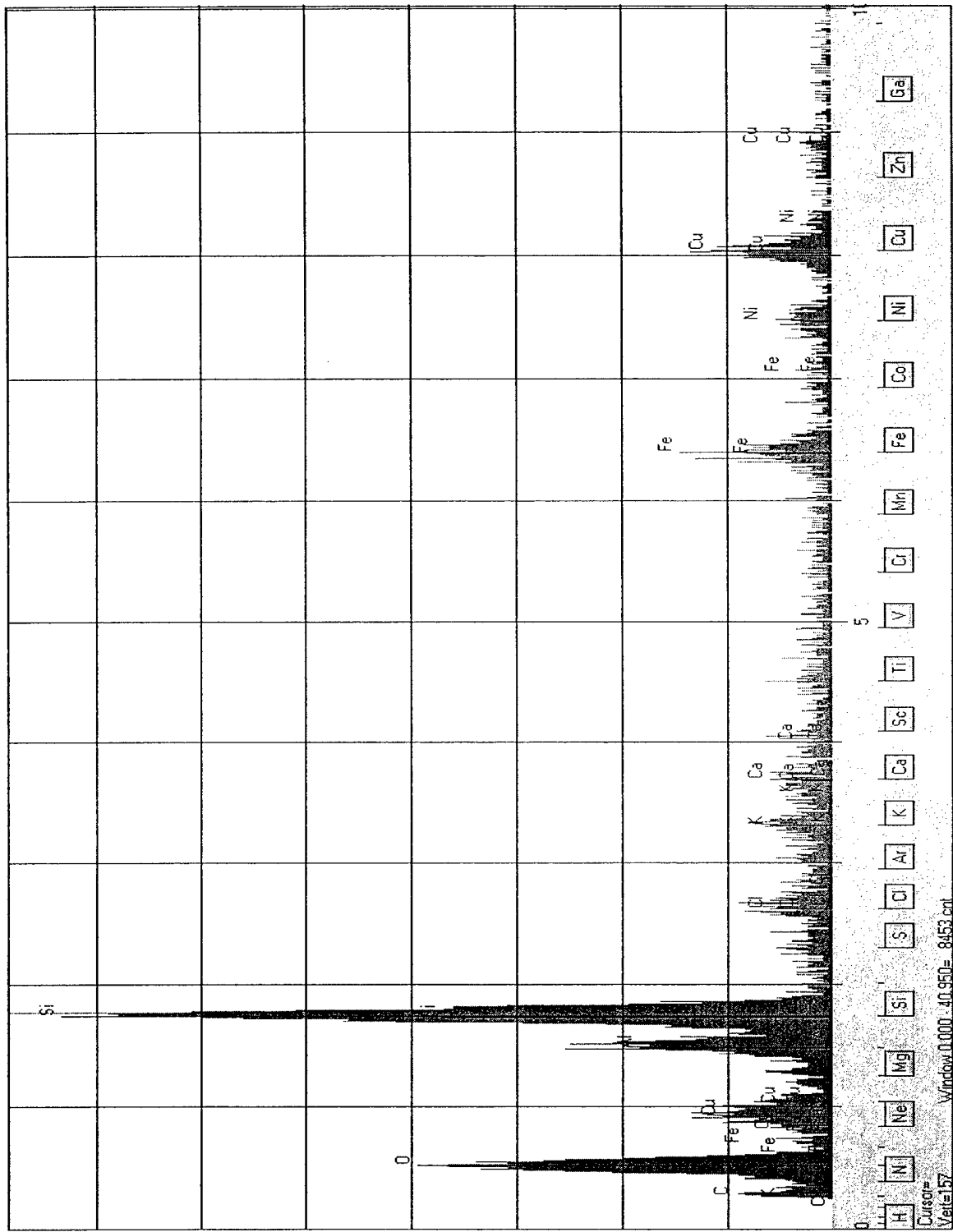


Figure C-18: EDS Spectrum A31c

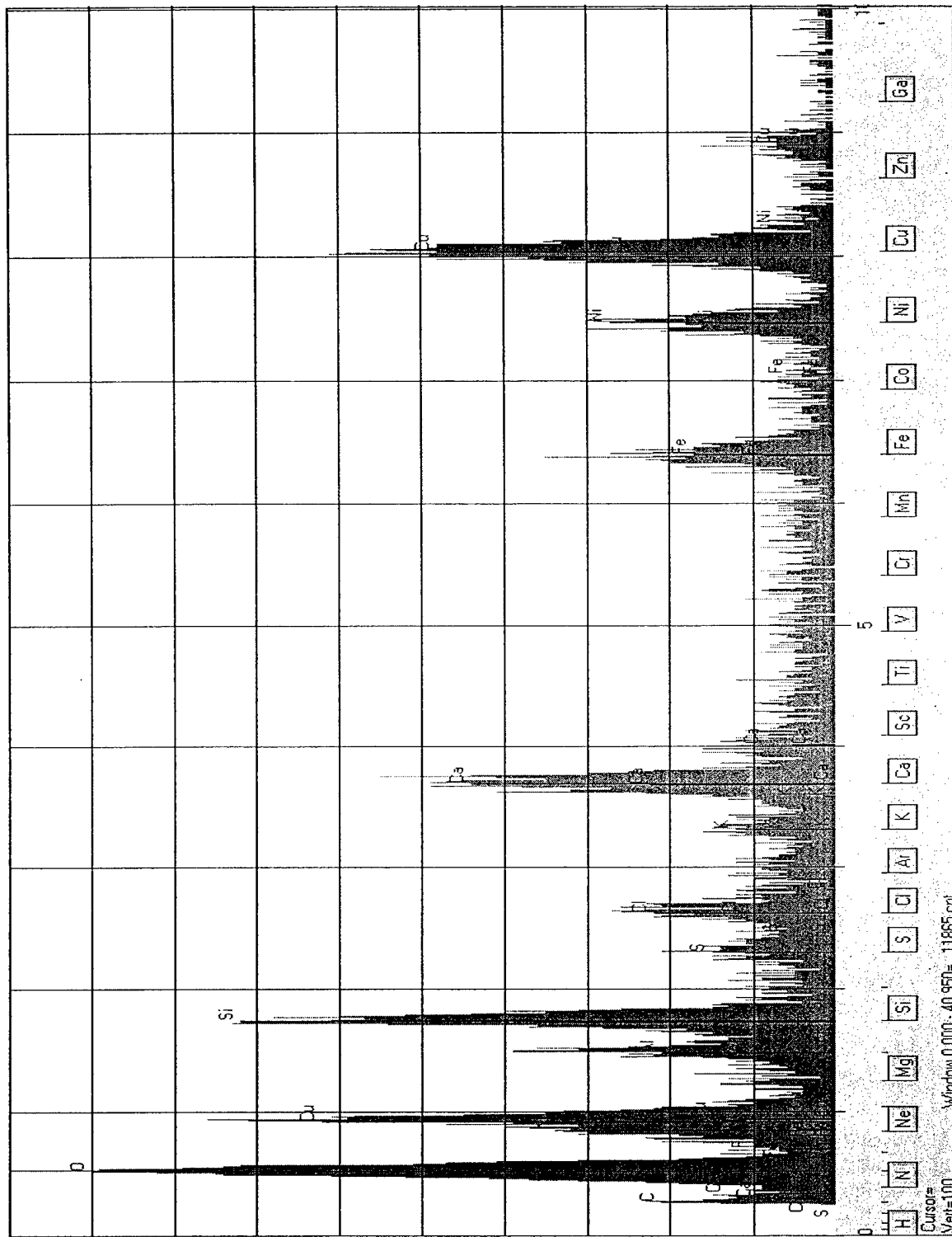


Figure C-19: EDS Spectrum A32a

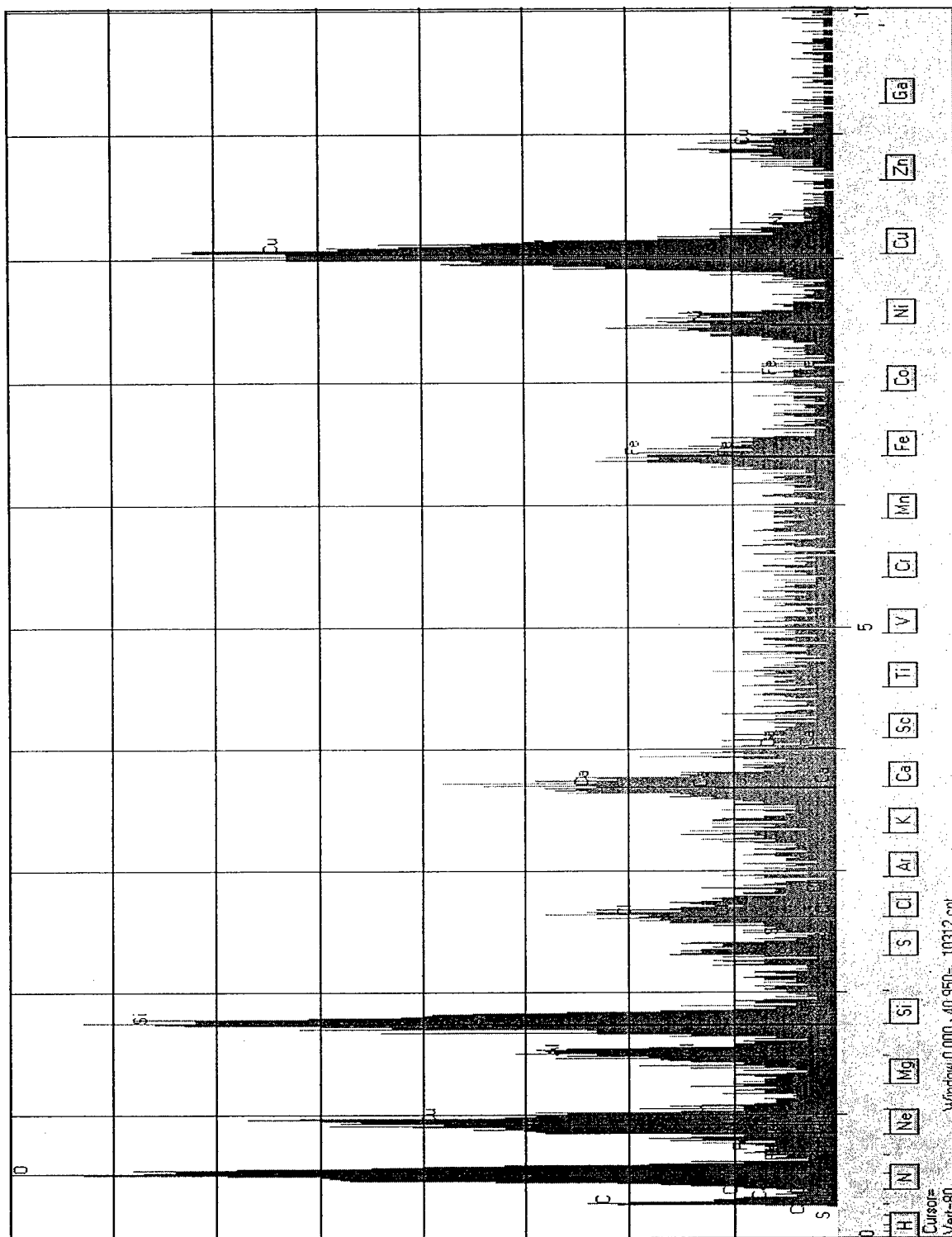


Figure C-20: EDS Spectrum A32b

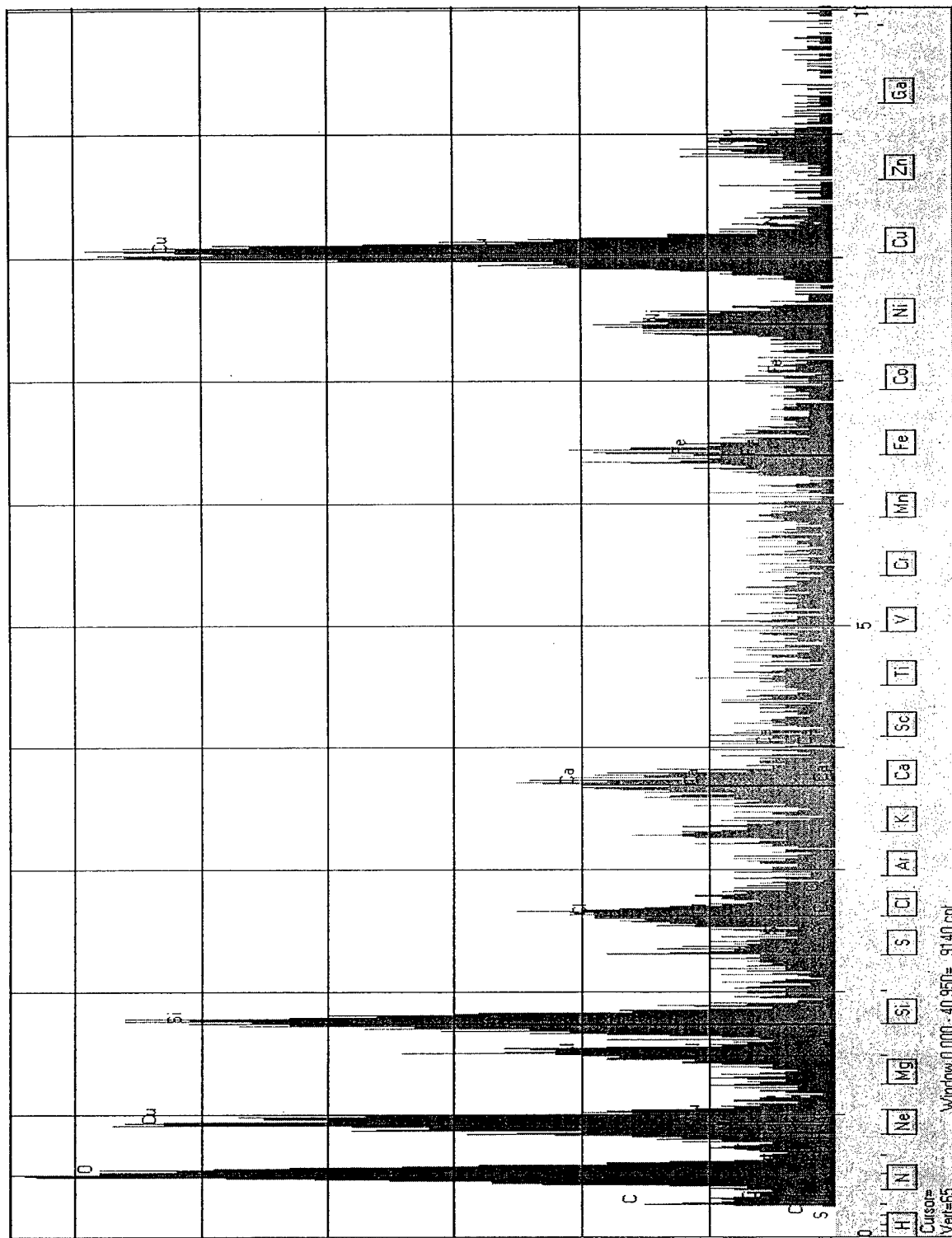


Figure C-21: EDS Spectrum A32c

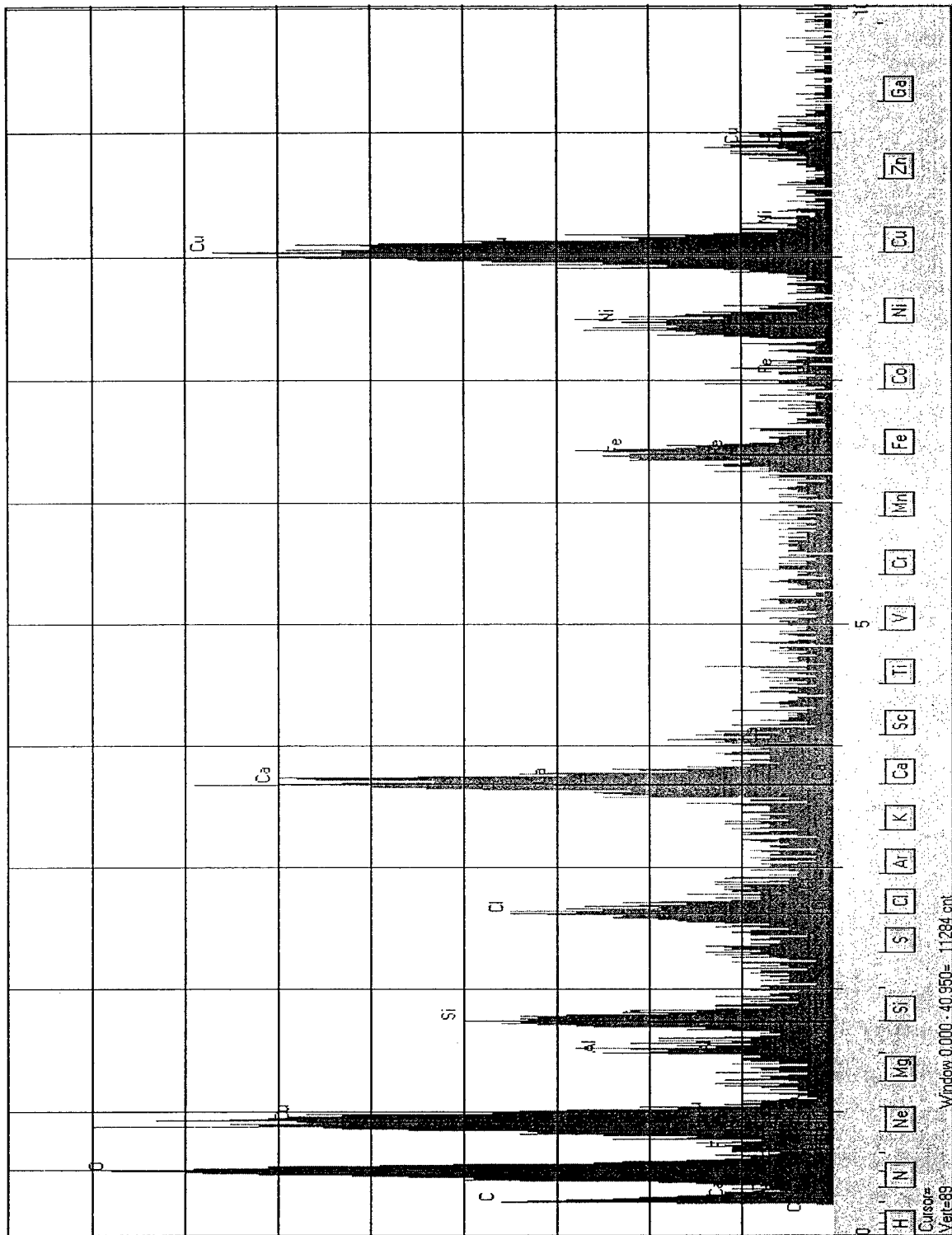


Figure C-22: EDS Spectrum A33a

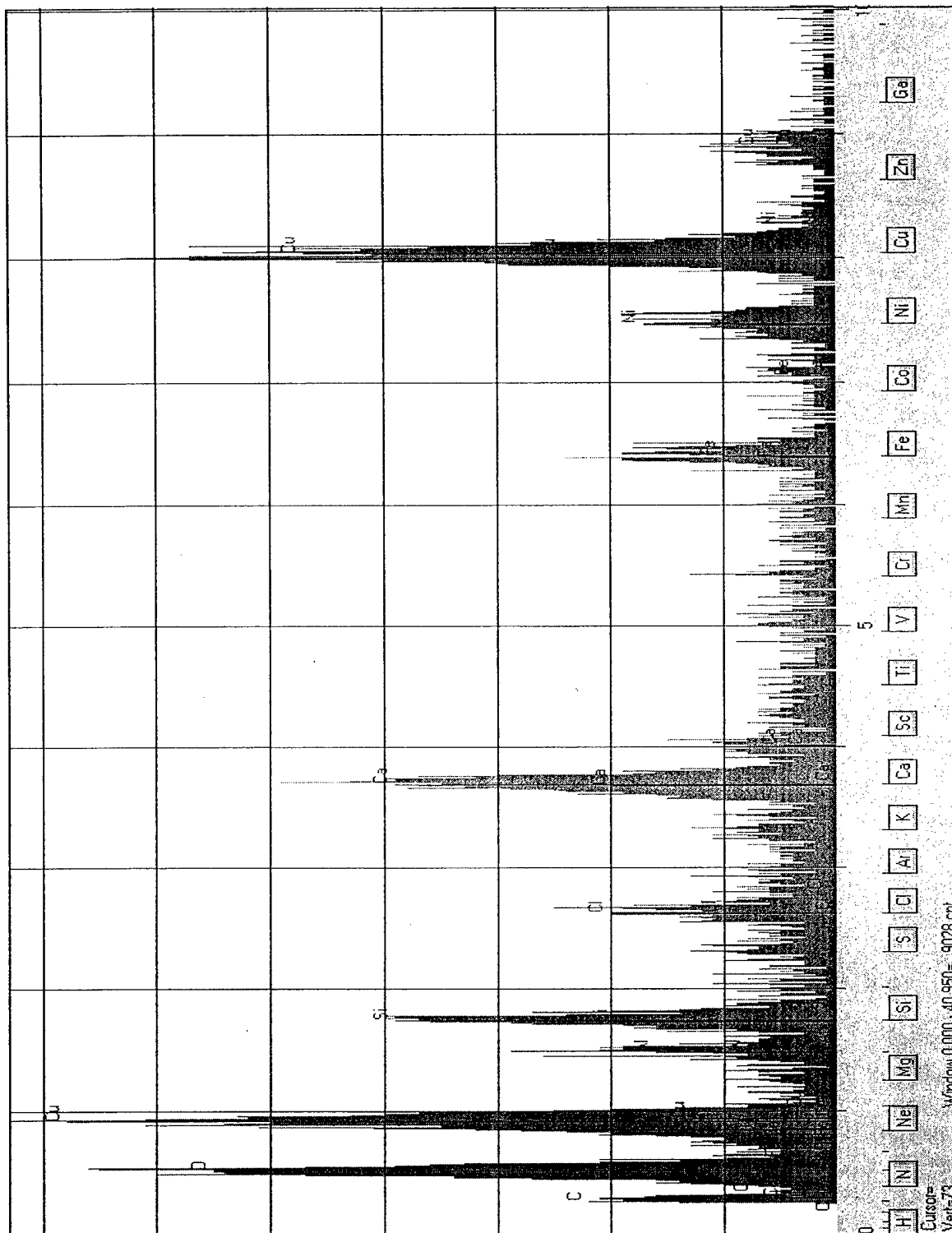


Figure C-23: EDS Spectrum A33b

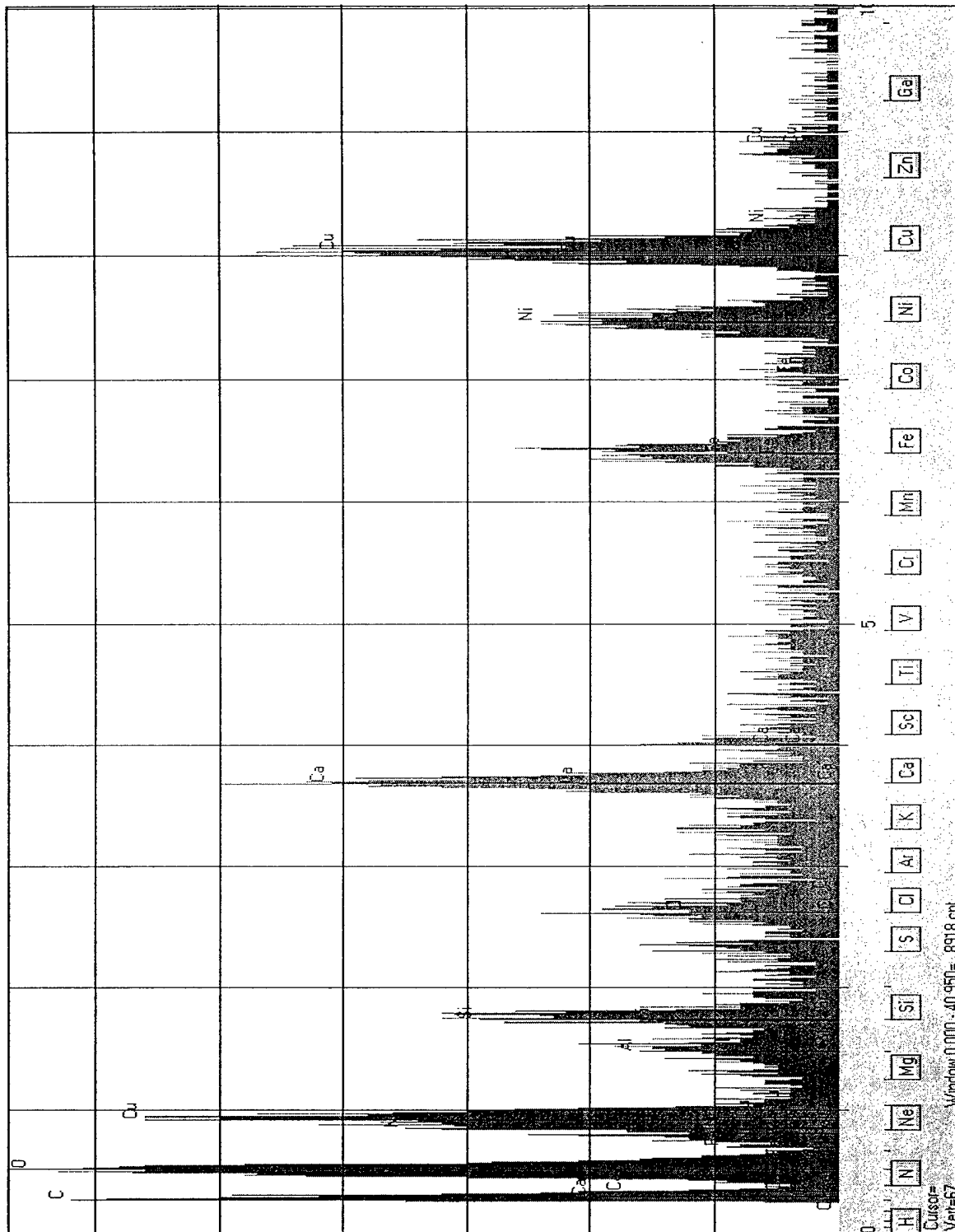


Figure C-24: EDS Spectrum A33c

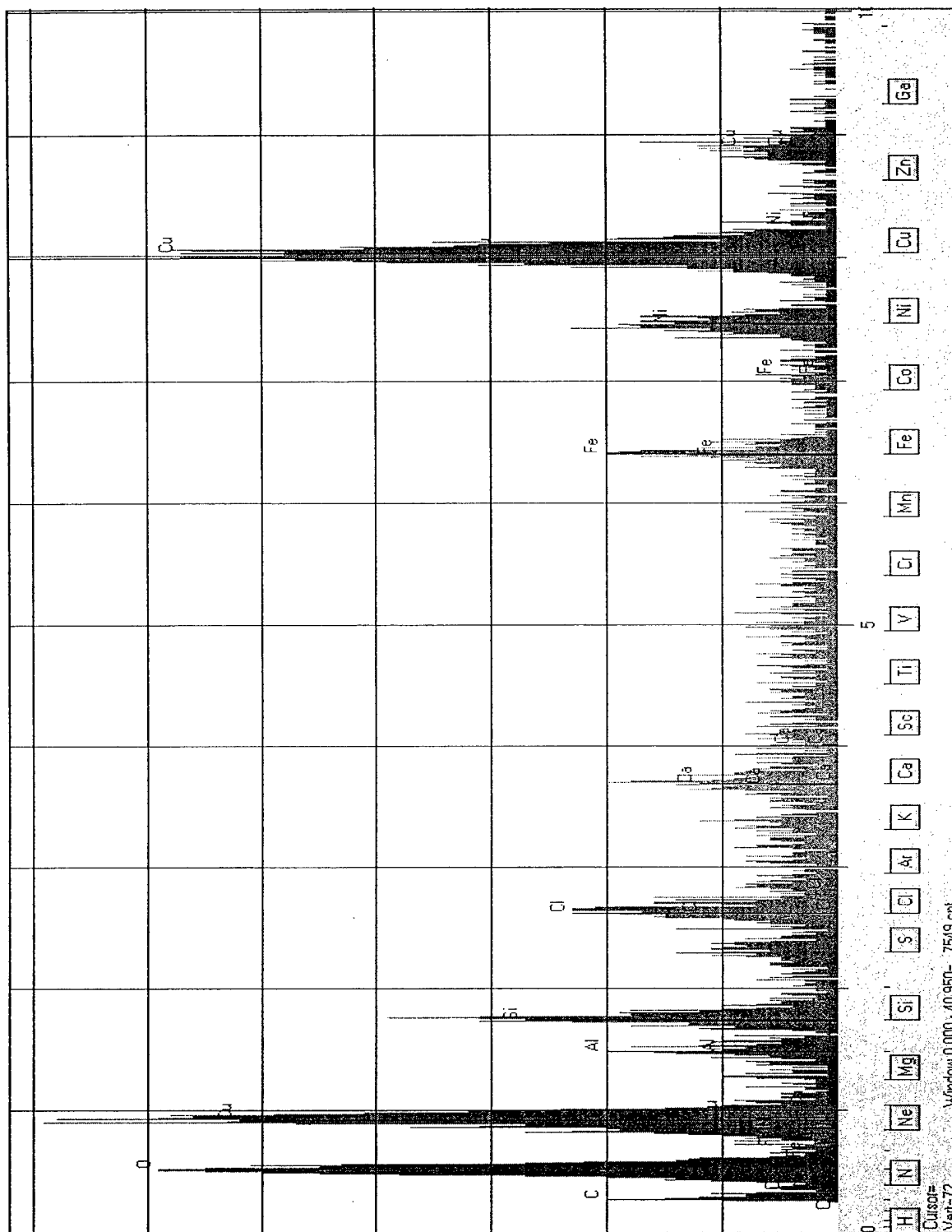


Figure C-25: EDS Spectrum A41a

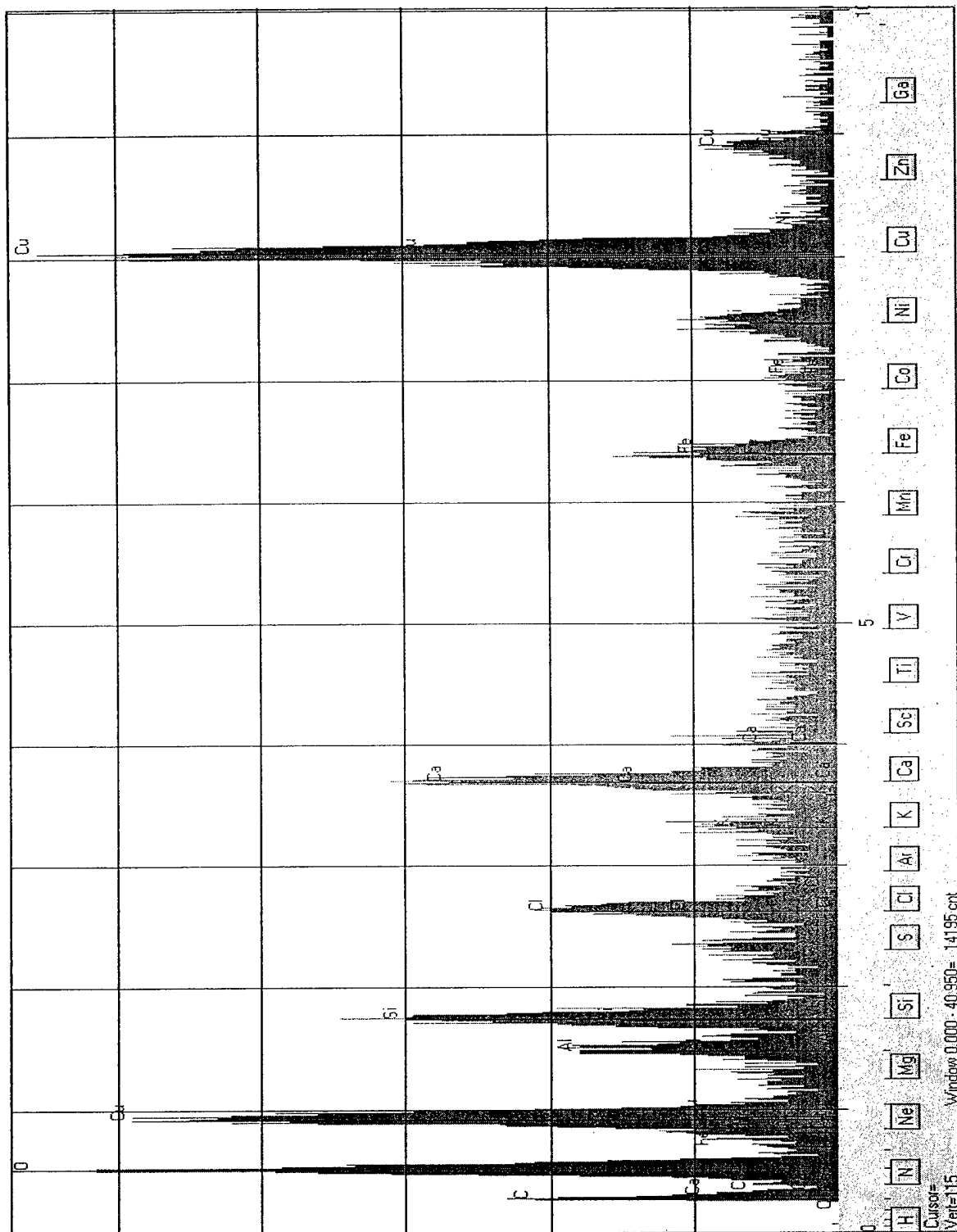


Figure C-26: EDS Spectrum A41b

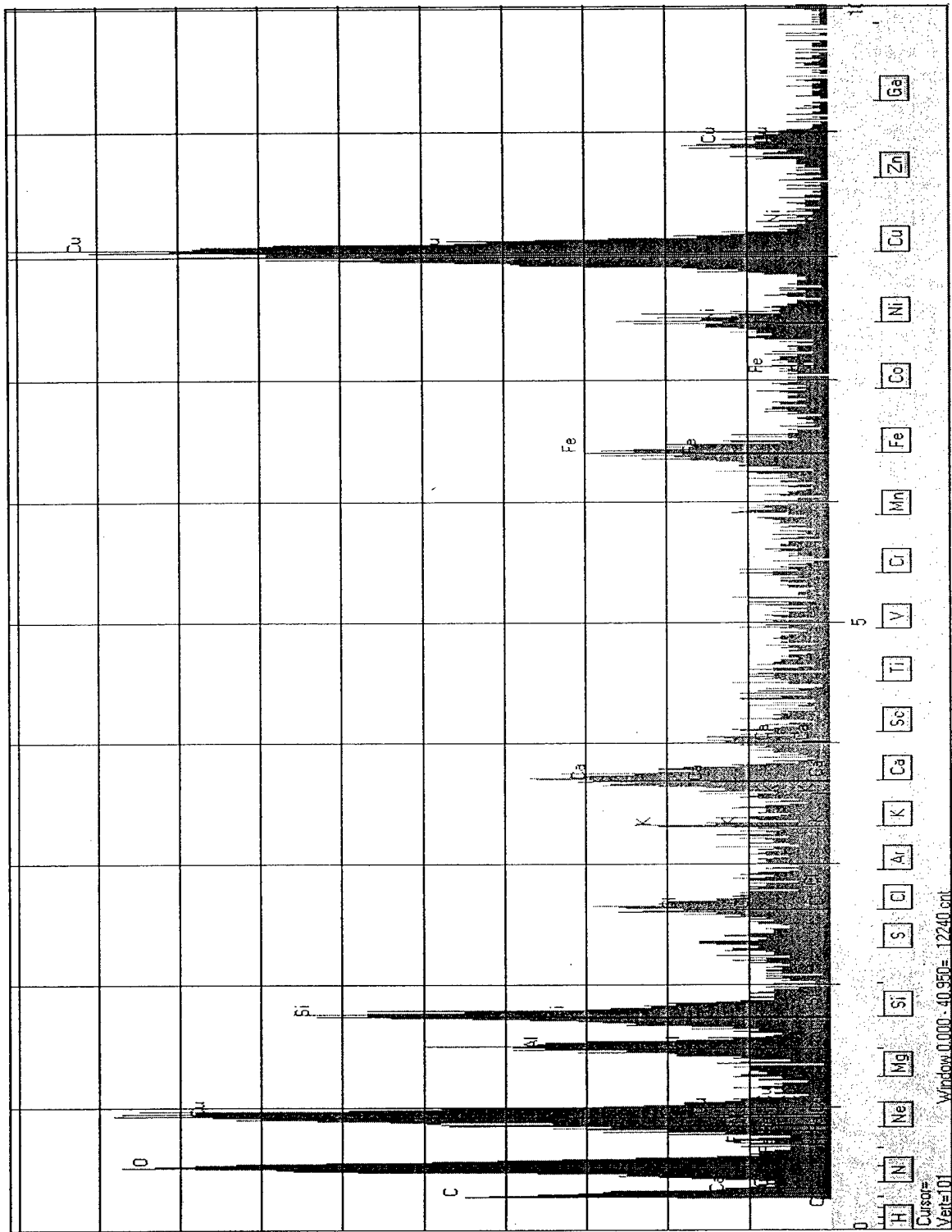


Figure C-27: EDS Spectrum A41c

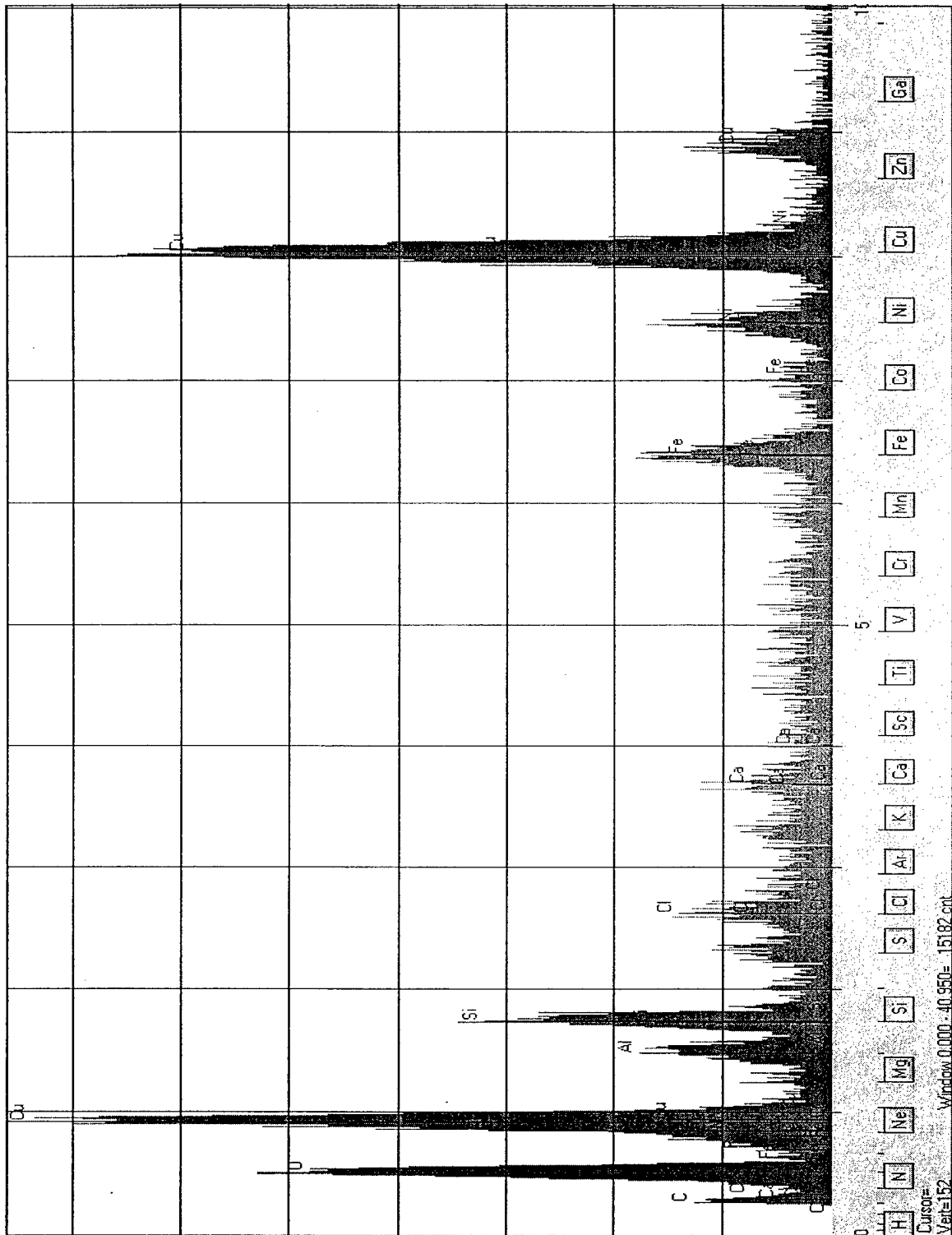


Figure C-28: EDS Spectrum A42a

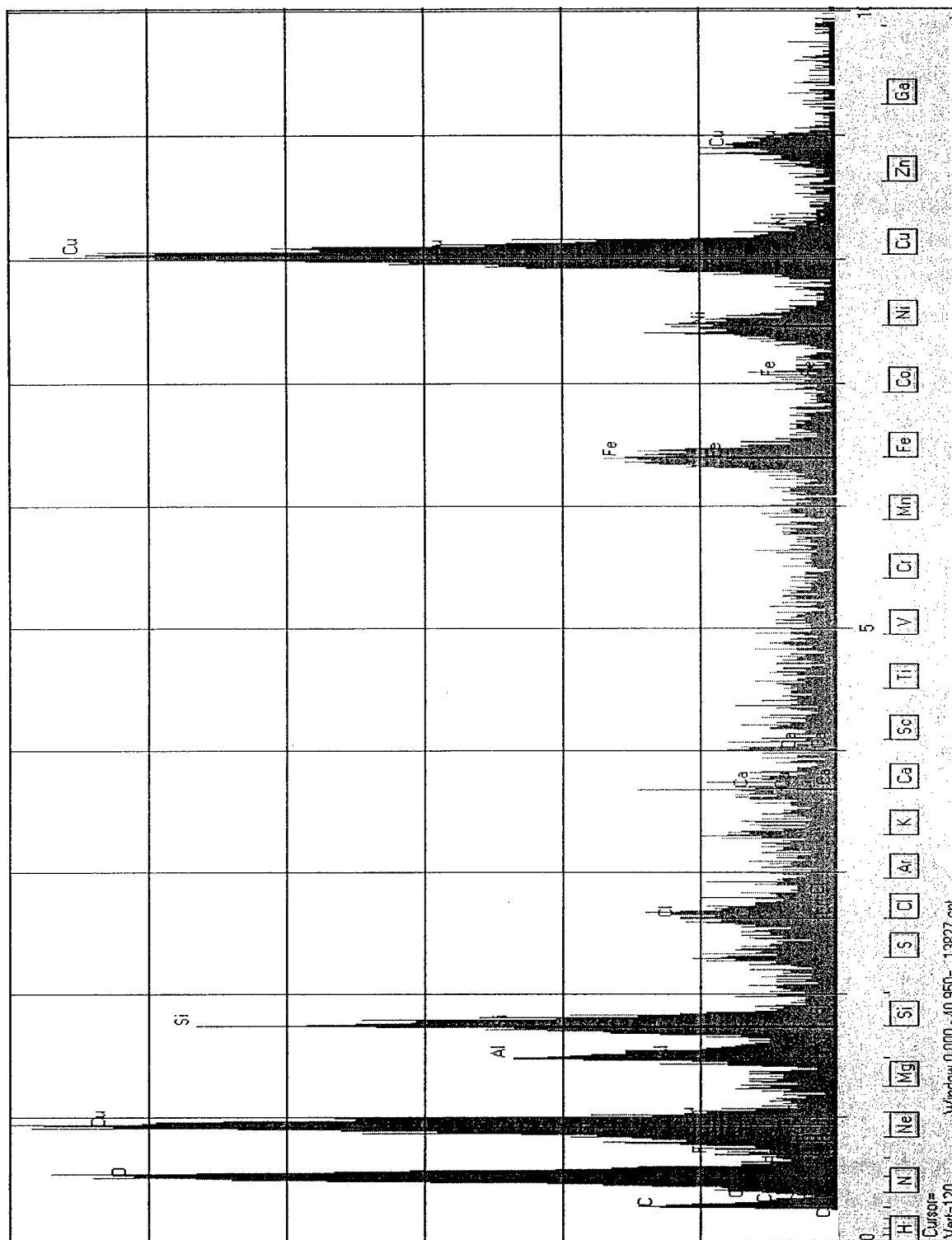


Figure C-29: EDS Spectrum A42b

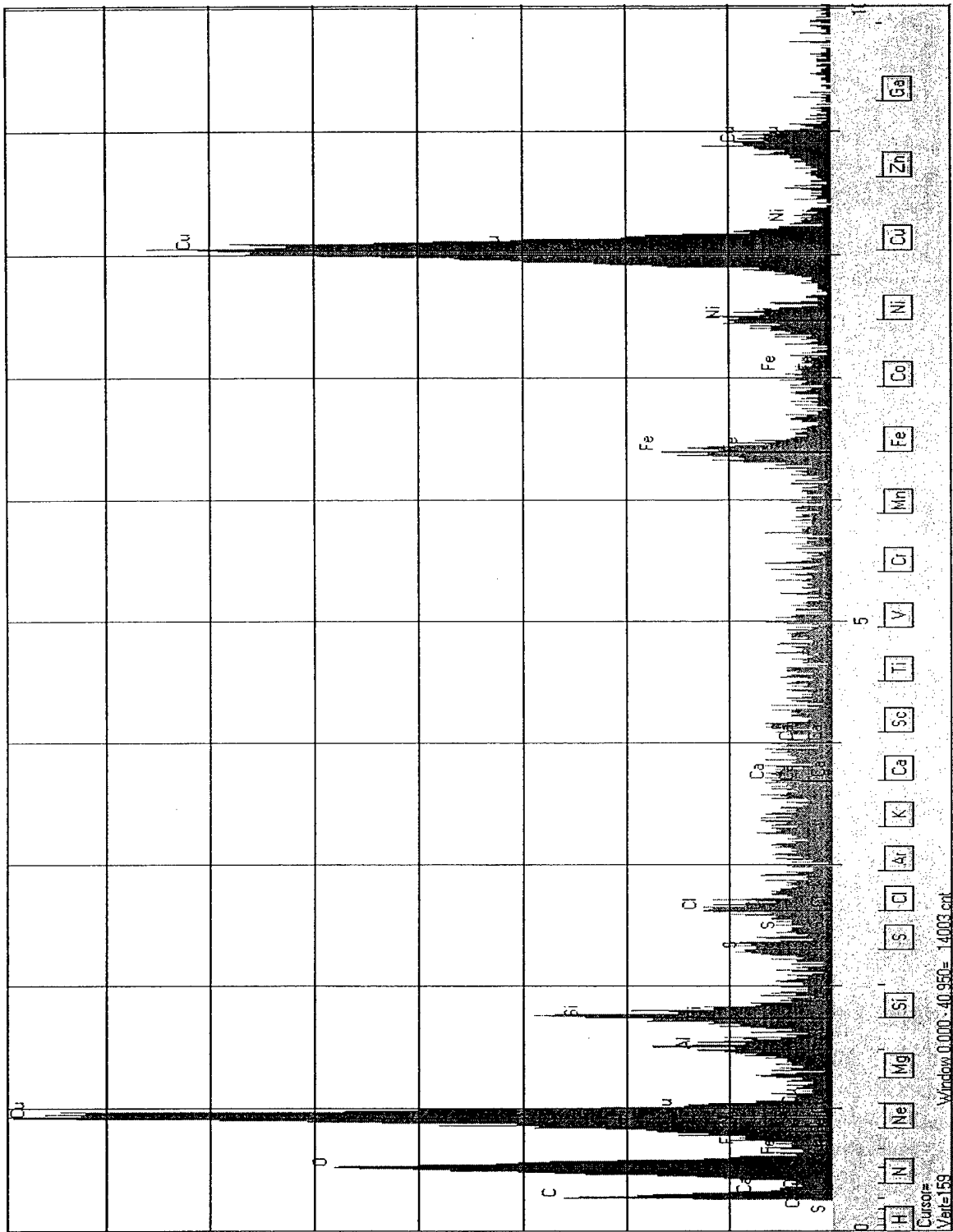


Figure C-30: EDS Spectrum A42c

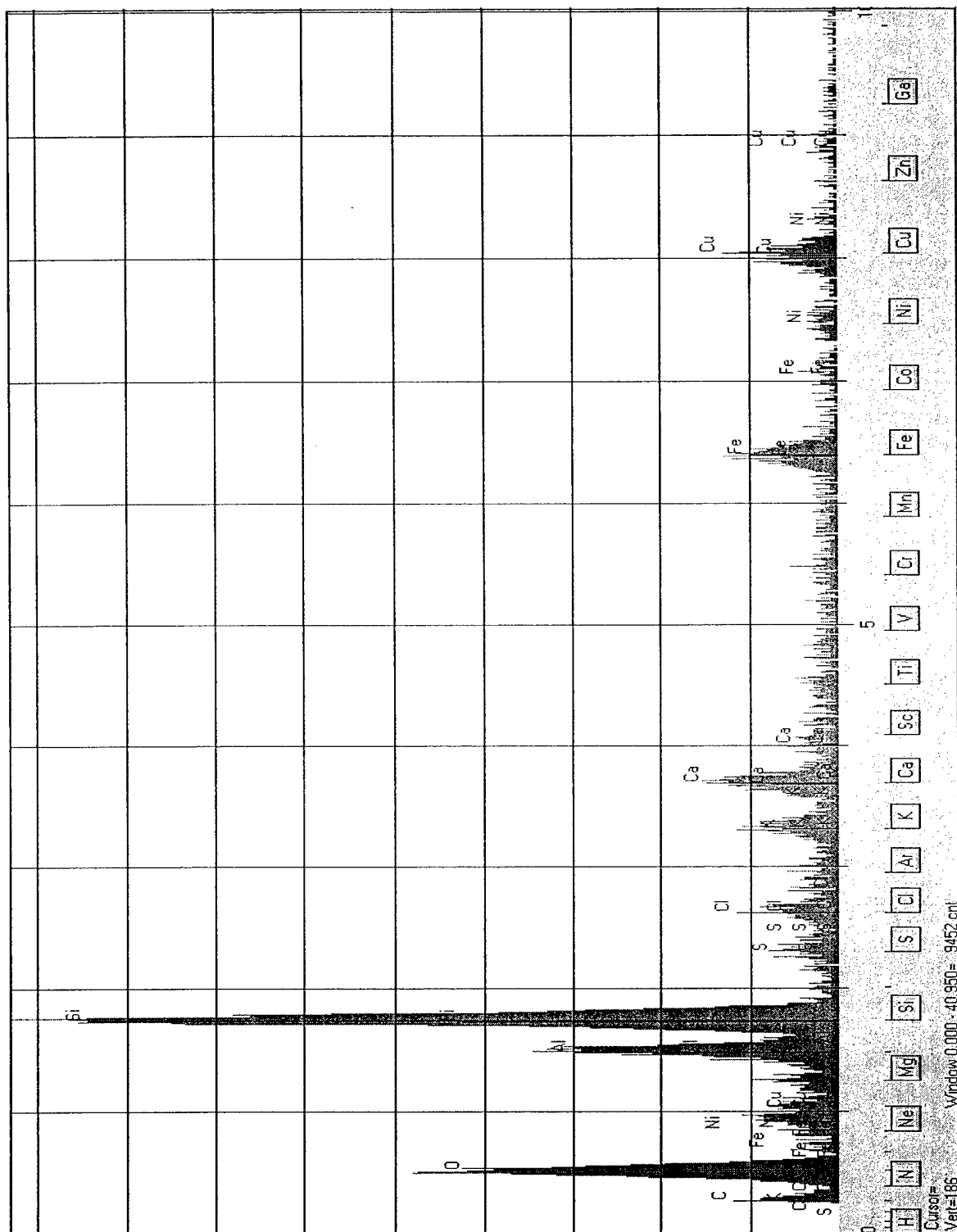


Figure C-31: EDS Spectrum A43a

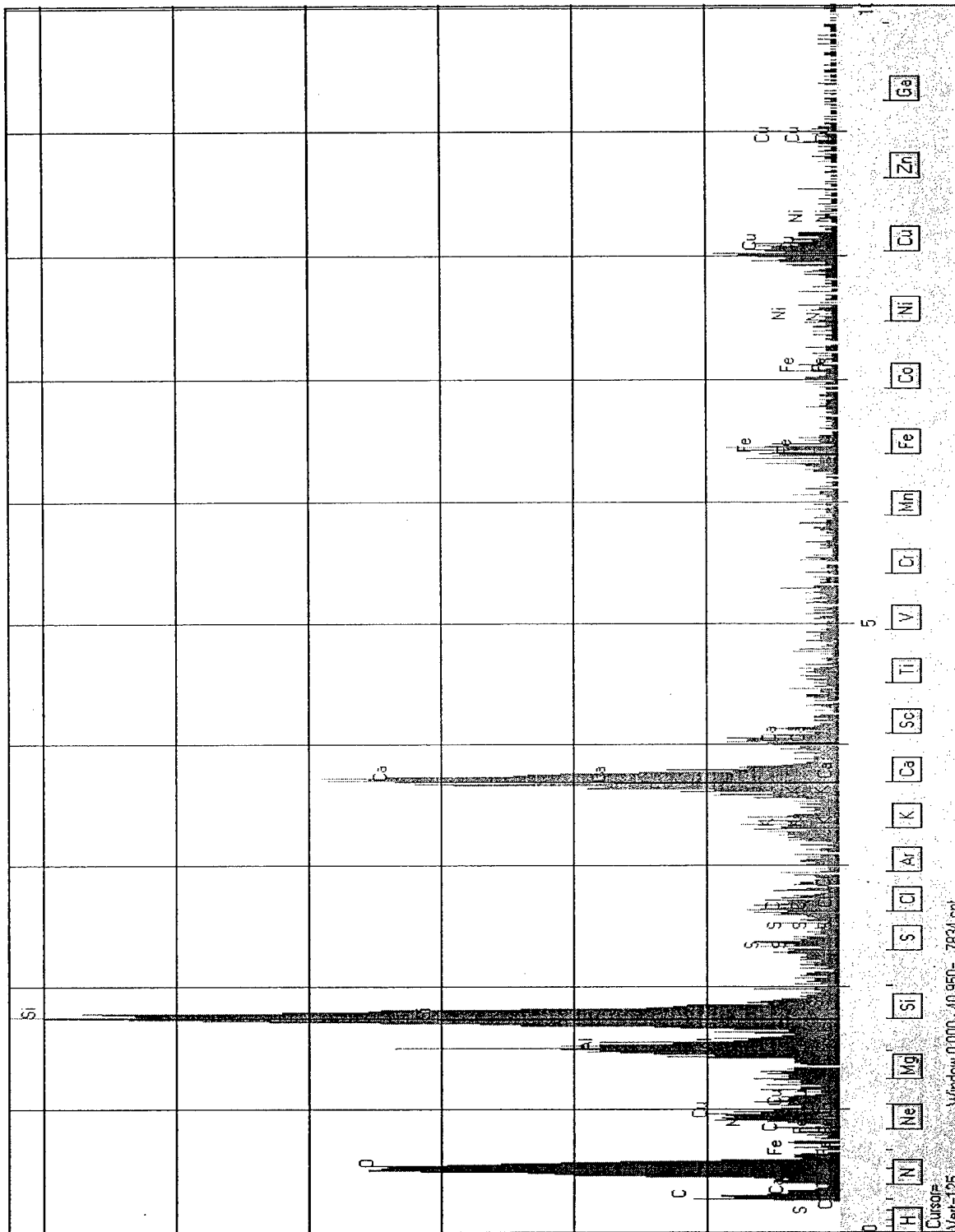


Figure C-32: EDS Spectrum A43b

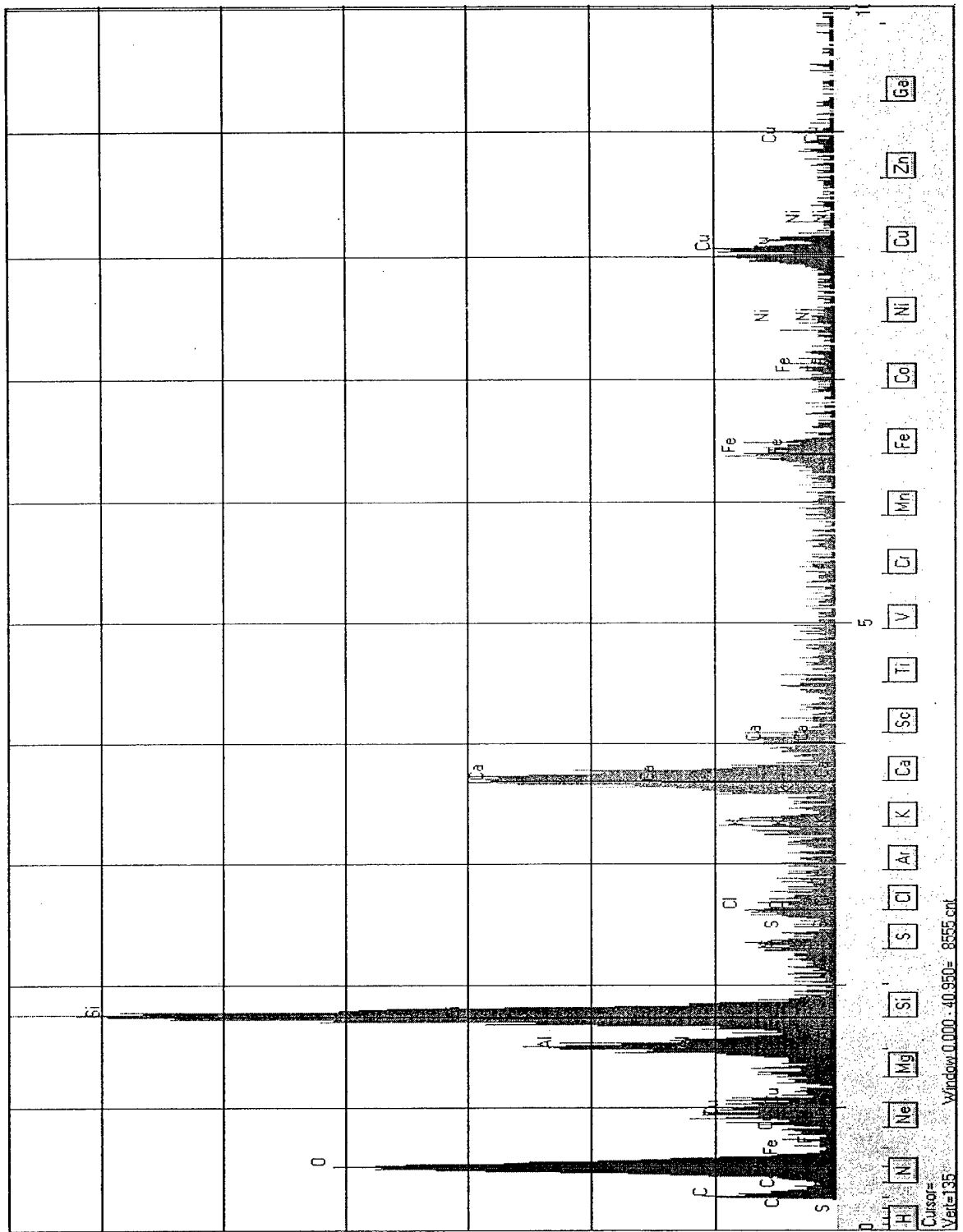


Figure C-33: EDS Spectrum A43c

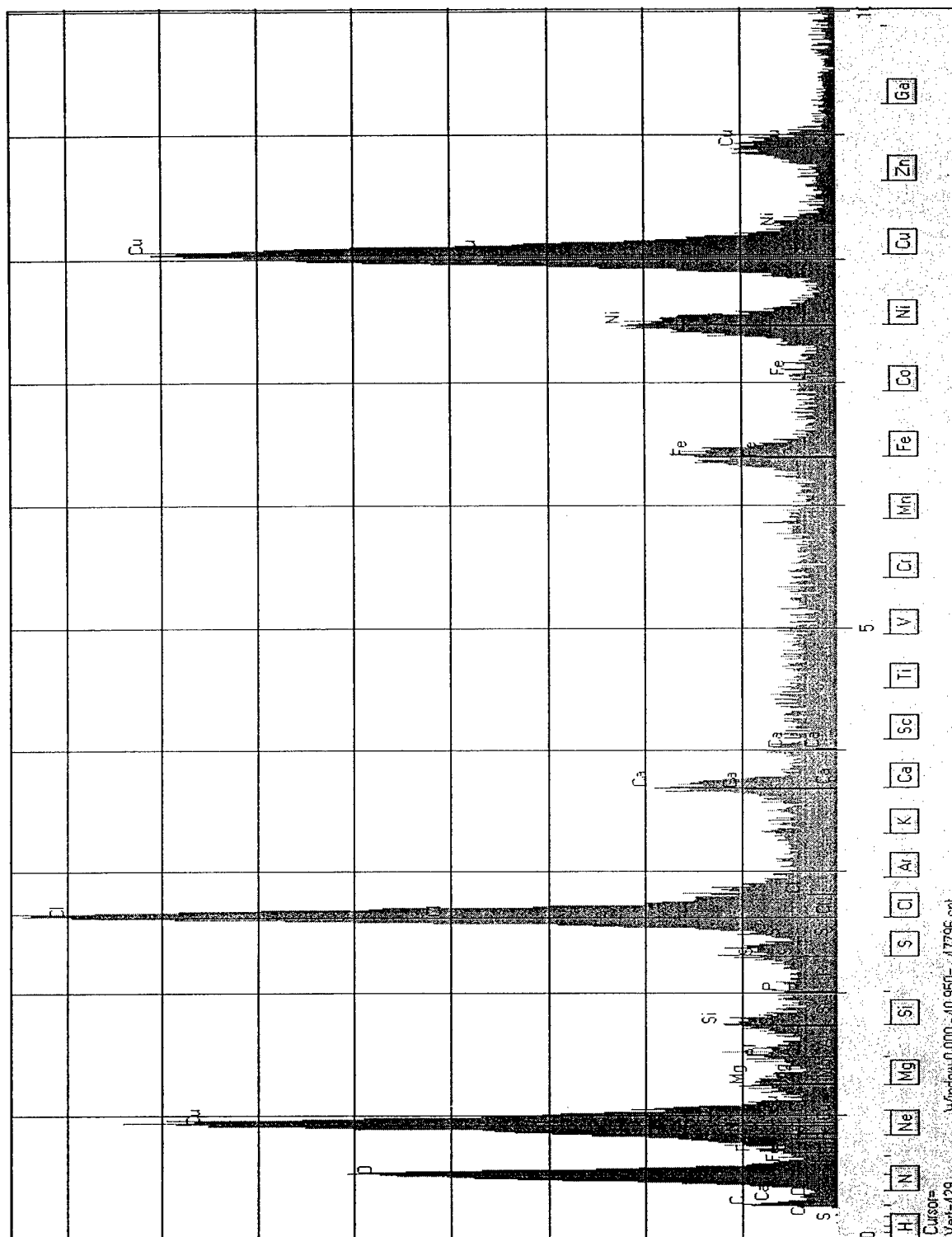


Figure C-34: EDS Spectrum C31

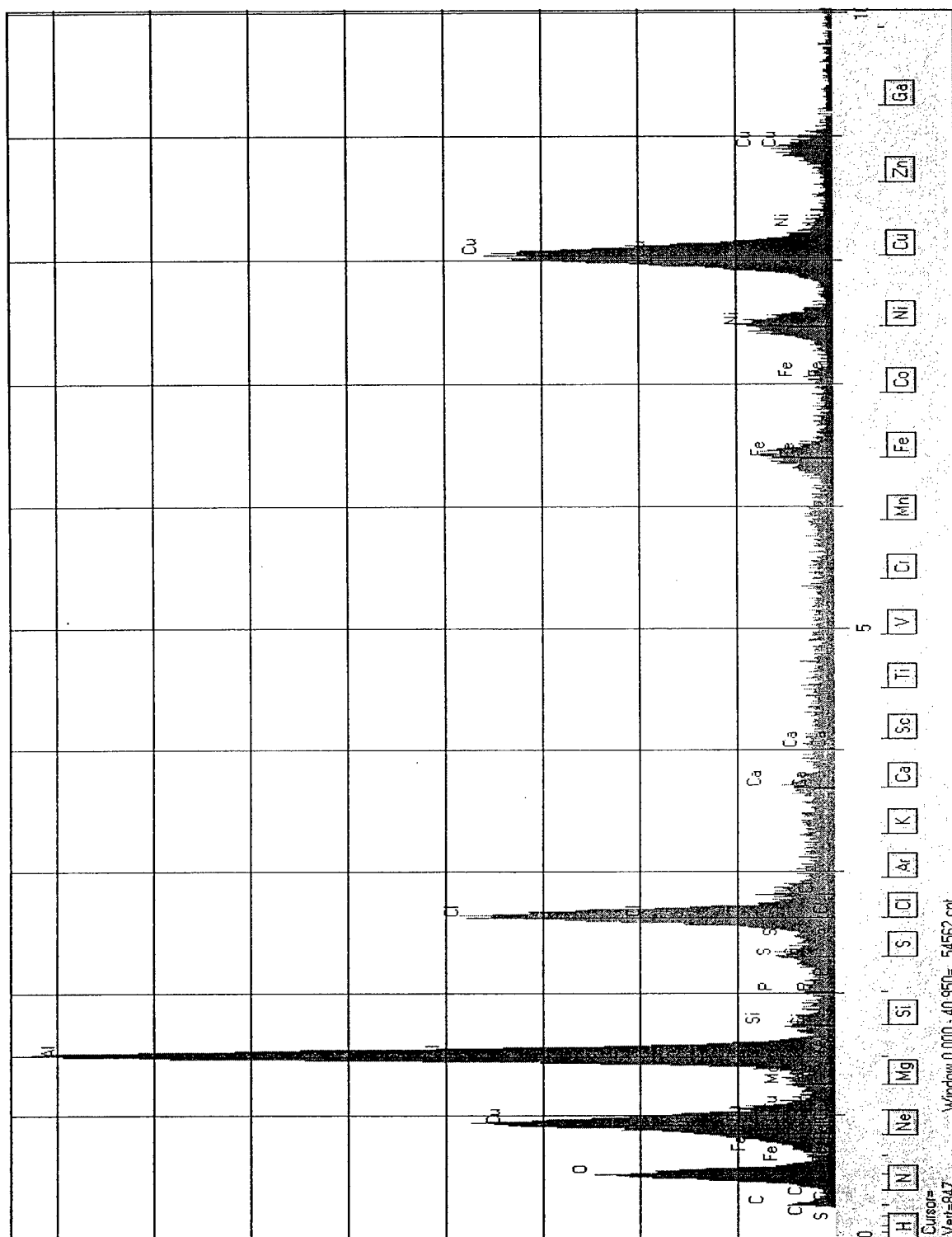


Figure C-35: EDS Spectrum C32

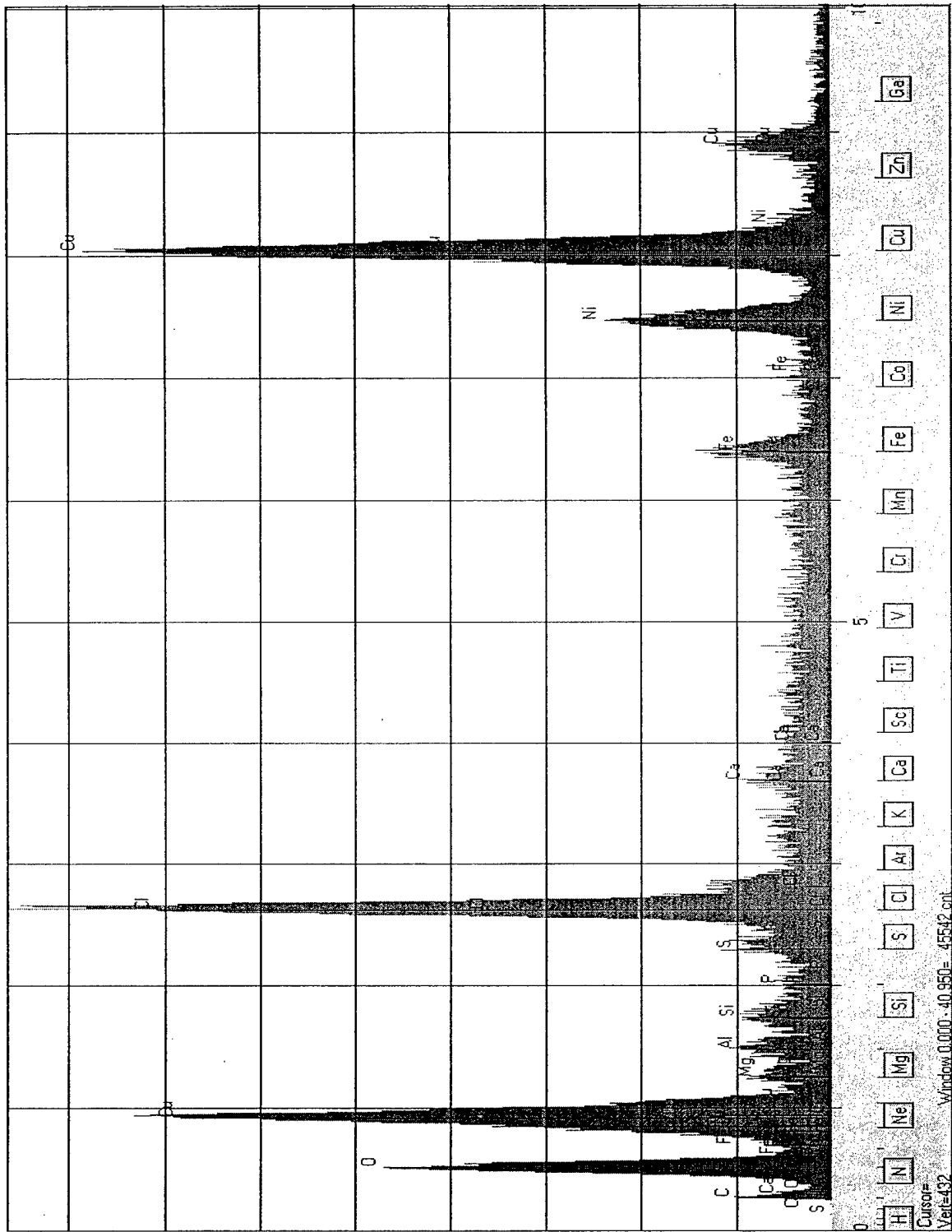


Figure C-36: EDS Spectrum C33



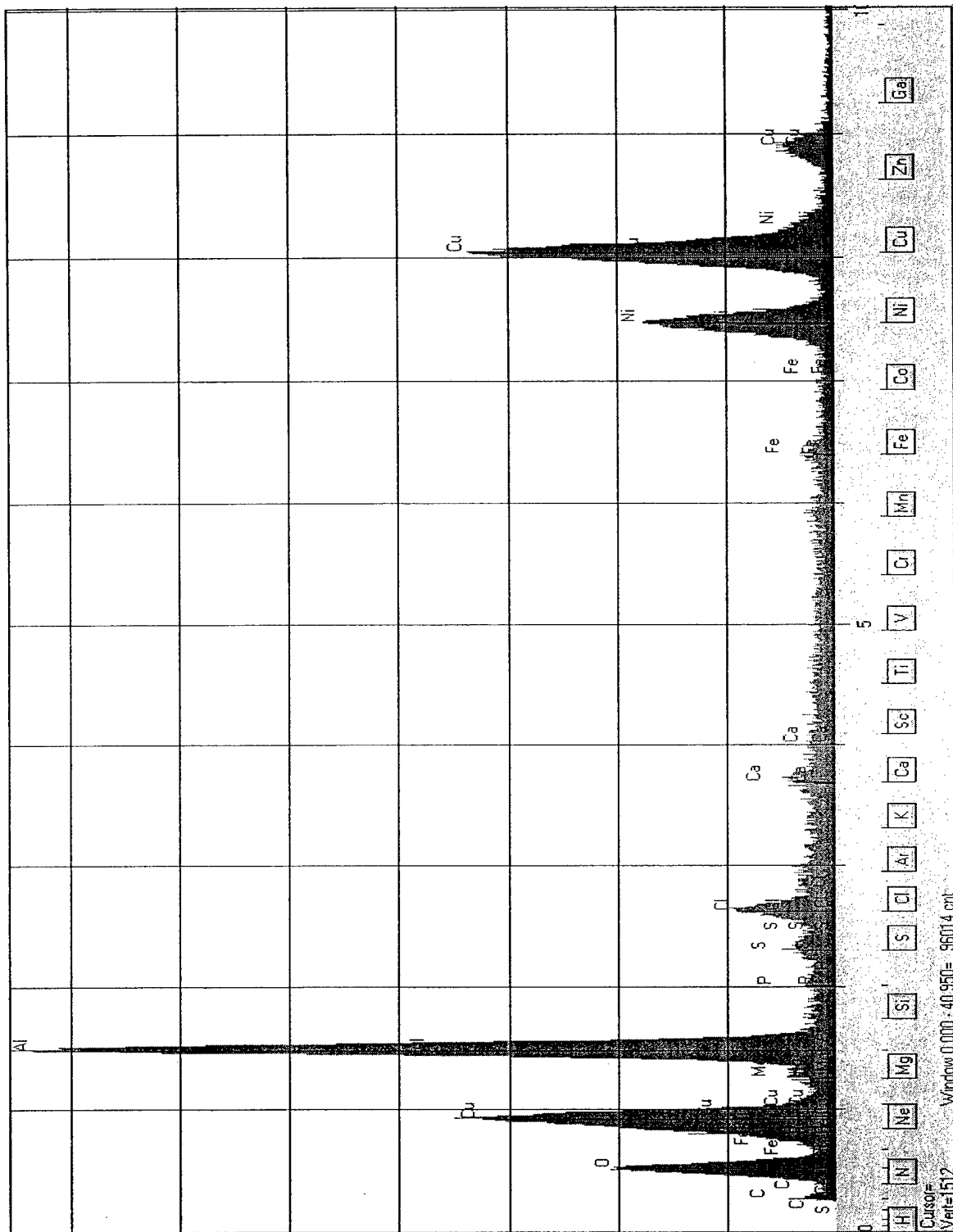


Figure C-38: EDS Spectrum C42

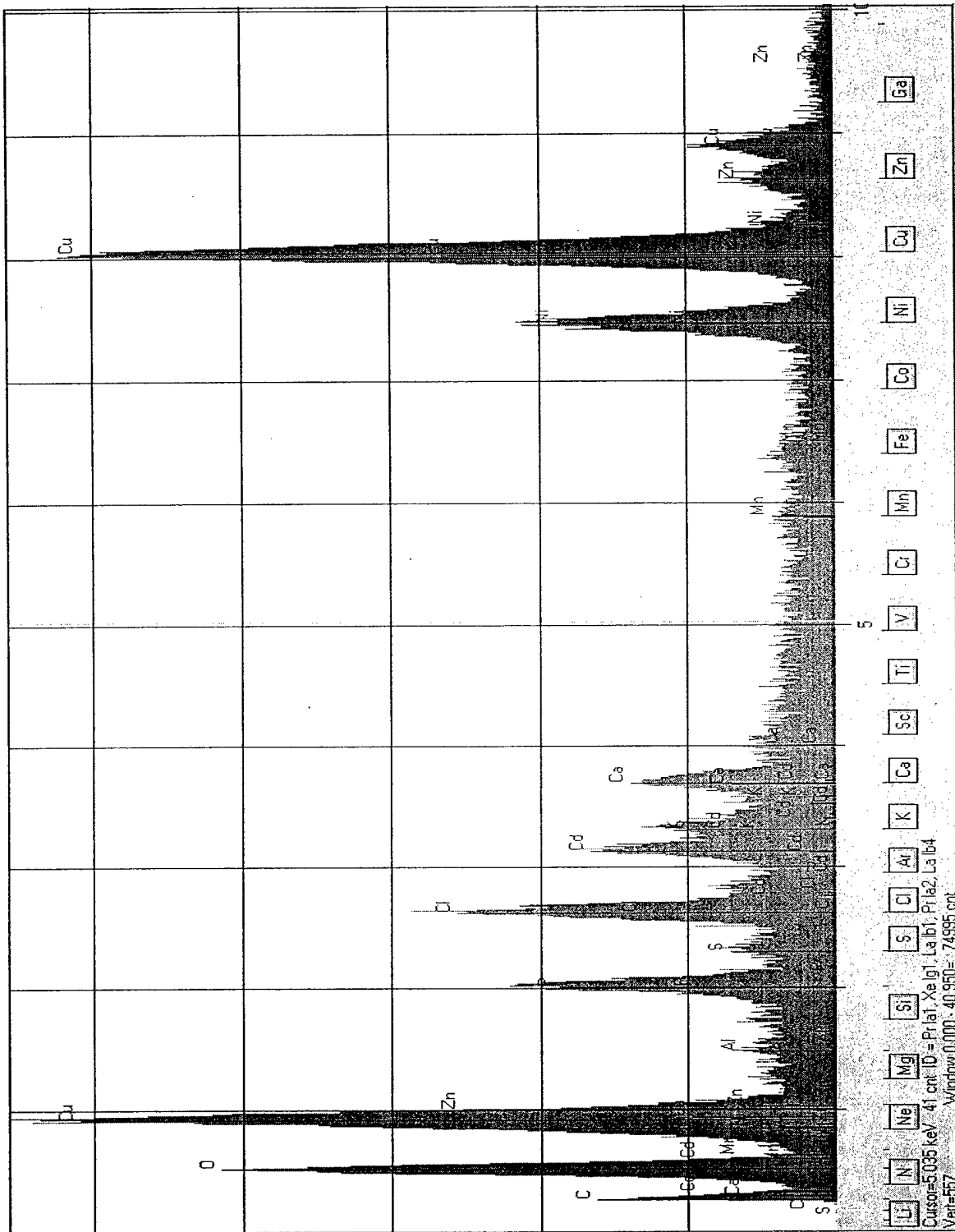


Figure C-39: EDS Spectrum C43

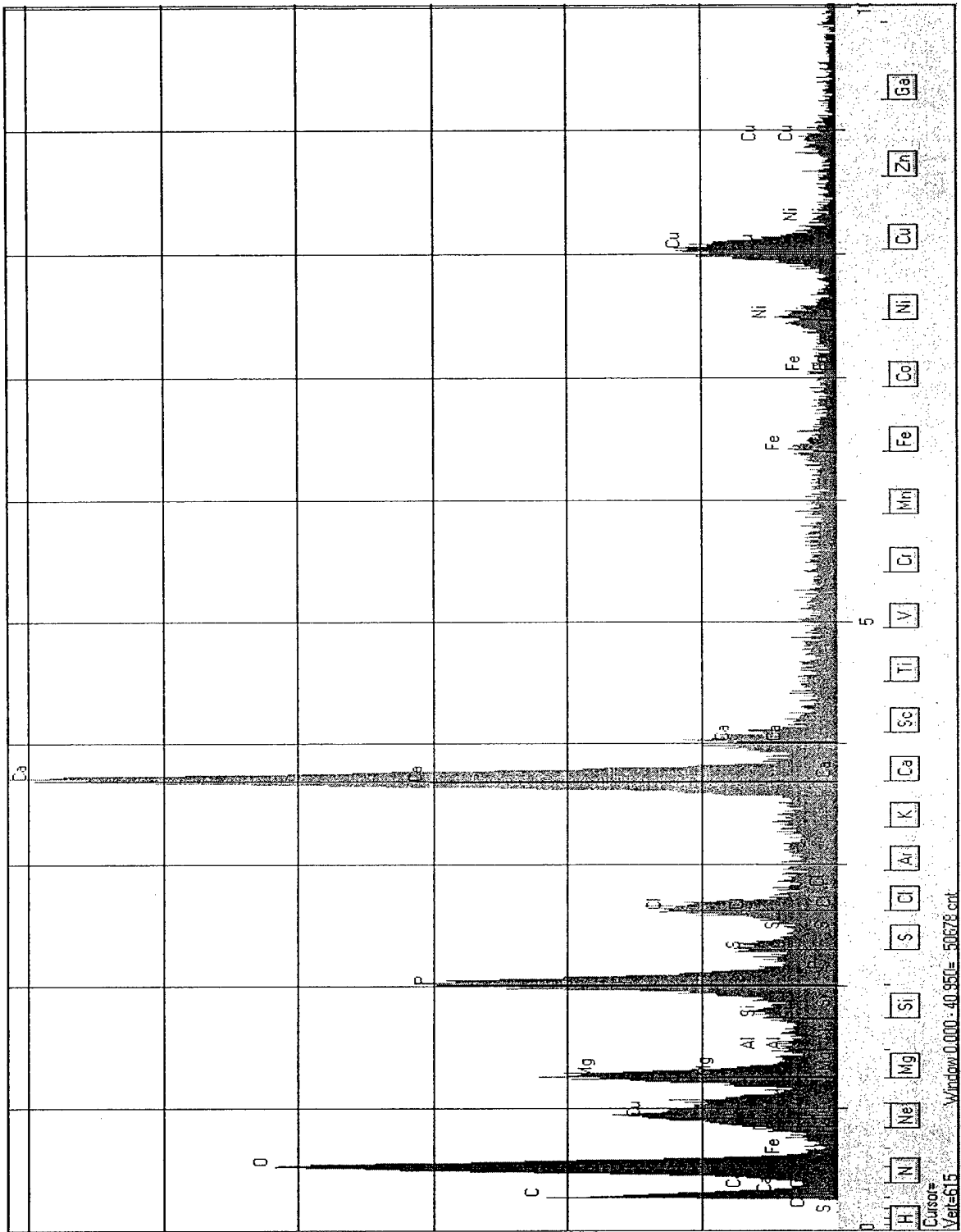


Figure C-40: EDS Spectrum C51

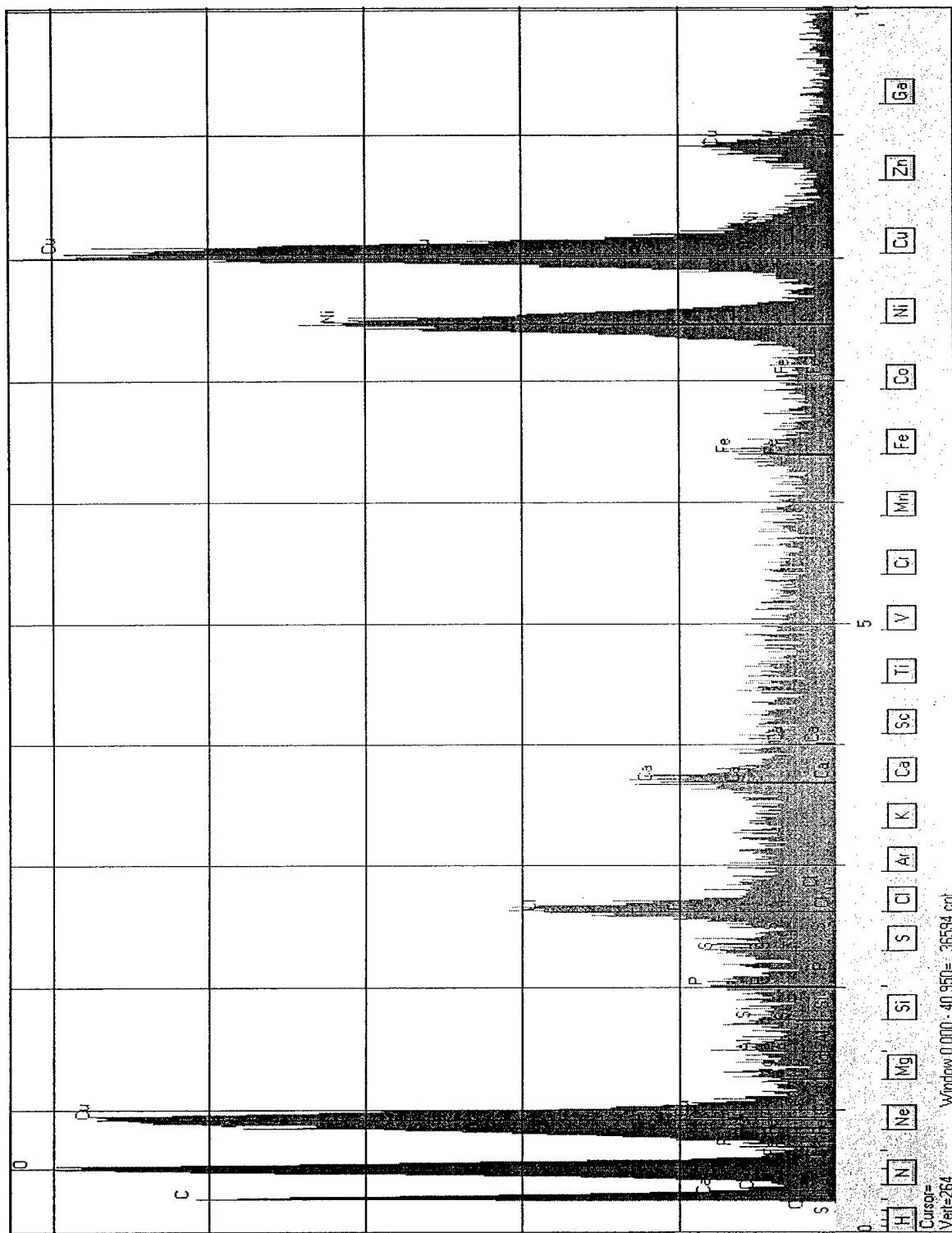


Figure C-41: EDS Spectrum C52

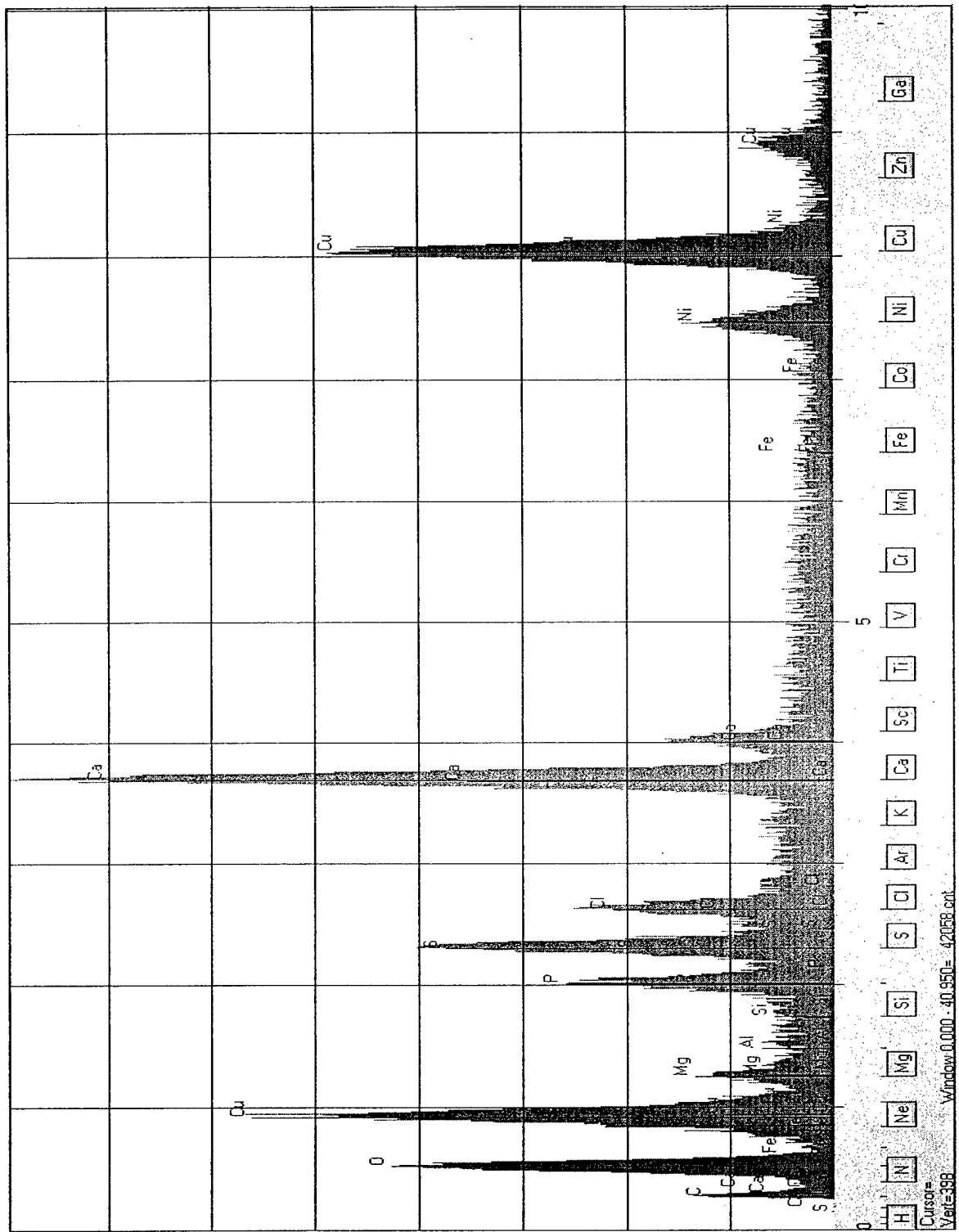


Figure C-42: EDS Spectrum C53

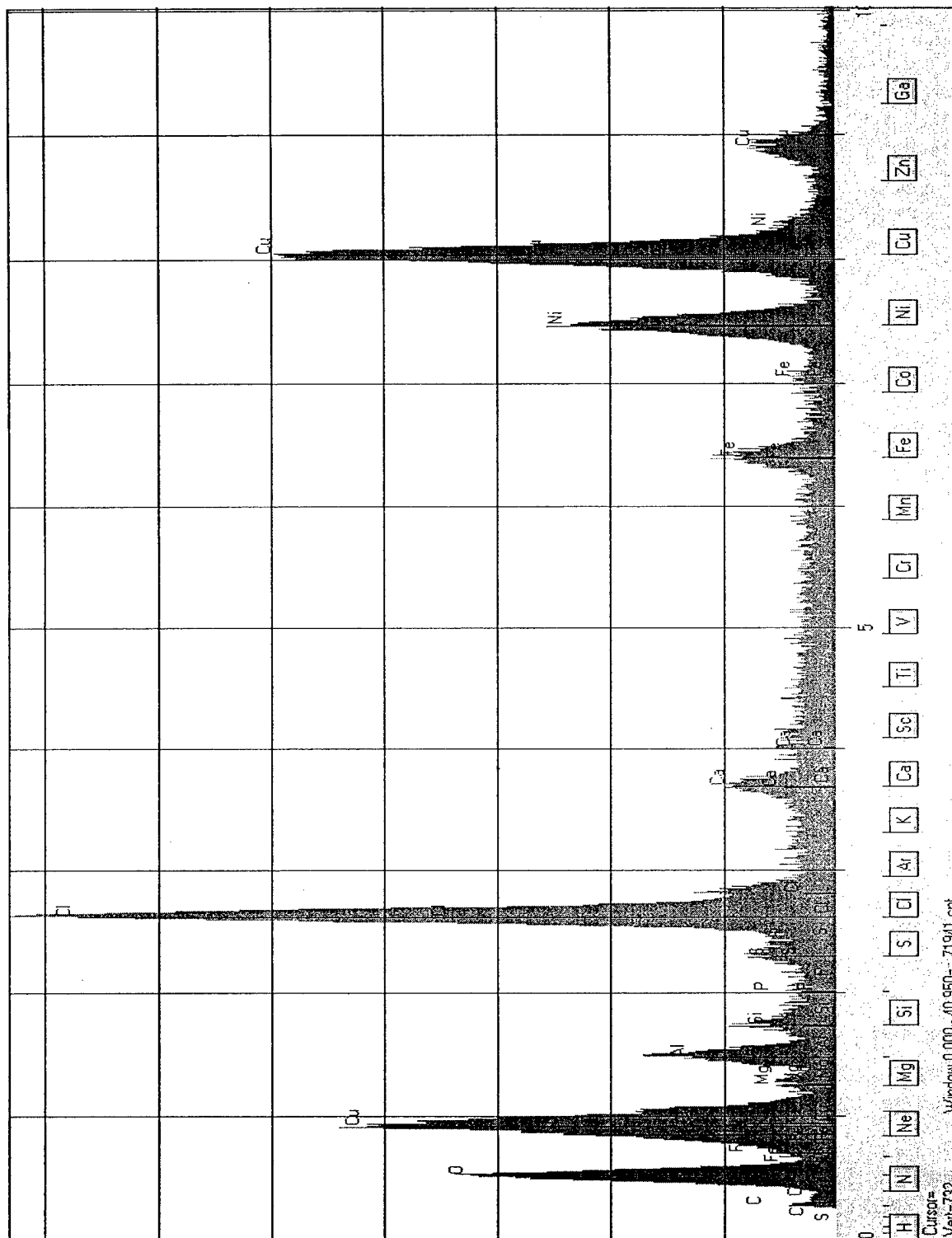


Figure C-43: EDS Spectrum C61

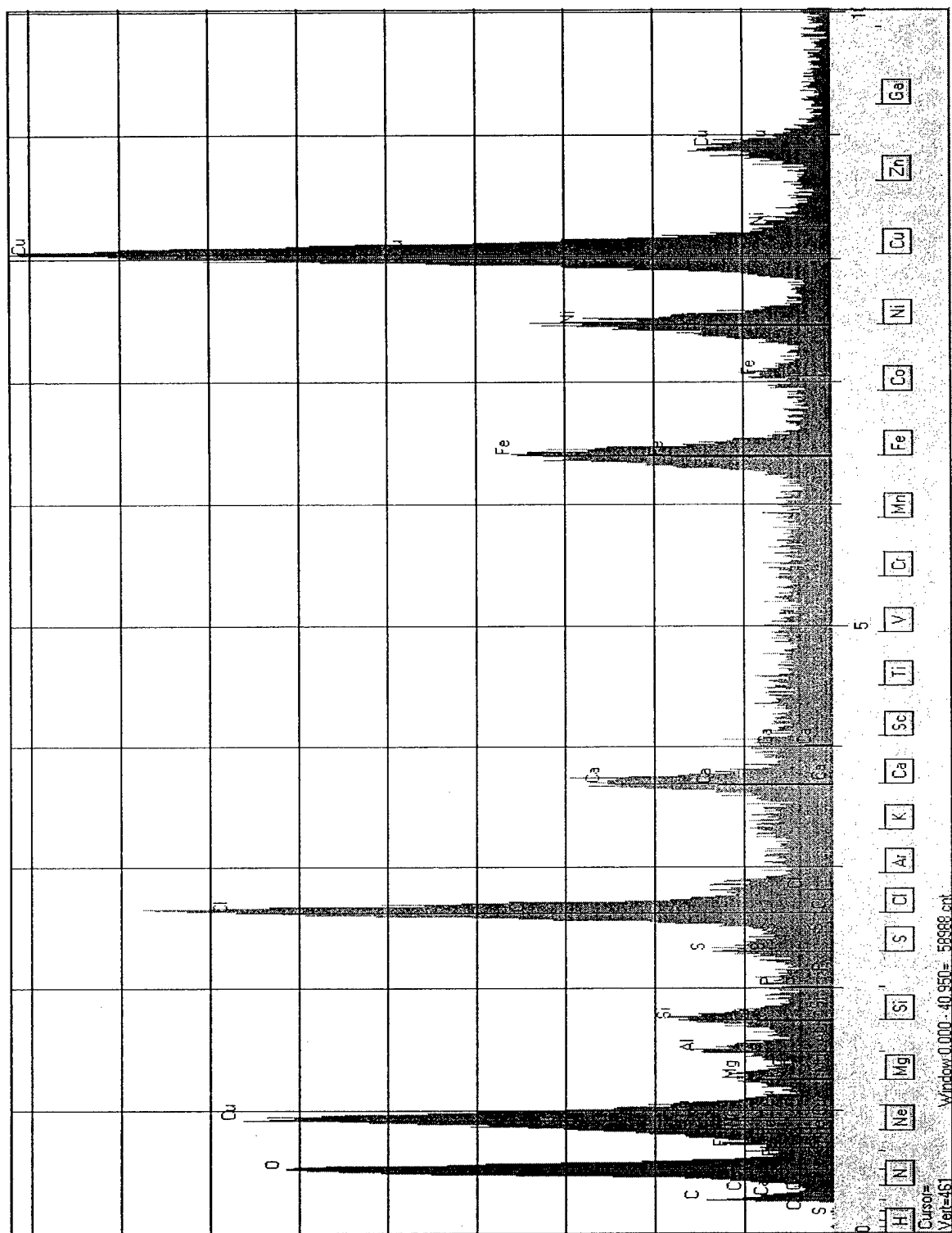


Figure C-44: EDS Spectrum C62

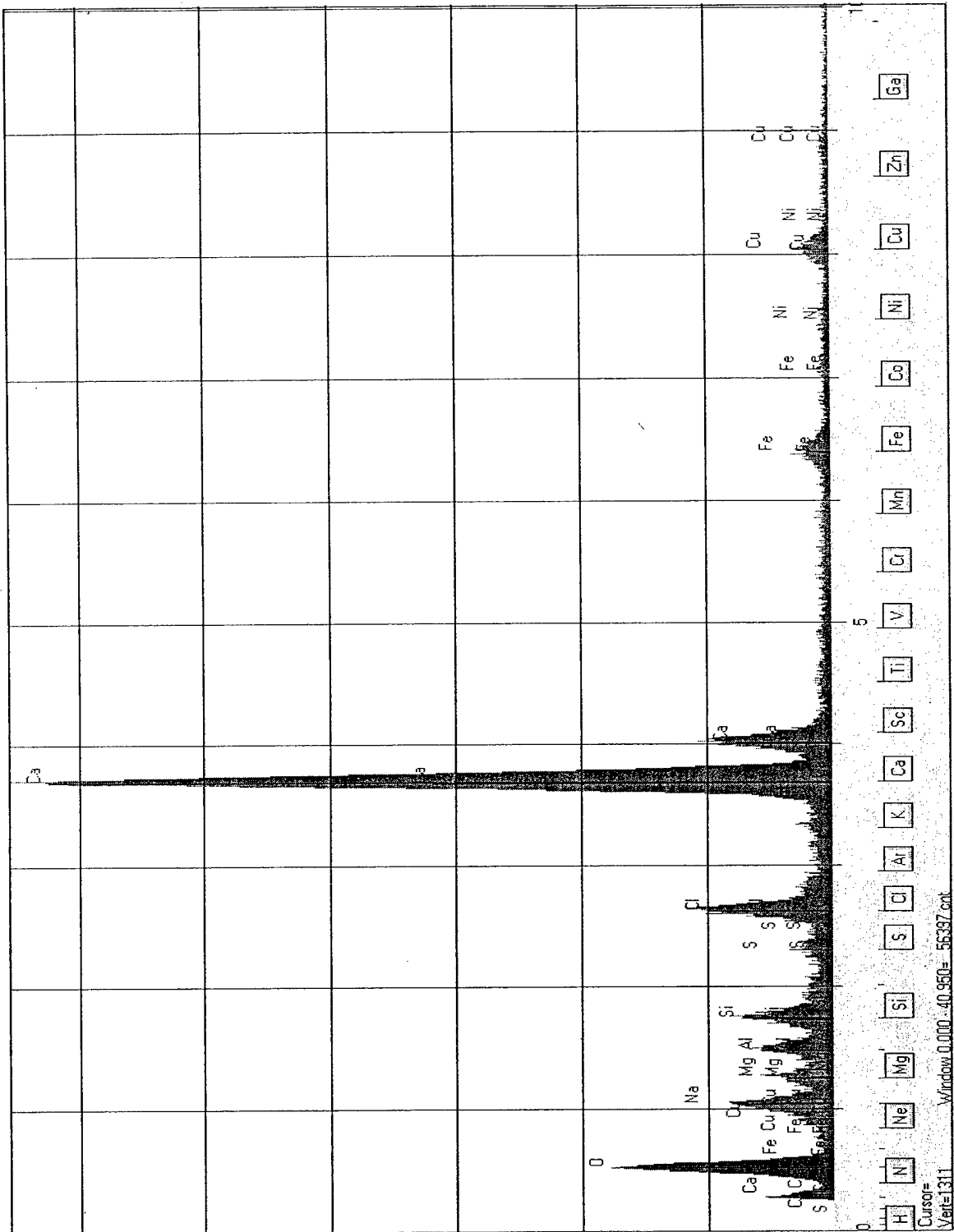


Figure C-45: EDS Spectrum C63

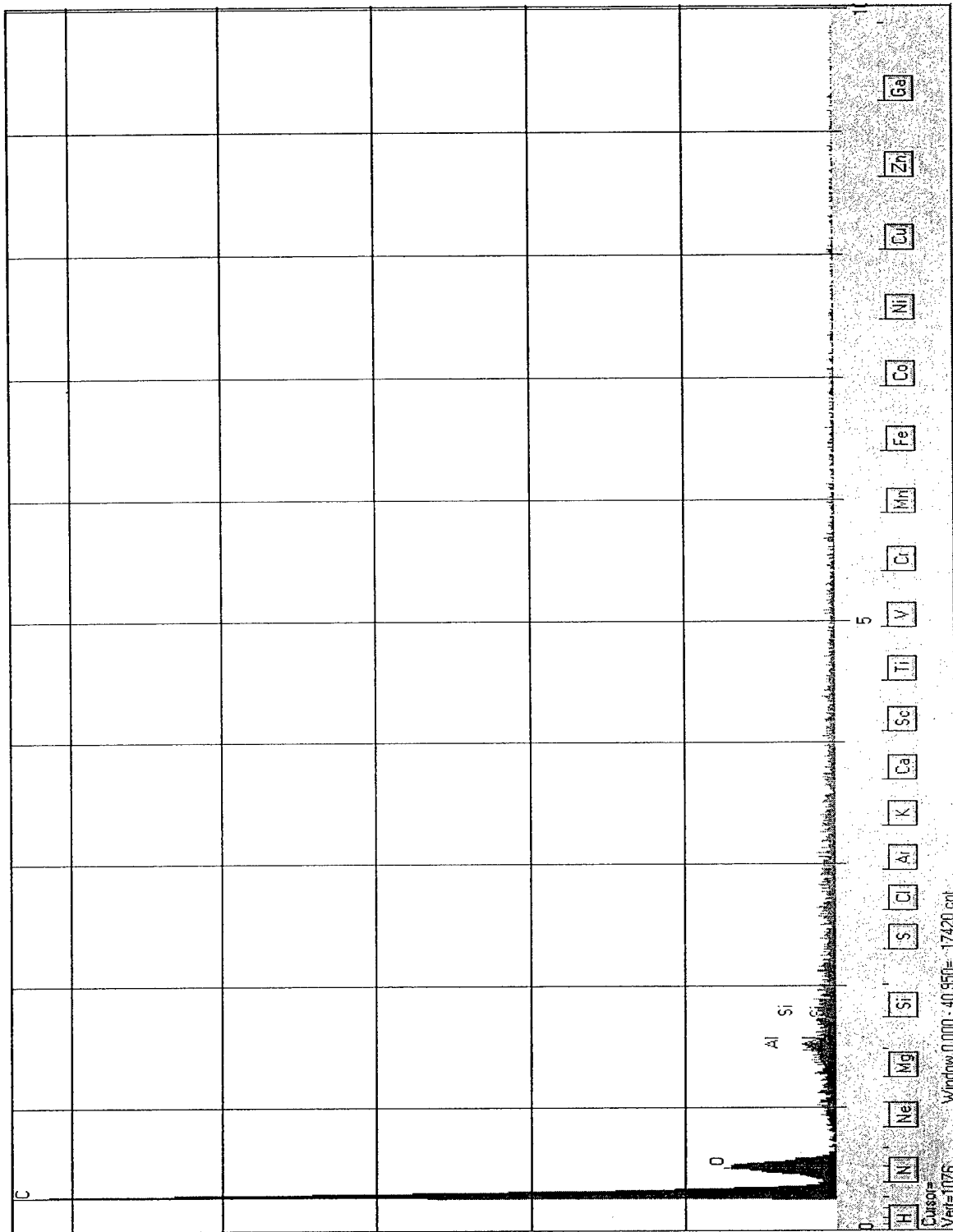


Figure C-46: EDS Spectrum Al Stub

## Appendix D

# EDS Spectra: Weldment Coupons

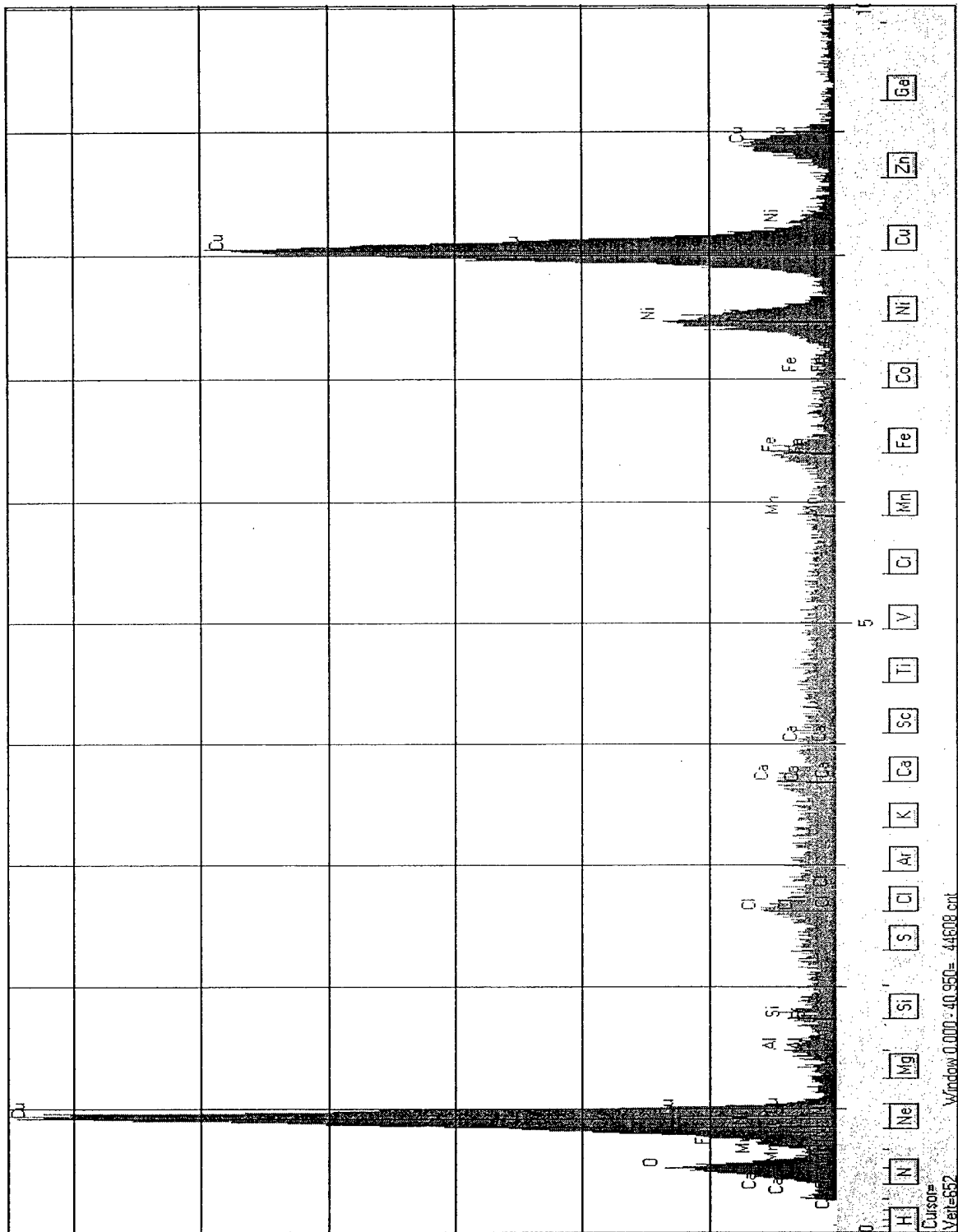


Figure D-1: EDS Spectrum Weld A2, Section 0-1, Base Metal

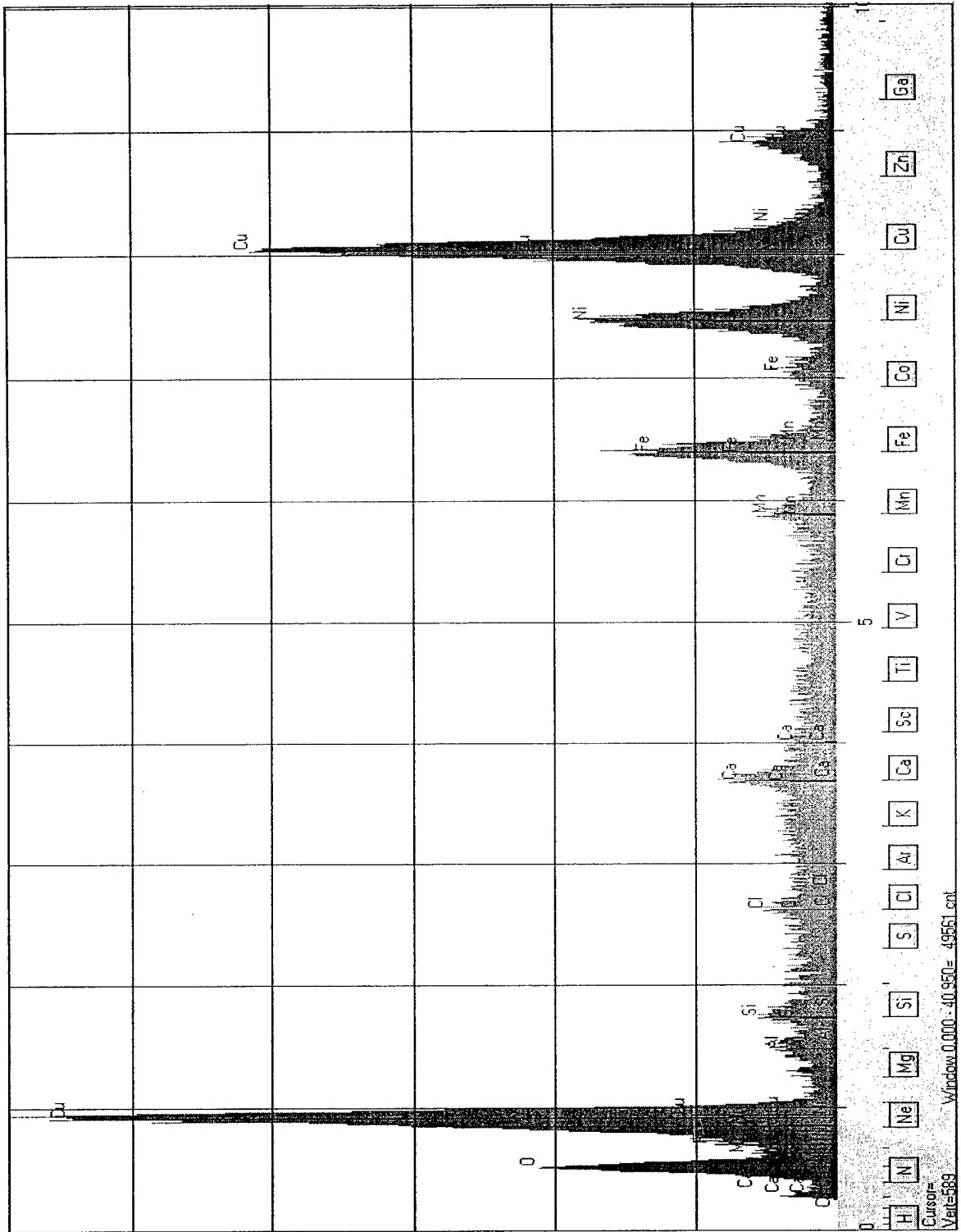


Figure D-2: EDS Spectrum Weld A2, Section 0-1, Weld Bead

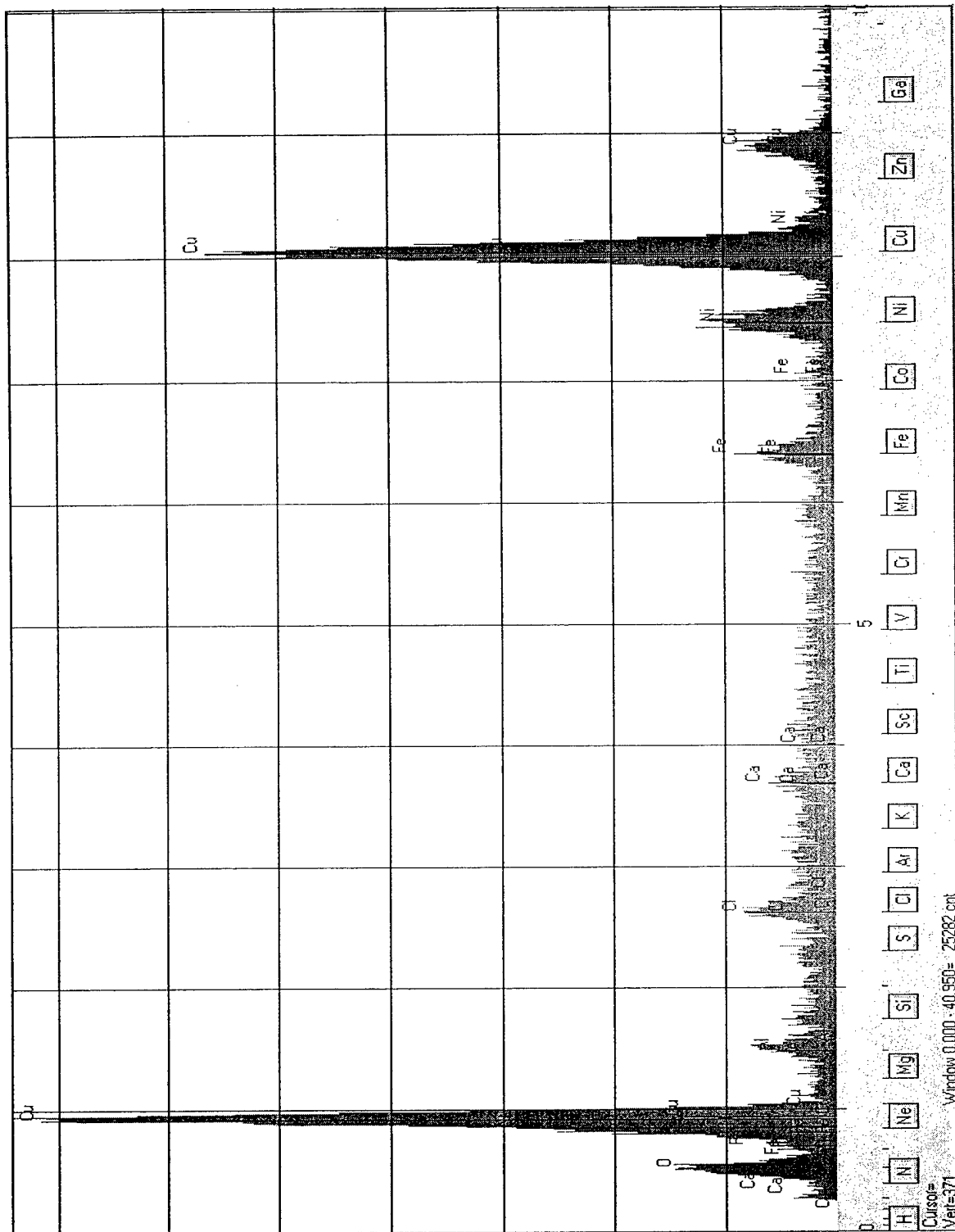


Figure D-3: EDS Spectrum Weld A3, Section 0-1, Base Metal

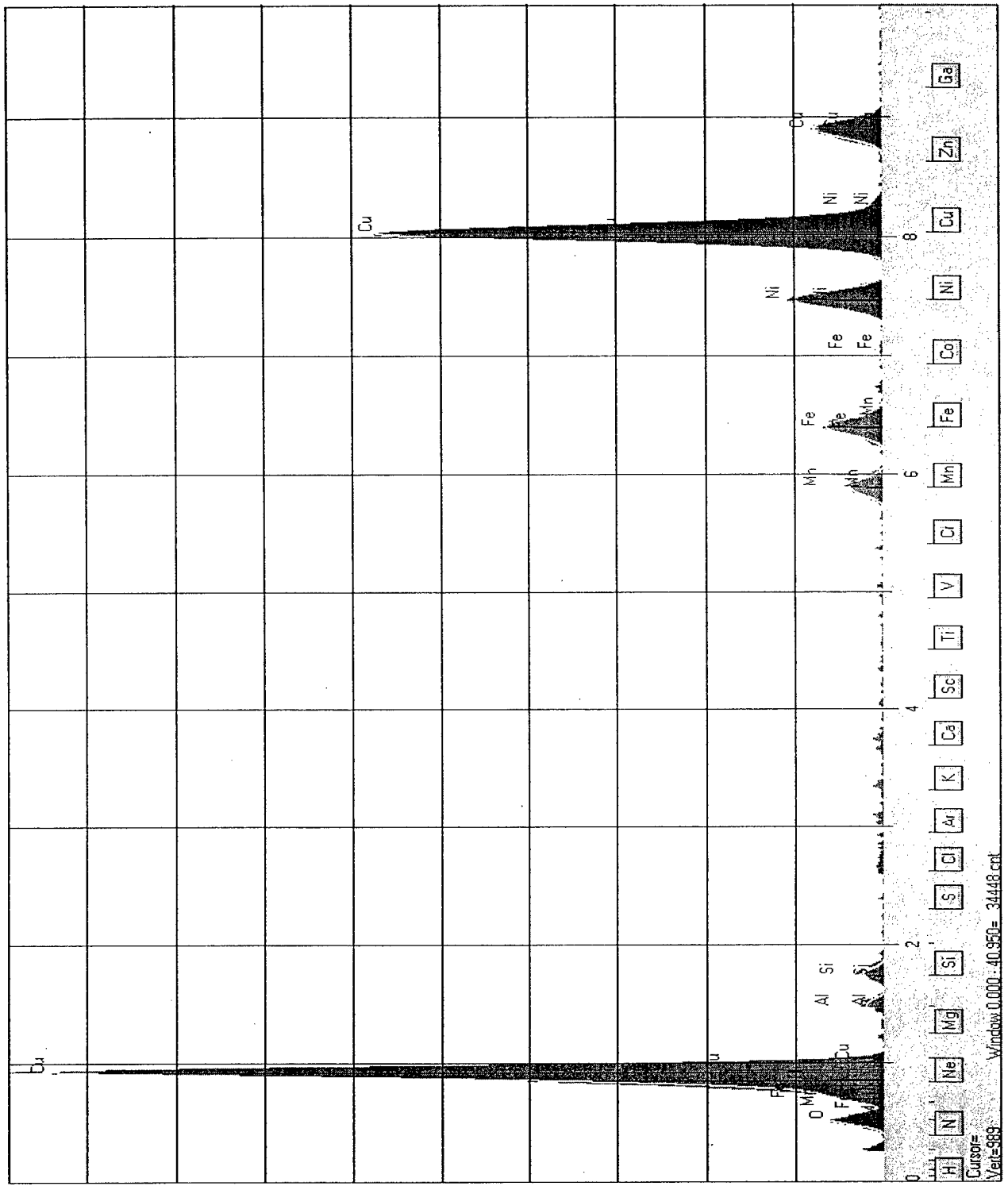


Figure D-4: EDS Spectrum Weld A3, Section 0-1, Weld Bead

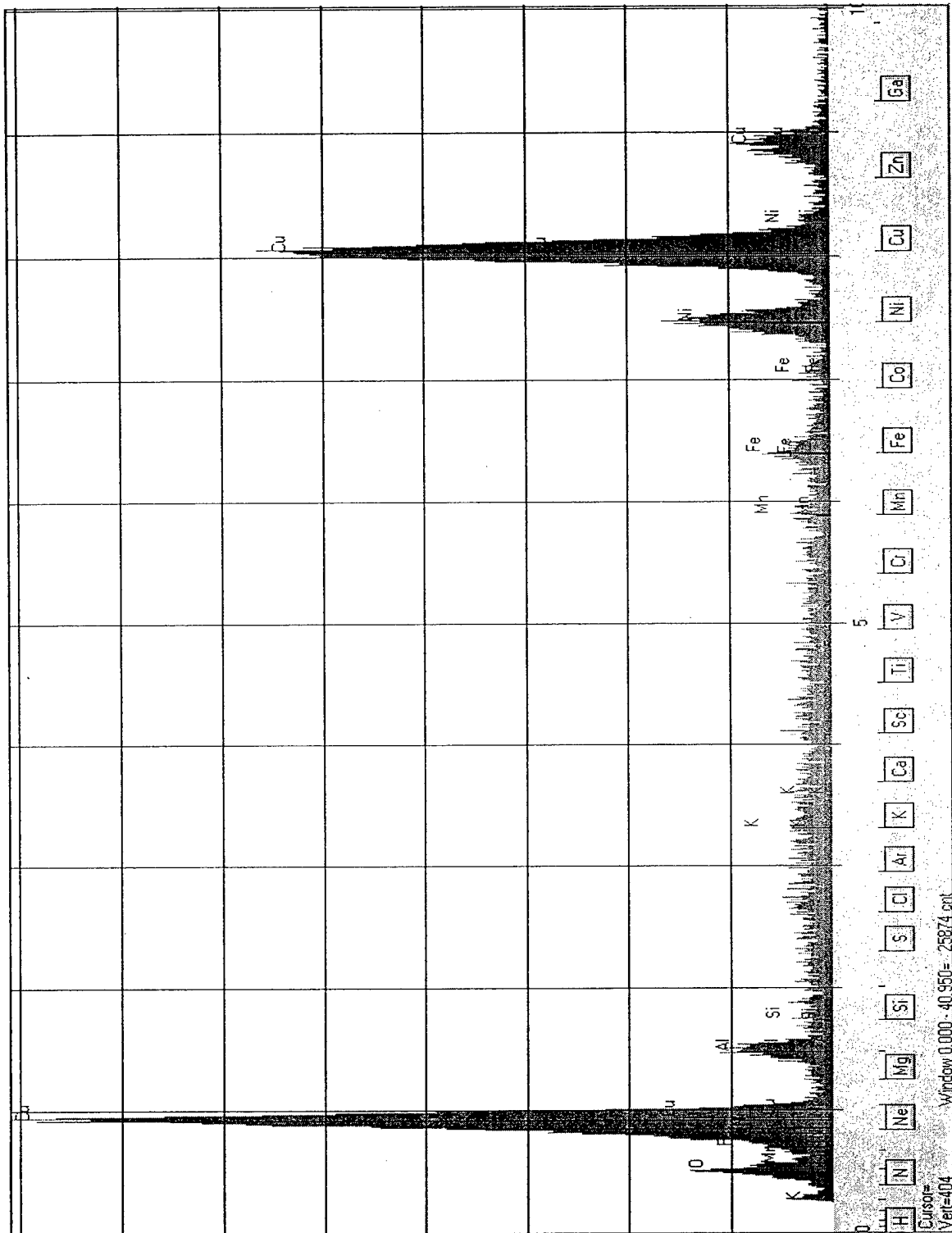


Figure D-5: EDS Spectrum Weld A4, Section 0-1, Base Metal

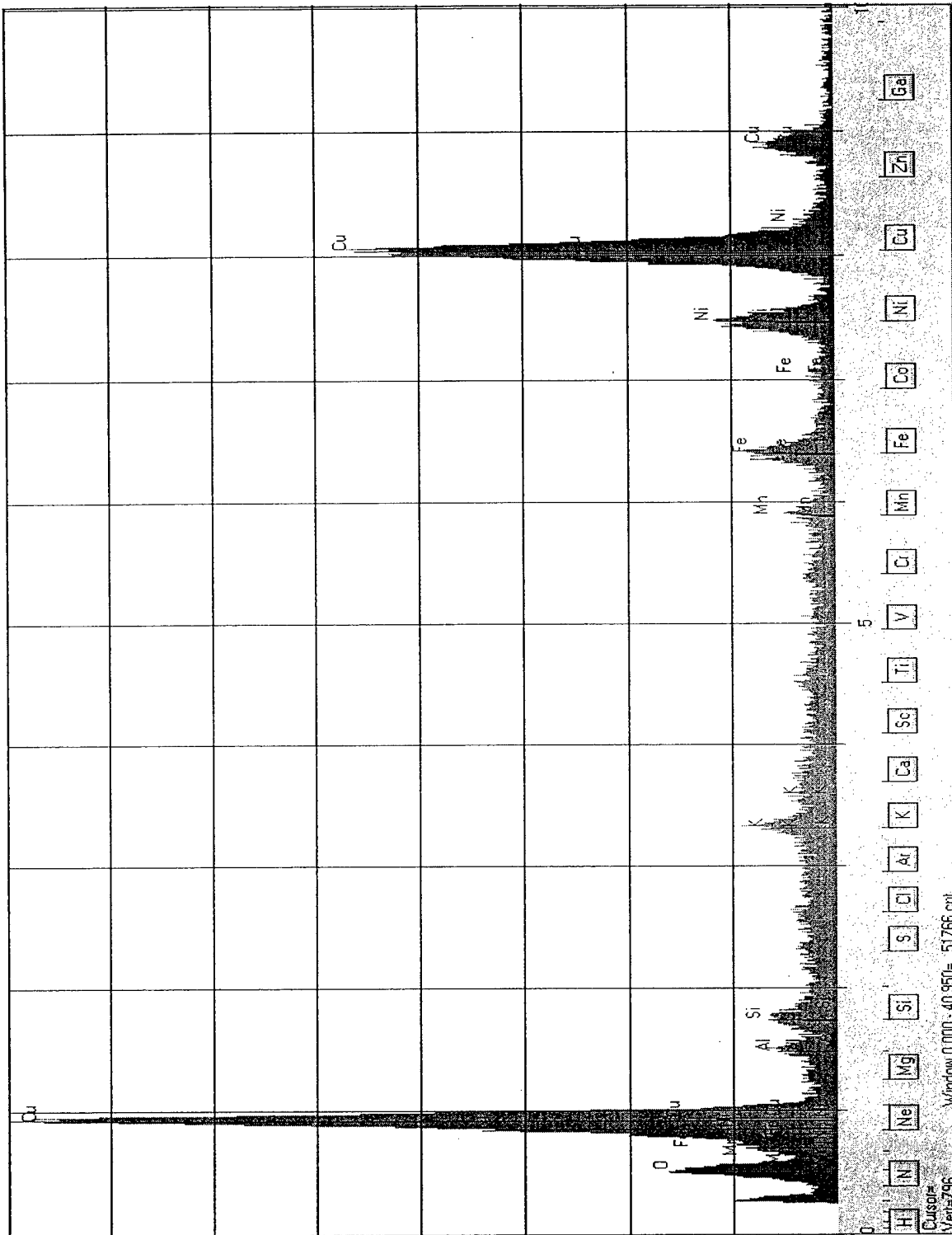


Figure D-6: EDS Spectrum Weld A4, Section 0-1, Weld Bead

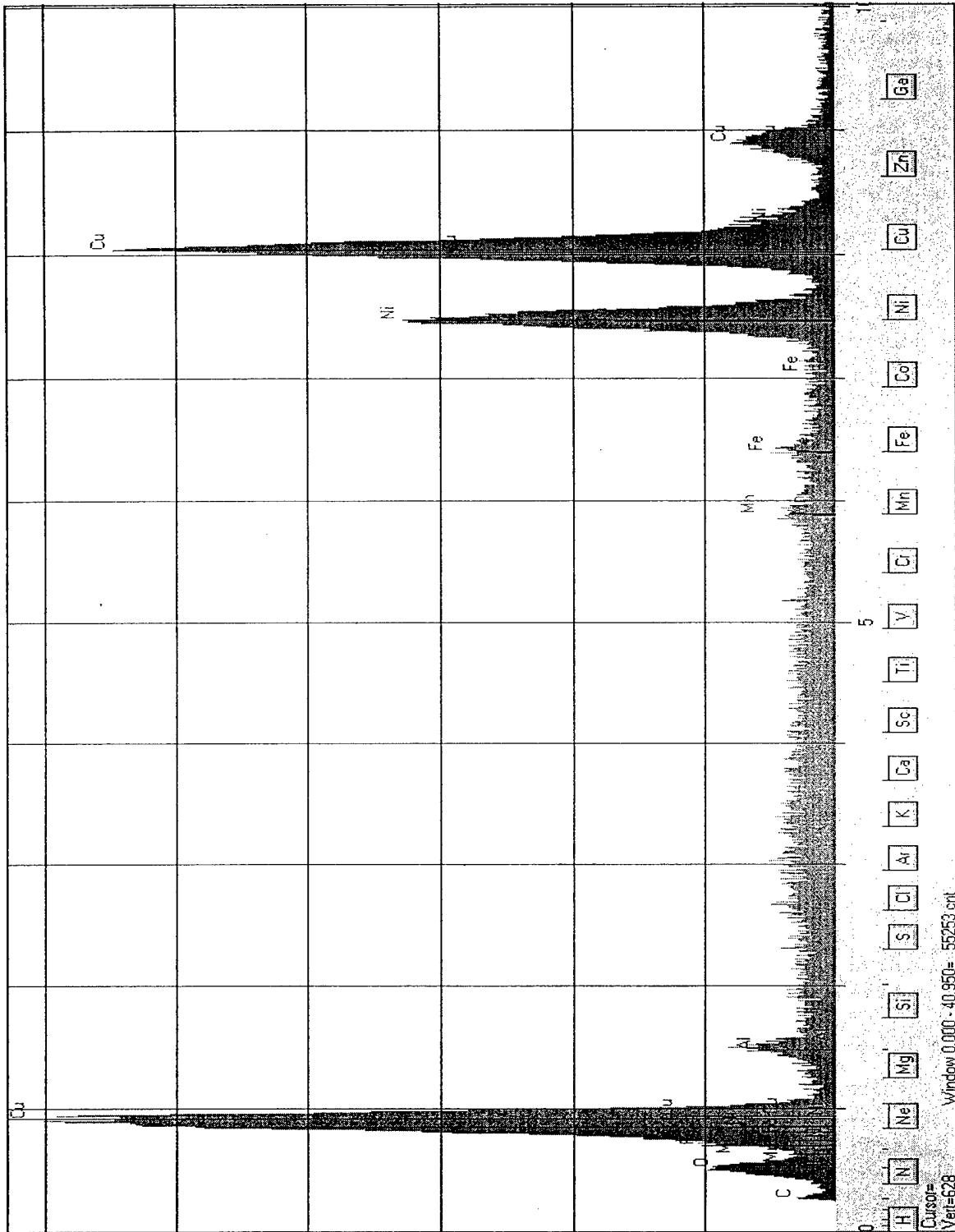


Figure D-7: EDS Spectrum Weld C4-A Base Metal

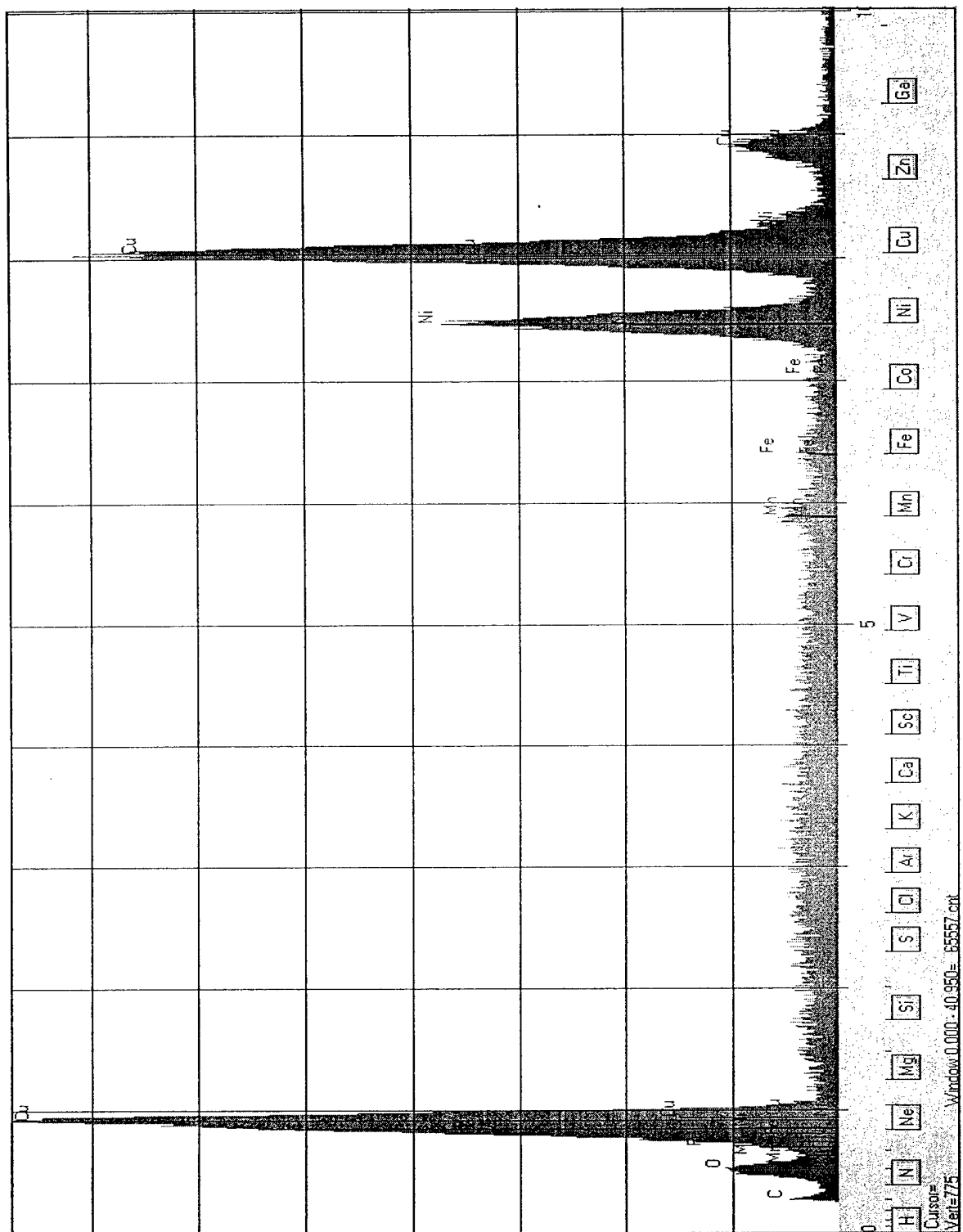


Figure D-8: EDS Spectrum Weld C4-A Weld Bead

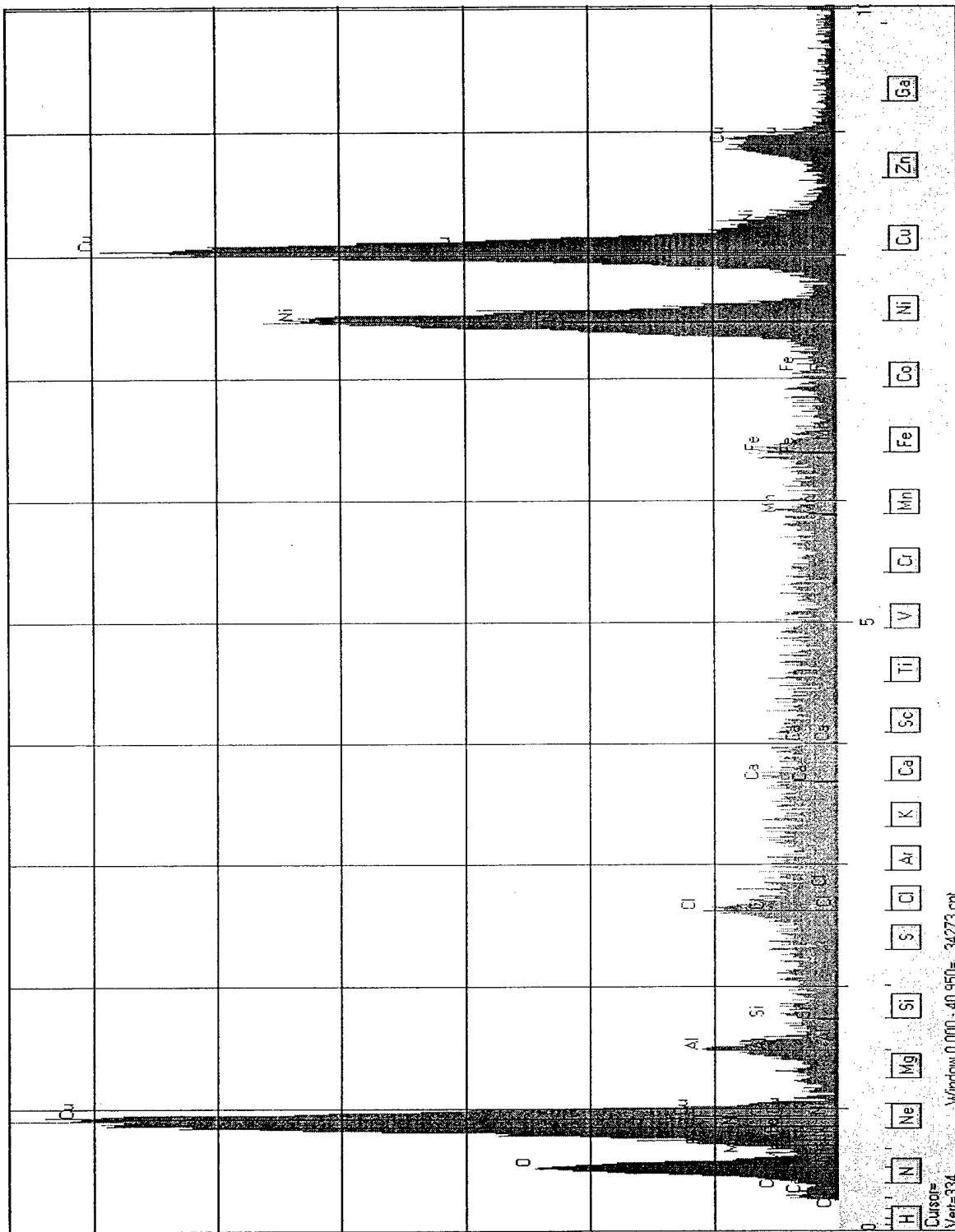


Figure D-9: EDS Spectrum Weld C6-A Base Metal

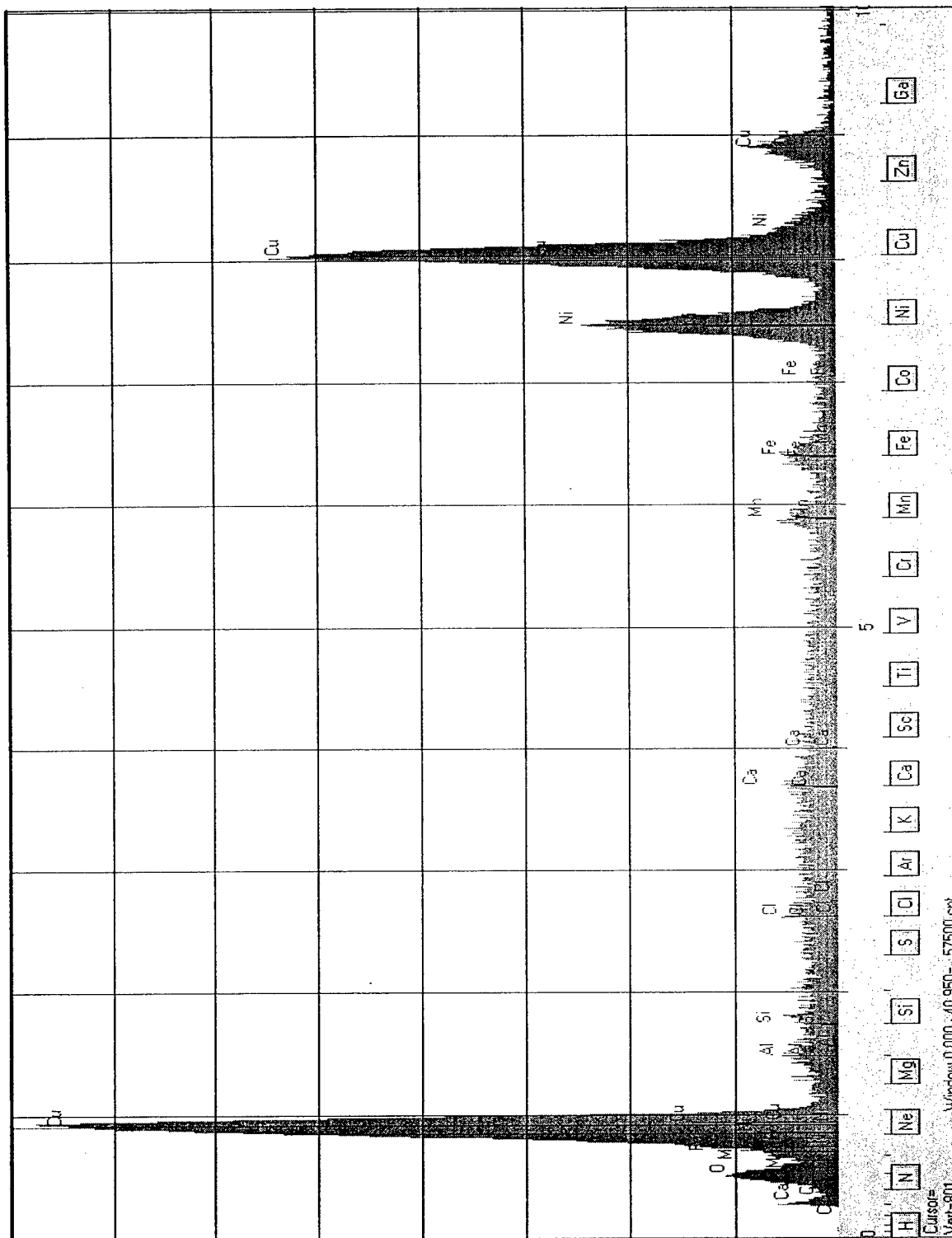


Figure D-10: EDS Spectrum Weld C6-A Weld Bead

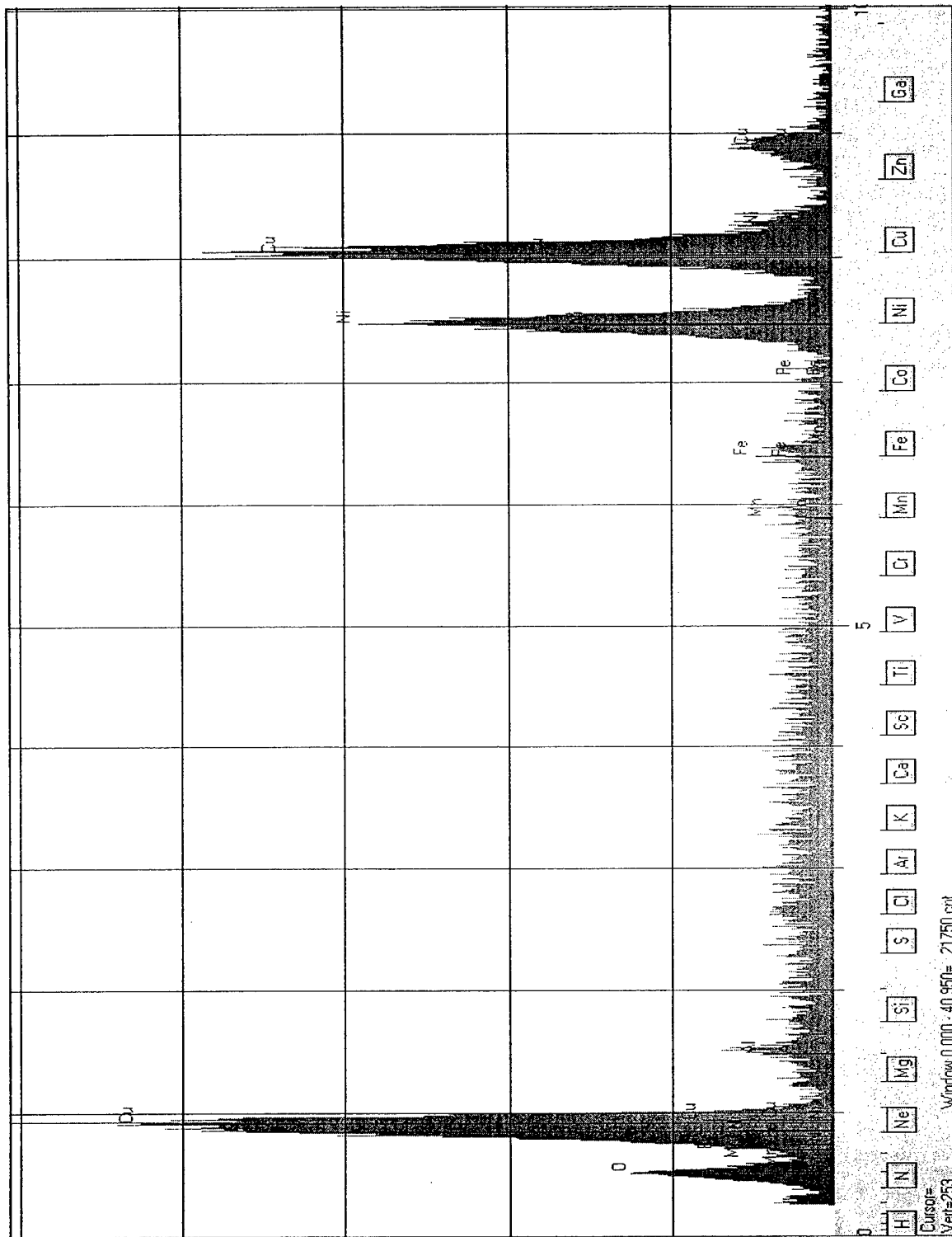


Figure D-11: EDS Spectrum Weld C6-C Base Metal

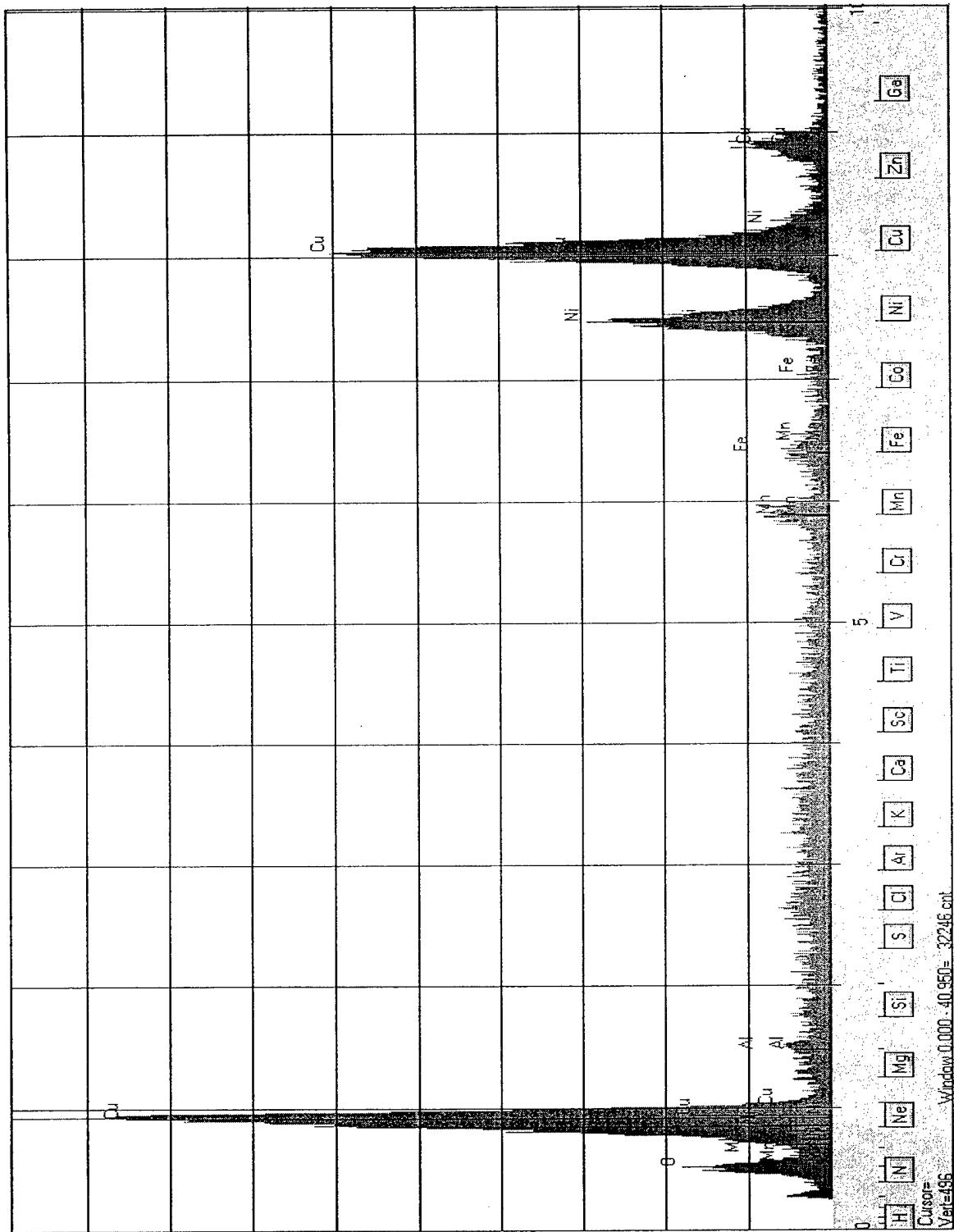


Figure D-12: EDS Spectrum Weld C6-C Weld Bead

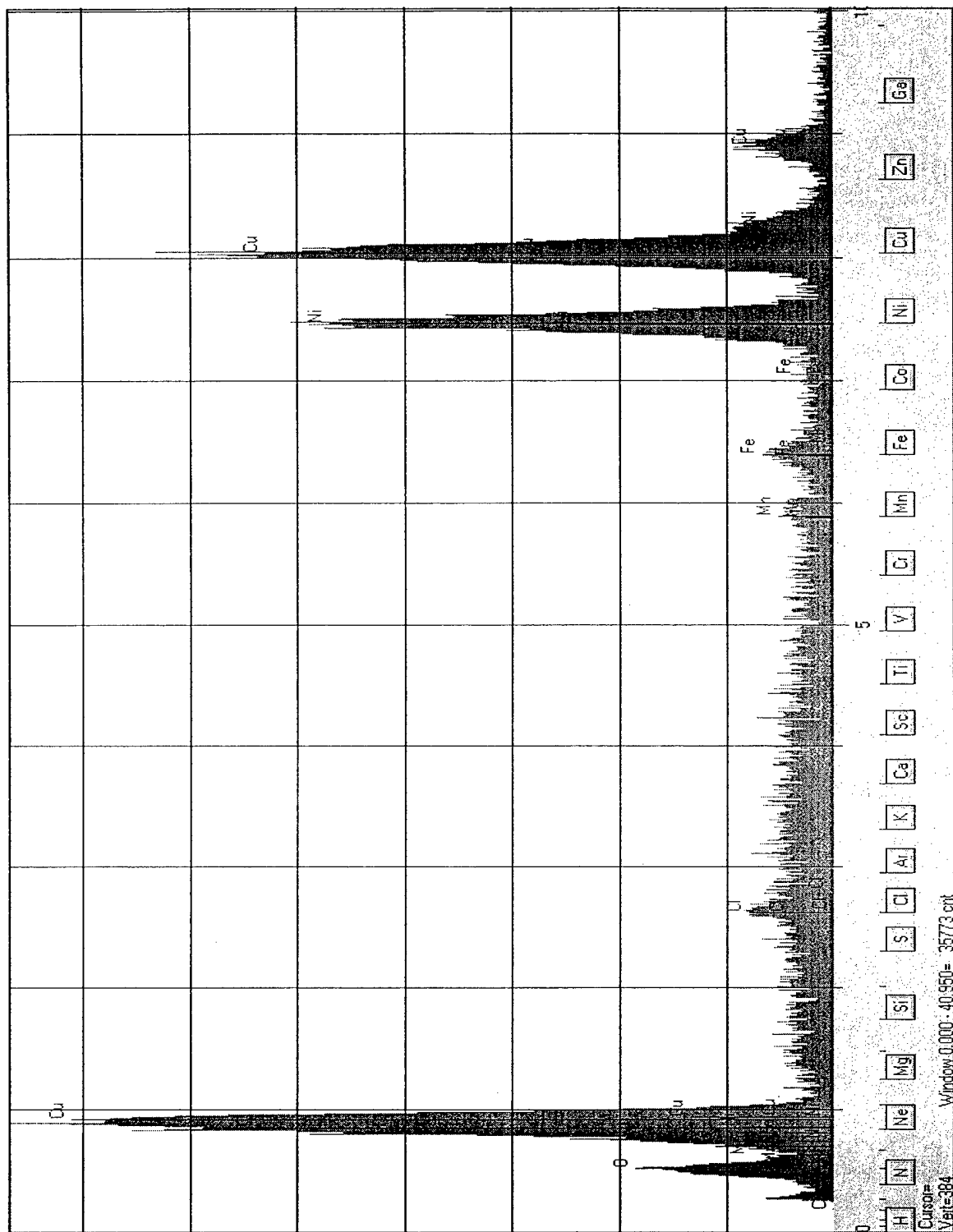


Figure D-13: EDS Spectrum Weld C6-D Base Metal

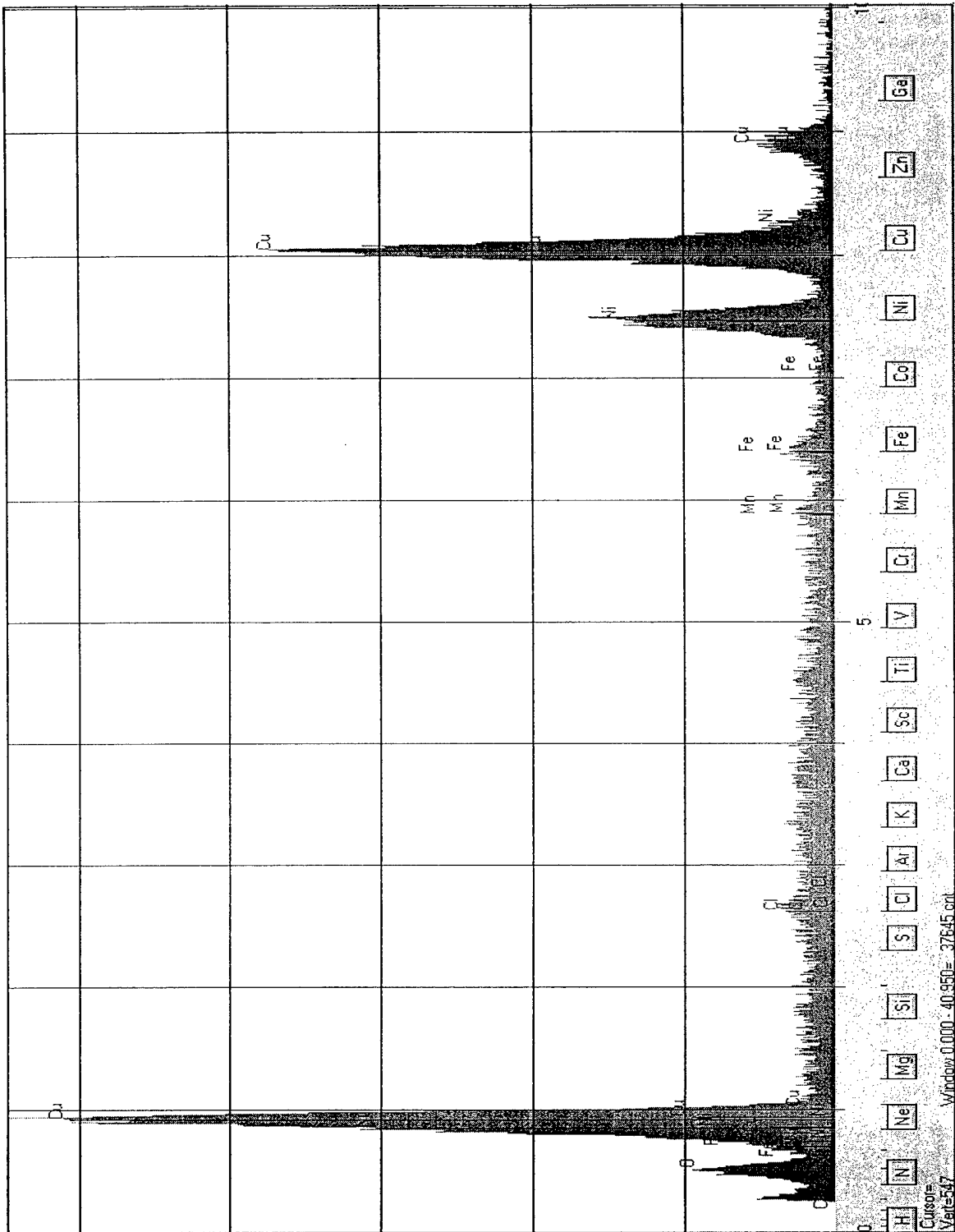


Figure D-14: EDS Spectrum Weld C6-D Weld Bead

# Bibliography

- [1] American Society for Testing and Materials. *1999 Annual Book of ASTM Standards, Section 2, Nonferrous Metal Products*. West Conshohocken, PA: ASTM, 1999.
- [2] *ASM Handbook, Vol. 10*. Materials Park, OH: ASM International, 1992.
- [3] Cary, Howard B. *Modern Welding Technology*. 2nd Edition. Englewood Cliffs, NJ: Prentice Hall, 1989.
- [4] Dawson, R. J. C. *Fusion Welding and Brazing of Copper and Copper Alloys*. New York: John Wiley and Sons, 1973.
- [5] Flinn, Richard A. and Paul K. Trojan. *Engineering Materials and Their Applications*. 3rd Edition. Boston: Houghton Mifflin, 1986.
- [6] Gabriel, Barbra L. *SEM: A User's Manual for Materials Science*. Metals Park, OH: American Society for Metals, 1985.
- [7] Jordan, M. F. and A. Duncan. *Final Report, INCRA Project 329: Cracking in the Welding of Cupronickel Alloys*. Birmingham, England: University of Aston in Birmingham, 1985.
- [8] Paskell, Troy, Matt Johnson, and Wangen Lin. *Development, Evaluation, and Deployment of Fluxes for GTAW That Increases Weld Penetration in Austenitic Stainless Steels, Carbon-Manganese Steel, and Copper-Nickel Alloys*. Report Project No. 08663GNF, NJC TDL No. 93-06, Columbus, OH: Edison Welding Institute, 1997.
- [9] *Requirements for Fabrication Welding and Inspection, and Casting Inspection and Repair for Machinery, Piping, and Pressure Vessels*. NAVSEA Technical Publication S9074-AR-GIB-010/278, 1995.

- [10] *Requirements for Welding and Brazing Procedure and Performance Qualification.* NAVSEA Technical Publication S9074-AQ-GIB-010/248, 1995.
- [11] *Source Book on Copper and Copper Alloys.* Metals Park, OH: American Society for Metals, 1979.
- [12] Wildsmith, G. "Copper-Nickel Seawater Piping Systems." *Marine Engineering with Copper-Nickel.* London: The Institute of Metals, 1988.
- [13] Witherell, C. E. "Some Factors Affecting the Weldability of the Cupro-Nickels." *Welding Journal* 39 (1960):411s-416s.